pISSN 2234-1900
eISSN 2234-3156

Radiation Oncology Journal

ROJ

Vol. 43, No. 1, March 2025

www.e-roj.org

The Korean Society for Radiation Oncology

www.e-roj.org

pISSN 2234-1900
eISSN 2234-3156

ROJ Radiation Oncology Journal

Vol. 43, No. 1, March 2025

Aims and Scope

The Radiation Oncology Journal (ROJ) is an official journal of the Korean Society for Radiation Oncology. It was launched in 1983 as the official journal of the Korean Society of Therapeutic Radiology. It was changed in 2000 as the official journal of the Korean Society for Therapeutic Radiology and Oncology and finally in 2011 as ROJ.

The aims of Radiation Oncology Journal are to contribute to the advancements in the fields of radiation oncology through the scientific reviews and interchange of all of radiation oncology. It encompasses all areas of radiation oncology that impacts on the treatment of cancer using radiation as well basic experimental work relating radiation oncology and health policy. It publishes papers describing clinical radiotherapy, combined modality therapy, radiation biology, cancer biology, radiation physics, radiation informatics and new technology including particle therapy.

The ROJ is published quarterly on the last day of March, June, September, and December, one volume per year. Any physicians or researchers throughout the world can submit a manuscript if the scope of the manuscript is appropriate. Articles in the following categories will be published: original articles, invited review articles, case reports, editorials, and letters to the editor related to basic or clinical radiation oncology. All of the manuscripts are peer-reviewed.

The ROJ is free open access journal. All articles published in ROJ are available through http://www.e-roj.org.

Open Access

This is an Open Access article distributed under the terms of the Creative Commons Attribution Non-Commercial License (https://creativecommons.org/licenses/by-nc/4.0/) which permits unrestricted non-commercial use, distribution, and reproduction in any medium, provided the original work is properly cited.

Publisher Hee Chul Park
Editor-in-Chief Sang Min Yoon

Editorial Office
Department of Radiation Oncology, Samsung Medical Center, Proton Therapy Center, B2, 81, Irwon-ro, Gangnam-gu, Seoul 06351, Republic of Korea
Tel: +82-2-3410-3617 E-mail: rojeditor@gmail.com, roj@kosro.or.kr

The Korean Society for Radiation Oncology
Department of Radiation Oncology, Samsung Medical Center, Proton Therapy Center, B2, 81, Irwon-ro, Gangnam-gu, Seoul 06351, Republic of Korea
Tel: +82-2-3410-3618 E-mail: kosro@kosro.or.kr

Printing Office
M2PI
#805, 26 Sangwon 1-gil, Seongdong-gu, Seoul 04779, Korea
Tel: +82-2-6966-4930 Fax: +82-2-6966-4945 E-mail: support@m2-pi.com

Published on March 31, 2025

© 2025 The Korean Society for Radiation Oncology
This paper meets the requirements of KS X ISO 9706, ISO 9706-1994 and ANSI/NISO Z39. 48-1992 (Permanence of paper)

ROJ Radiation Oncology Journal

Editorial Board

Publisher	Hee Chul Park	*Sungkyunkwan University, Korea*
Editor-in-Chief	Sang Min Yoon	*University of Ulsan, Korea*
Associate Editor	Dongryul Oh	*Sungkyunkwan University, Korea*
Editorial Board	Zishan Allibhai	*Southlake Regional Health Centre, Canada*
	Sevil Aliyeva Bagaturovna	*N. N. Blokhin Cancer Research Center, Russia*
	Miriam Joy C. Calaguas	*St. Luke's Medical Center, Philippines*
	Yu-Jen Chen	*National Yang-Ming University and MacKay Medical College, Taiwan*
	Jason Chia-Hsien Cheng	*National Taiwan University, Taiwan*
	Jeng-Fong Chiou	*Taipei Medical University, Taiwan*
	Changhoon Choi	*Sungkyunkwan University, Korea*
	Jin Hwa Choi	*Chung-Ang University, Korea*
	Youngmin Choi	*Dong-A University, Korea*
	Hak Choy	*UT Southweastern Medical Center, USA*
	Mantana Dhanachai	*Mahidol University, Thailand*
	Soehartati Gondhowiardjo	*University of Indonesia, Indonesia*
	Chul Soo Ha	*The University of Texas Health Science Center at San Antonio, USA*
	Ji Hong Hong	*Chang Gung Memorial Hospital, Taiwan*
	Byoung Hyuck Kim	*SMG-SNU Boramae Medical Center, Korea*
	Jin Sung Kim	*Yonsei University, Korea*
	Kyubo Kim	*Ewha Womans University, Korea*
	Tae Hyun Kim	*National Cancer Center, Korea*
	Woong Sub Koom	*Yonsei University, Korea*
	Jong Hoon Lee	*Catholic University, Korea*
	Vedang Murthy	*Tata Memorial Centre, India*
	O Kyu Noh	*Ajou University, Korea*
	Won Park	*Sungkyunkwan University, Korea*
	Jae Won Park	*Yeungnam University, Korea*
	Umberto Ricardi	*University of Turin, Italy*
	Vinay Sharma	*University of the Witwatersrand, South Africa*
	Tarek Shouman	*Cairo University, Egypt*
	Chang Won Song	*University of Minnesota, USA*
	Ekkasit Tharavichitkul	*Chiang Mai University, Thailand*
	Dang Huy Quoc Thinh	*HCMC Oncology Hospital, Vietnam*
	Joseph Tien-Seng Wee	*National Cancer Center, Singapore*
	Seung-Gu Yeo	*Soon Chun Hyang University, Korea*
	Zhao Chong Zeng	*Fudan Univerisity, China*
	Eduardo H. Zubizarreta	*International Atomic Energy Agency, Argentina*
Editorial Assistant	Horim Yang	*KOSRO, Korea*
Manuscript Editor	Soo-Hee Chang	*Infolumi, Korea*

ROJ Radiation Oncology Journal

Radiat Oncol J
pISSN 2234-1900 eISSN 2234-3156

Vol. 43, No. 1, March 2025

Editorials

1 De-escalation of regional nodal management for breast cancer patients after primary systemic therapy: from radiation oncologist's perspectives
Yong Bae Kim

4 Establishing protocols and standards for cardiac radioablation: a path toward clinical integration
Ji Hyun Chang

Original Articles

6 Feasibility and safety study of ultra-hypofractionated neoadjuvant radiotherapy to margins-at-risk in retroperitoneal sarcoma
Ru-Xin Wong, Valerie Shi Wen Yang, Clarame Shulyn Chia, Wen Shen Looi, Wen Long Nei, Chin-Ann Johnny Ong

13 Reducing clinical target volume margins for multifocal glioblastoma: a multi-institutional analysis of patterns of recurrence and treatment response
Francesco Marampon, Giovanni Luca Gravina, Elisa Cinelli, Lucy Zaccaro, Miriam Tomaciello, Nunzia Di Meglio, Francesco Gentili, Alfonso Cerase, Armando Perrella, Mariya Yavorska, Sami Aburas, Luciano Mutti, Maria Antonietta Mazzei, Giuseppe Minniti, Paolo Tini

22 Promising application of nano-WO_3/epoxy composite in intensity-modulated brachytherapy: a simulation study
Erfan Saatchian, Shahrokh Naseri, Sare Hosseini, Hamid Gholamhosseinian

30 Hounsfield units predict vertebral compression fractures in gastric cancer survivors after adjuvant irradiation
Pervin Hurmuz, Yasin Ozyurek, Ecem Yigit, Suayib Yalcin, Fazli Yagiz Yedekci, Faruk Zorlu, Mustafa Cengiz

40 Planning evaluation of stereotactic magnetic resonance–guided online adaptive radiosurgery for kidney tumors close to the organ at risk: is it valuable to wait for good timing to perform stereotactic radiosurgery?
Takaya Yamamoto, Shohei Tanaka, Noriyoshi Takahashi, Rei Umezawa, Yu Suzuki, Keita Kishida, So Omata, Kazuya Takeda, Hinako Harada, Kiyokazu Sato, Yoshiyuki Katsuta, Noriyuki Kadoya, Keiichi Jingu

Case Report

49 Long-term outcomes of radiotherapy for inoperable benign soft tissue tumors in the skull base or head
Joo-Hyun Chung, Hak Jae Kim, Hyun-Cheol Kang, Il Han Kim, Joo Ho Lee

ⓒ 2025 The Korean Society for Radiation Oncology

ROJ Radiation Oncology Journal

Editorial

pISSN 2234-1900 · eISSN 2234-3156
Radiat Oncol J 2025;43(1):1-3
https://doi.org/10.3857/roj.2025.00108

De-escalation of regional nodal management for breast cancer patients after primary systemic therapy: from radiation oncologist's perspectives

Yong Bae Kim

Department of Radiation Oncology, Heavy Ion Therapy Research Institute, Yonsei Cancer Center, Yonsei University Health System, Yonsei University College of Medicine, Seoul, Republic of Korea

Received: February 27, 2025
Revised: March 6, 2025
Accepted: March 10, 2025

Correspondence:
Yong Bae Kim
Department of Radiation Oncology, Heavy Ion Therapy Research Institute, Yonsei Cancer Center, Yonsei University Health System, Yonsei University College of Medicine, 50-1 Yonsei-ro, Seodaemun-gu, Seoul 03722, Republic of Korea
Tel: +82-2-2228-8095
E-mail: ybkim3@yuhs.ac
ORCID:
https://orcid.org/0000-0001-7573-6862

Breast cancer has increasingly been recognized as a systemic disease, leading to the understanding that if positive axillary disease is confirmed at diagnosis, primary systemic therapy should be prioritized, even when the tumor volume is small. The advent of targeted agents for the human epidermal growth factor receptor 2–positive type and the introduction of pembrolizumab in triple-negative breast cancer have significantly increased the rates of pathologic complete response [1,2]. Following surgery after neoadjuvant systemic therapy (NAST) when regional lymph node metastasis is confirmed at diagnosis, various scenarios may arise depending on the initial diagnosis, surgical interventions, and pathological findings.

A crucial issue is the administration of radiation therapy (RT). The results of the NRG Oncology/NSABP B-51/RTOG 1304 study were presented at the 2023 San Antonio Breast Cancer Symposium, indicating no significant difference in 5-year invasive breast cancer recurrence-free interval between the no regional nodal irradiation (RNI) and RNI groups after a follow-up of 59.5 months. Although further follow-up is warranted, if these results are confirmed, they are expected to establish Level 1 evidence that will be incorporated into routine clinical practice guidelines.

A consensus is yet to be reached regarding axillary management options such as axillary lymph node dissection (ALND), targeted axillary dissection, or axillary RT, and it will take considerable clinical experience to establish clear guidelines. However, in cases where ypN1 or higher is observed postoperatively, there seems to be a consensus on the necessity of RT, regardless of the surgical technique or number of lymph nodes involved. Current guidelines primarily recommend postmastectomy RT for patients with persistent axillary nodal involvement after NAST, as specified in the 2016 American Society of Clinical Oncology/American Society for Radiation Oncology/Society of Surgical Oncology guideline update [3].

Variability and uncertainty surrounding the RT exist, particularly in the two aforementioned scenarios. Moderate hypofractionation of the RNI has been established as the standard treatment in standard guidelines, suggesting a more uniform approach in this domain [4]. However, various delivery methodologies exist, ranging from anatomical landmark-based field delivery to anatomy-based delivery, all of which are used in real-world practice. The selected method inherently influences the policies surrounding volume coverage. The international European Breast Cancer Research Association of Surgical Trialists survey, in a recent issue of the Radiation Oncology Journal,

© 2025 The Korean Society for Radiation Oncology
This is an Open Access article distributed under the terms of the Creative Commons Attribution Non-Commercial License (http://creativecommons.org/licenses/by-nc/4.0/) which permits unrestricted non-commercial use, distribution, and reproduction in any medium, provided the original work is properly cited.

reflected remarkable variability in responses regarding volume management [5].

Presently, the prevailing trend in breast cancer treatment is the optimization of therapy through de-escalation strategies, which will ultimately reflect on both surgical and RT approaches, gradually shifting towards de-escalation. Our understanding suggests that as research data and real-world experiences accumulate, a distinct preference will develop for sentinel lymph node dissection (SLND) over ALND. Similarly, RNI practices adapt to reflect a reduction in volume for optimization.

In scenarios in which a disease-free status is confirmed after ALND or SLND, emerging evidence suggests that RNI may soon be safely omitted from oncological practice. Conversely, various opinions arise as to whether axillary residual disease is detected post-ALND or SLND. Generally, if ypN2 or higher residual disease is noted post-ALND, the implementation of a wide RNI is deemed necessary. However, more nuanced discussions exist concerning ypN1, in which the necessity of RT may depend on the number of nodes removed and the lymph nodes involved, resulting in a range of opinions regarding the extensive application of RNI. As classifications lean towards N1mic or N0(+i), the inclination to limit or omit RT coverage may increase. For cases with post-SLND–positive disease, there may be a tendency to select a broader RNI when adding RT as opposed to relying on ALND, yet some advocate for implementing a limited RNI in line with the ACOSOG Z0011 findings.

De-escalation of RT volume requires robust anatomical treatment planning, which is crucial for high-precision therapy. This entails advanced anatomical contouring and intensity-modulated radiation therapy (IMRT) planning. Although IMRT has been used for a long time in breast cancer treatment, oncologists have been hesitant to adoption because of concerns about the lack of supporting evidence, despite clear dosimetric advantages. The high costs associated with demonstrating the utility of treatment techniques through clinical trials, particularly for RT, which lacks substantial backing entities compared to chemotherapy, pose significant barriers to achieving Level 1 evidence.

Currently, the execution of IMRT depends on adequate resources, including equipment and personnel. The severe workload of radiation oncologists presents a notable hurdle, with IMRT demanding exponentially greater execution compared to that in 2-dimensional and 3-dimensional conformal technique. Defining not only the target but also the organs at risk, along with establishing planning goals and conducting quality assurance processes, requires substantial time commitments. Auto-contouring systems under development may alleviate some of this burden and auto-planning processes are likely to find their way into real-world applications.

Ultimately, de-escalation of both surgery and RT seeks to minimize toxicity and improve the quality of life, addressing issues such as lymphedema, which significantly affects daily living [6]. Minimizing the RT fields and employing high-precision therapies should guide treatment strategies to reduce complications without compromising efficacy. The increased use of breast reconstruction with implants following mastectomy is noteworthy, particularly because RT is known to correlate with a heightened risk of reconstructive complications such as capsular contracture [7]. Therefore, the oncological safety of omitting RT may be a pivotal factor in reducing adverse outcomes.

In conclusion, the optimal use of RT, including dosage and field, is still debated due to differing pathological results after NAST and surgical intervention. As we align with the de-escalation trend, adjustments in RT practices are also expected to evolve. However, the processes involved in optimizing the treatment could contribute to rising costs. Therefore, radiation oncologists should judiciously determine appropriate treatment policies, taking the available equipment and workforce resources into account. This balance is essential to ensure quality patient care while effectively managing economic considerations.

Conflict of Interest

No potential conflict of interest relevant to this article was reported.

References

1. Schmid P, Cortes J, Pusztai L, et al. Pembrolizumab for early triple-negative breast cancer. N Engl J Med 2020;382:810–21.
2. Cortes J, Rugo HS, Cescon DW, et al. Pembrolizumab plus chemotherapy in advanced triple-negative breast cancer. N Engl J Med 2022;387:217–26.
3. Recht A, Edge SB, Solin LJ, et al. Postmastectomy radiotherapy: clinical practice guidelines of the American Society of Clinical Oncology. J Clin Oncol 2001;19:1539–69.
4. Balic M, Thomssen C, Gnant M, Harbeck N. St. Gallen/Vienna 2023: optimization of treatment for patients with primary breast cancer - a brief summary of the consensus discussion. Breast Care (Basel) 2023;18:213–22.
5. Gasparri ML, Kaidar-Person O, Gentilini OD, de Boniface J, Kuehn T, Poortmans P. Radiation therapy volumes after primary systemic therapy in breast cancer patients: an international EUBREAST survey. Radiat Oncol J 2024;42:308–18.
6. Byun HK, Chang JS, Im SH, et al. Risk of lymphedema following contemporary treatment for breast cancer: an analysis of 7617 consecutive patients from a multidisciplinary perspective. Ann

 https://doi.org/10.3857/roj.2025.00108

Surg 2021;274:170–8.
7. Chung SY, Chang JS, Shin KH, et al. Impact of radiation dose on complications among women with breast cancer who underwent breast reconstruction and post-mastectomy radiotherapy: a multi-institutional validation study. Breast 2021;56:7–13.

ROJ Radiation Oncology Journal

Editorial

pISSN 2234-1900 · eISSN 2234-3156
Radiat Oncol J 2025;43(1):4-5
https://doi.org/10.3857/roj.2025.00094

Establishing protocols and standards for cardiac radioablation: a path toward clinical integration

Ji Hyun Chang

Department of Radiation Oncology, Seoul National University Hospital, Seoul National University College of Medicine, Seoul, Republic of Korea

Received: February 25, 2025
Revised: March 10, 2025
Accepted: March 10, 2025

Correspondence:
Ji Hyun Chang
Department of Radiation Oncology, Seoul National University Hospital, Seoul National University College of Medicine, 101 Daehak-ro, Jongno-gu, Seoul 03080, Republic of Korea
Tel: +82-2-2072-4940
E-mail: jh.chang@snu.ac.kr
ORCID:
https://orcid.org/0000-0001-5921-5522

Ventricular tachycardia (VT) and other cardiac arrhythmias are treated with antiarrhythmic drugs, catheter ablation, implantable cardioverter defibrillators, or surgical intervention. In cases where such treatments are ineffective or contra-indicated, these conditions can become life-threatening. Cardiac radioablation, specifically stereotactic ablative body radiotherapy (SABR), offers a promising noninvasive alternative for treating refractory VT. After the first case report from Stanford University, a case series presentation at Washington University in St. Louis contributed to its global expansion [1,2].

A recent paper by Kim et al. [3] outlines an institutional workflow for VT-SABR, emphasizing its technical aspects, treatment planning, and quality assurance (QA) measures. This paper presents two example cases in which advanced multimodal imaging techniques, including electrocardiographic-gated computed tomography (CT), 4-dimensional cone-beam CT (CBCT), and intrafractional CBCT were employed. Despite current capabilities, challenges persist in meeting planned target volume coverage and constraints for specific cardiac substructures, such as the left coronary artery and adjacent structures, illustrating the complexity of balancing therapeutic efficacy against safety. As shown in this study, clearly defining an institutional protocol is crucial as it enables consistent treatment delivery and facilitates standardized reporting of clinical outcomes.

Achieving dose constraints for organs at risk (OARs), including critical cardiac substructures, remains a significant challenge in cardiac radioablation [4]. While insufficient clinical data currently exist to determine the actual incidence of expected toxicities, existing studies have not reported a substantial decline in left ventricular function or a significant increase in coronary artery events after cardiac radioablation [5,6]. To date, long-term effects on myocardial tissue and surrounding OARs remain insufficiently studied, underscoring the need for prospective randomized controlled trials (RCTs) to assess therapeutic efficacy and potential late toxicities. As this treatment is introduced among a high-risk patient population, its integration into standard care requires rigorous procedural frameworks and robust clinical evidence. Concerns among cardiologists remain considerable, emphasizing the importance of interdisciplinary collaboration. In a survey conducted by the European Heart Rhythm Association, 48.1% of respondent cardiologists reported having either performed cardiac radioablation or referred patients for the procedure. Although many acknowledged the potential indications for VT/ventricular fibrillation in patients with underlying structural heart disease, 63% of respondents cited the perceived lack of reliable outcome data as a significant concern [7].

© 2025 The Korean Society for Radiation Oncology
This is an Open Access article distributed under the terms of the Creative Commons Attribution Non-Commercial License (http://creativecommons.org/licenses/by-nc/4.0/) which permits unrestricted non-commercial use, distribution, and reproduction in any medium, provided the original work is properly cited.

The distinct clinical characteristics of cardiac and oncology patients must be considered when defining and interpreting study endpoints. Researchers in this field must develop a comprehensive understanding of the disciplines involved to foster effective collaboration and ensure meaningful clinical outcomes.

A United States RCT (NCT05765175) aims to address several of these concerns. This study will evaluate the efficacy of cardiac radioablation in reducing arrhythmia burden, assess safety profiles, particularly regarding radiation-induced cardiotoxicity and collateral damage to adjacent organs, and establish benchmarks for imaging, dose delivery, and QA standards applicable across diverse clinical settings [8]. The results of this trial will be instrumental in shaping clinical guidelines and determining whether cardiac radioablation can transition from an experimental procedure to a standard treatment option.

Conflict of Interest

No potential conflict of interest relevant to this article was reported.

References

1. Loo BW Jr, Soltys SG, Wang L, et al. Stereotactic ablative radiotherapy for the treatment of refractory cardiac ventricular arrhythmia. Circ Arrhythm Electrophysiol 2015;8:748–50.
2. Cuculich PS, Schill MR, Kashani R, et al. Noninvasive cardiac radiation for ablation of ventricular tachycardia. N Engl J Med 2017;377:2325–36.
3. Kim H, Park S, Kim J, et al. Reinforcing treatment and evaluation workflow of stereotactic ablative body radiotherapy for refractory ventricular tachycardia. Radiat Oncol J 2024;42:319–29.
4. Gupta A, Sattar Z, Chaaban N, et al. Stereotactic cardiac radiotherapy for refractory ventricular tachycardia in structural heart disease patients: a systematic review. Europace 2024;27:euae305.
5. van der Ree MH, Dieleman EM, Visser J, et al. Non-invasive stereotactic arrhythmia radiotherapy for ventricular tachycardia: results of the prospective STARNL-1 trial. Europace 2023;25:1015–24.
6. Robinson CG, Samson PP, Moore KM, et al. Phase I/II trial of electrophysiology-guided noninvasive cardiac radioablation for ventricular tachycardia. Circulation 2019;139:313–21.
7. Kovacs B, Lehmann HI, Manninger M, et al. Stereotactic arrhythmia radioablation and its implications for modern cardiac electrophysiology: results of an EHRA survey. Europace 2024;26:euae110.
8. Cardiac RADIoablation versus repeat catheter ablation: a pivotal randomized clinical trial evaluating safety and efficacy for patients with high-risk refractory ventricular tachycardia (RADIATE-VT) [Internet]. Bethesda, MD: National Library of Medicine; 2025 [cited 2025 Feb 20]. Available from: https://clinicaltrials.gov/study/NCT05765175.

ROJ Radiation Oncology Journal

Original Article

pISSN 2234-1900 · eISSN 2234-3156
Radiat Oncol J 2025;43(1):6-12
https://doi.org/10.3857/roj.2024.00297

Feasibility and safety study of ultra-hypofractionated neoadjuvant radiotherapy to margins-at-risk in retroperitoneal sarcoma

Ru-Xin Wong[1,2], Valerie Shi Wen Yang[2,3,4], Clarame Shulyn Chia[2,5,6,7], Wen Shen Looi[1,2], Wen Long Nei[1,2], Chin-Ann Johnny Ong[2,5,6,7,8,9]

[1]*Division of Radiation Oncology, National Cancer Centre Singapore, Singapore*
[2]*SingHealth Duke-NUS Oncology Academic Clinical Program, Duke-NUS Medical School, Singapore*
[3]*Division of Medical Oncology, National Cancer Centre Singapore, Singapore*
[4]*Translational Precision Oncology Laboratory, Institute of Molecular and Cell Biology, Agency for Science, Technology and Research, Singapore*
[5]*Division of Surgery and Surgical Oncology, Department of Sarcoma, Peritoneal and Rare Tumours, National Cancer Centre Singapore, Singapore*
[6]*Division of Surgery and Surgical Oncology, Department of Sarcoma, Peritoneal and Rare Tumours, Singapore General Hospital, Singapore*
[7]*SingHealth Duke-NUS Surgery Academic Clinical Program, Duke-NUS Medical School, Singapore*
[8]*Laboratory of Applied Human Genetics, Division of Medical Sciences, National Cancer Centre Singapore, Singapore*
[9]*Institute of Molecular and Cell Biology, Agency for Science, Technology and Research, Research Entities, Singapore*

Received: April 22, 2024
Revised: July 3, 2024
Accepted: July 5, 2024

Correspondence:
Ru-Xin Wong
Division of Radiation Oncology, National Cancer Centre Singapore, 30 Hospital Blvd, 168583 Singapore
Tel: +65-91522720
E-mail: wongruxin@gmail.com
ORCID:
https://orcid.org/0000-0002-4973-7404

Purpose: Retroperitoneal sarcomas (RPS) are rare tumors that present unique challenges, often due to late presentation, and the proximity of critical organs makes complete surgical resection challenging. This study aimed to assess the feasibility of neoadjuvant short-course radiotherapy (SCRT) targeting margins-at-risk and to assess its potential impact on outcomes.

Materials and Methods: This is a single-center, prospective, non-randomized feasibility study. SCRT was administered via image-guided volumetric modulated arc therapy, consisting of 5 fractions of daily radiotherapy followed by immediate surgery. As a starting dose, patients were prescribed 25 Gy in 5 fractions. For the escalation stage, patients were prescribed 30 Gy in 5 fractions. Only the presumed threatened surgical margins were delineated for large tumors.

Results: Patients with either primary or recurrent RPS were recruited. Eight patients underwent SCRT but one patient did not have a resection as planned. Seven patients underwent surgical resection, of whom one passed away 3 months postoperative from a cardiac event. After a median follow-up of 20.5 months for the six postoperative survivors, there were no overt long-term toxicities and one patient relapsed out-of-radiotherapy-field.

Conclusion: SCRT to RPS with a margin boost followed by immediate surgery is worth investigating. A starting dose of 30 Gy in 5 fractions is recommended for further studies. Longer-term follow-up is necessary.

Keywords: Sarcoma, Radiotherapy, Neoadjuvant therapy, Preoperative procedures

Introduction

Retroperitoneal sarcomas (RPS) are rare malignancies arising within the retroperitoneal space, characterized by their infiltrative nature and propensity for local recurrence. Optimal management typically involves surgical resection; however, achieving negative margins can be challenging due to anatomical constraints and proximity to critical structures. As a result, local recurrence rates for RPS

© 2025 The Korean Society for Radiation Oncology
This is an Open Access article distributed under the terms of the Creative Commons Attribution Non-Commercial License (http://creativecommons.org/licenses/by-nc/4.0/) which permits unrestricted non-commercial use, distribution, and reproduction in any medium, provided the original work is properly cited.

are high. Neoadjuvant radiotherapy aims to reduce tumor size and improve resectability but is associated with toxicity and delayed wound healing. While long-course radiotherapy has been employed with some success in a sub-group of RPS, it often requires prolonged treatment courses and can delay surgical resection [1]. Short-course radiotherapy (SCRT) offers the advantage of delivering a higher dose of radiation over a shorter time frame, made possible with conformal technologies with image guidance and volumetric modulation. There has been a paradigm shift in recent years on other cancer types favoring SCRT [2,3]. For sarcomas, there have been a few small prospective studies on soft tissue sarcomas of the extremities and trunk [4,5].

In this study, we sought to investigate the feasibility and utility of neoadjuvant SCRT for retroperitoneal liposarcoma, followed by immediate surgery. This feasibility study aimed to assess whether neoadjuvant SCRT targeting margins can be integrated into the treatment paradigm for RPS, and to report on early safety outcomes of ultra-fractionated radiotherapy.

The hypothesis is that SCRT to threatened margins is a safe and efficacious treatment method for retroperitoneal sarcomas. The primary objectives are to assess the safety and acute toxicities, including postoperative complications, of neoadjuvant short-course radiotherapy followed by immediate surgery in resectable retroperitoneal sarcomas, to evaluate the effects of neoadjuvant short-course radiotherapy on surgical procedures, e.g., frequency of intra-operative fibrosis, and to report short-term tumor control outcomes.

Materials and Methods

Eight patients diagnosed with retroperitoneal sarcoma were enrolled in this single-center, prospective feasibility study. Eligible patients were scheduled to receive ultra-fractionated radiotherapy before surgical resection. Safety assessments were conducted regularly throughout treatment and included monitoring of acute toxicity, wound healing complications, and surgical outcomes. Feasibility endpoints included treatment compliance, completion rates, and technical feasibility of radiotherapy delivery. This is a single-center, prospective, non-randomized feasibility study.

Patients were recruited by surgical oncologists, discussed at multi-disciplinary meetings, and referred to a radiation oncologist for discussion, communicating that neoadjuvant radiotherapy is not routine, and that SCRT is novel. Fig. 1 illustrates the flowchart for the study pathway.

SCRT was administered via image-guided-volumetric modulated arc therapy following four-dimensional computed tomography simulation. Treatment consisted of 5-fraction radiotherapy, followed by immediate surgery. Patients were prescribed 25 Gy for the first stratum. At the next level, patients were prescribed 25 Gy with simultaneous integrated boost of 30 Gy. When tumors were small, the entire tumor was treated. When tumors were deemed too large to be entirely encompassable by the radiotherapy fields, only threatened margins were irradiated. Where margins were antici-

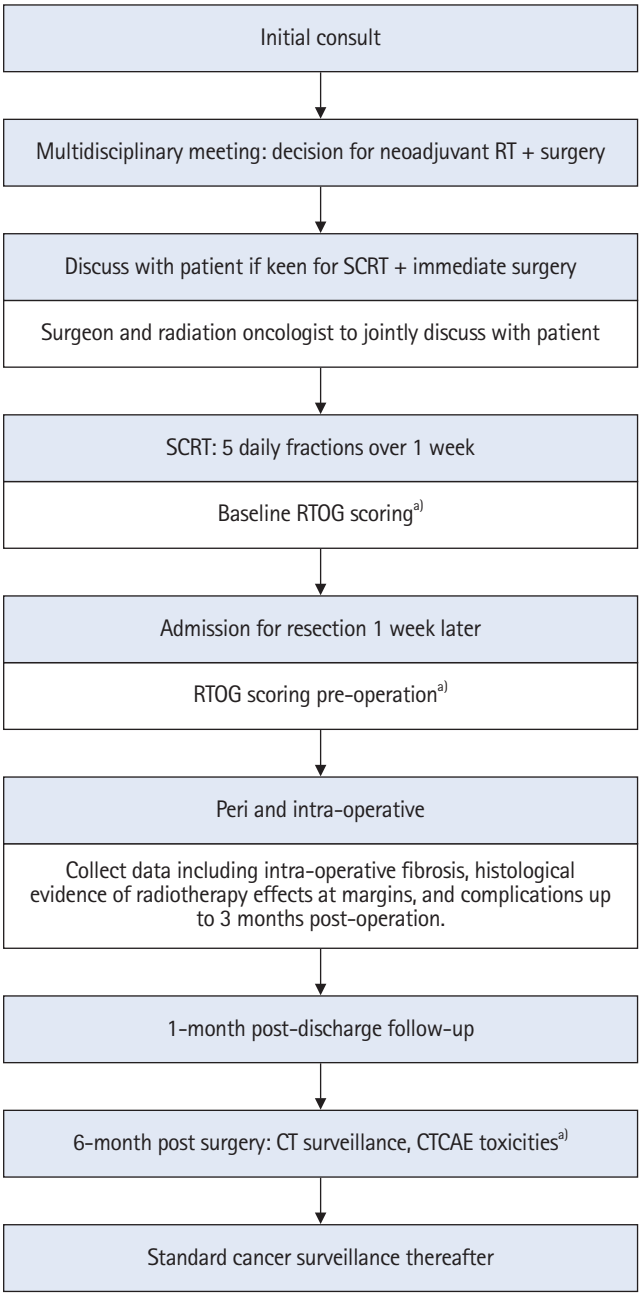

Fig. 1. Flow chart for patients' recruitment and study journey. RT, radiotherapy; SCRT, short-course radiotherapy; RTOG, Radiation Therapy Oncology Group; CT, computed tomography; CTCAE, Common Terminology Criteria for Adverse Events. [a)]Time points for toxicities scoring.

pated to be "air" margins; pushing instead of infiltrative, a joint decision by radiation oncologists and surgeons was made only to include threatened margins, which typically included tumor interfaces with vertebral bodies, great vessels (aorta, inferior vena cava, portal vein), and abdominal wall musculature up to an anticipated location of the free intra-abdominal cavity, by international guidelines [6]. Dose constraints were met and were extrapolated from guidelines from Task Group 101 [7] and UK stereotactic ablative radiotherapy [8].

The study would be stopped if one or more postoperative complications of fistula or perforation happened at the site of anastomosis within the high-dose irradiation field since such events are rare. Adverse events were graded using Radiation Therapy Oncology Group score during the acute phase and National Cancer Institute Common Terminology Criteria for Adverse Events version 5.0, up to 6 months post-operation.

Any patient diagnosed clinically, radiologically, and histology-proven to have RPS and deemed operable would be considered. The patient may have primary or locally recurrent RPS.

Clinical, radiological, and pathological assessments were conducted before and after SCRT. Surgical resection with the intent of achieving negative margins was performed as soon as logistically possible upon completion of SCRT. Surgical outcomes, including margin status and postoperative outcomes, were assessed.

Results

Eight patients were treated with SCRT; Table 1 summarizes the included patients' characteristics. All patients completed the planned course of ultra-fractionated radiotherapy without interruptions.

Patient 8 developed coronavirus disease 2019 (COVID-19) infection before her planned surgery. She had a recurrent multi-focal low-grade dedifferentiated liposarcoma and a joint decision was made to abandon surgical salvage for palliative chemotherapy. Patient number 8 tolerated the SCRT well and remained progression-free for 18 months after SCRT while she was maintained on palliative trabectedin. The sarcoma surgeons did not report intra-operative fibrosis for the seven patients who underwent resection. All seven patients, but one (patient 7), recovered well post-operatively. Patient 7 was an elderly patient with a large undifferentiated pleomorphic sarcoma, with pre-existing cardiac and pulmonary co-morbidities who developed an infected abscess at the distal pancreatomy bed and passed away 3 months postoperative from an unrelated sudden cardiac event. After excluding patients 7 and 8, with a median follow-up of 20.5 months, six patients were eligible for evaluation; five patients were disease-free except for one who developed an out-of-field relapse (patient 4) as she did not receive an en bloc multi-organ extended resection due to the large and central nature of her tumor, and only the central vessels were irradiated (Fig. 2).

The surgeons did not report intra-operative fibrosis for the seven

Table 1. Patients' demographic, tumor and treatment characteristics

Patient No.	Primary or recurrent	Dose/Fraction/ Treatment field/ Volume (cm^3)	Age (year)	Histology	Margins	Follow-up (months)	Disease-free	Toxicities	Interval between SCRT and surgery (week)
1	Primary	25 Gy/5#/margins/150	58	Low-grade dedifferentiated LPS	Atypical stromal cells present	23	Yes	None	1
2	Primary	25 Gy/5#/entire tumor/400	54	Low-grade dedifferentiated LPS	Well-diffrentiated present	22	Yes	None	1
3	Primary	25 Gy/5#/margins/200	64	Low-grade dedifferentiated LPS	Clear	21	Yes	None	3
4	Primary	30 Gy/5#/margins/246	45	Well-dedifferentiated LPS	Clear	20	Out-of-field relapse	None	6
5	Primary	30 Gy/5#/entire tumor/680	54	High-grade dedifferentiated LPS	Clear	19	Yes	Postoperative chyle leak	1
6	Primary	30 Gy/5#/margins/575	69	Low-grade dedifferentiated LPS	Dedifferentiated cells present	18	Yes	None	2
7	Primary	30 Gy/5#/margins/643	83	Undifferentiated pleomorphic sarcoma	High-grade sarcoma present	3	n.a.	Pancreatic abscess	1
8	Recurrent	30 Gy/5#/entire tumor/300	62	Dedifferentiated LPS (from the first laparotomy)	n.a.	24	n.a.	None	n.a. (developed COVID-19)

SCRT, short-course radiotherapy; LPS, lipopolysaccharide; n.a., not available; COVID-19, coronavirus disease 2019.
# denotes number of fractions.

https://doi.org/10.3857/roj.2024.00297

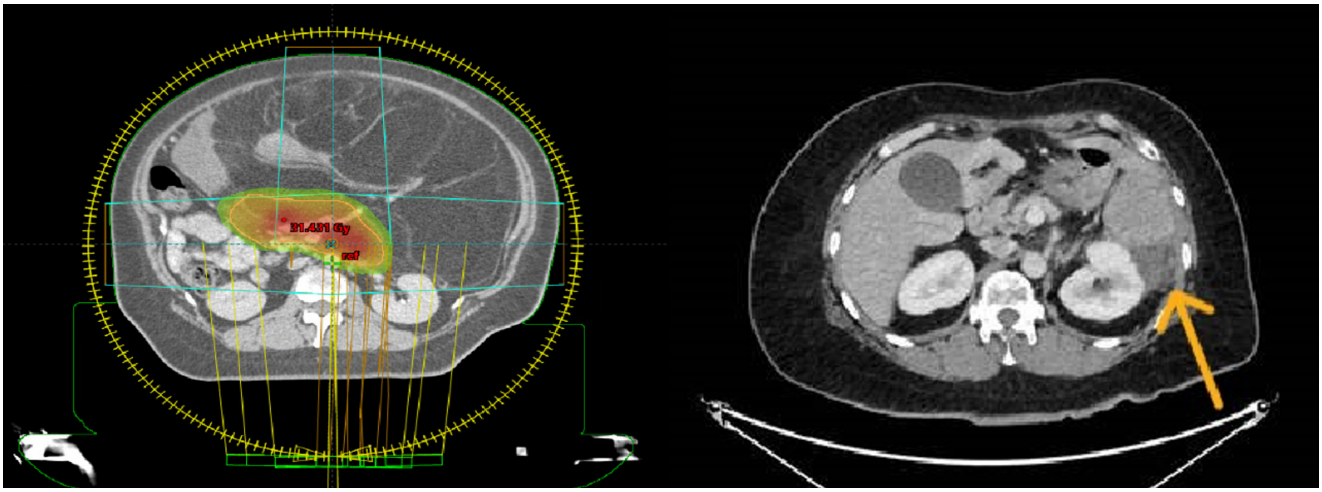

Fig. 2. Patient 4 received 30 Gy in 5 fractions to the inferior vena cava, abdominal aorta, and mesenteric vessels where the surgical margins were anticipated to be R1 (left). Eighteen months later she had a relapse out-of-field adjacent to the left kidney (right). She underwent a salvage resection with a nephrectomy successfully without complications. Arrow indicates the area of local relapse, which is out of radiotherapy field.

patients who had resection. There were no acute toxicities greater than grade 2 during and immediately after radiotherapy. Post-operatively, patient 7 developed an abscess at the pancreatic bed and passed away from a sudden cardiac event. Patient 5 developed a chyle-leak post-operatively which was self-resolving. There were no long-term toxicities > grade 3.

Discussion and Conclusion

RPS remains a challenging malignancy to treat due to its complex anatomical location. Currently, survival rates for low and intermediate-grade RPS are about 50% at 5 years [9]. Oncologic en bloc extended resection is required for the cure of non-metastatic retroperitoneal sarcoma [10]. Recurrent RPS also requires resection, considering the patient's age and performance status, pace of disease, and type of initial resection. Current evidence suggests that while neoadjuvant radiotherapy was not associated with an overall benefit, the STRASS and STREXIT trials showed a consistent signal that well-differentiated (WD) and low-grade dedifferentiated liposarcomas (DDLS) demonstrated improved abdominal recurrence-free survival [1,11]. Currently, neoadjuvant radiotherapy is not routinely recommended. Recent evidence has shed light on the different behaviors of different histology subtypes of RPS, prompting STRASS 2, which is investigating the role of systemic therapies in subtypes that have a high propensity for distant metastases (high-grade DDLS, undifferentiated sarcomas, and leiomyosarcomas) [12]. Until more evidence comes to light, the use of neoadjuvant radiotherapy remains controversial and is to be discussed on an individual patient basis for WD and low-grade DDLS.

The current standard dose-fraction is about 50 Gy over 5 weeks of daily treatment (long-course radiotherapy [LCRT]) followed by delayed surgery. While LCRT may be considered for certain RPS subtypes, there are significant logistical issues. Surgeons are unwilling, understandably, to delay curative surgery for LCRT in the absence of very compelling evidence. SCRT may overcome these issues, although its toxicity may not be insignificant in patients with very large tumors. Involved margins are common in RPS and associated with worse local controls [12]. Hence, we were prompted to investigate the feasibility of a novel approach using SCRT, targeting especially the margins-at-risk in these patients. Other than logistical convenience, there could be inherent biological benefits. As the alpha/beta ratio of soft tissue sarcomas, especially low-grade, is presumably low, a high dose per fraction is more desirable, hence favoring SCRT. Boosts to high-risk margins are sometimes given as reported in some studies, with some suggesting a benefit [13,14]. There is an ongoing trial to study SCRT using proton therapy with boosts to the margins [15]. In the STRASS study, 16% of the patients had tumor progression before surgery was administered. SCRT can mitigate this problem. This sentiment is echoed by Istl and Gronchi [12].

We have provided early and small evidence that SCRT to the margins is safe, intra-, and peri-operatively, with minimal logistical difficulties for patients with RPS that are located near critical structures. One patient died from a sudden cardiac event and he did develop an abscess at the distal pancreatectomy site. We investigated and found that the radiotherapy dose at the distal pancreas was 27 Gy in 5 fractions, and our surgeon did not report increased fibrosis intra-operatively. Regarding pancreatic SCRT and extrapo-

Table 2. Different dose fractionation regimens and EQD_2

Dose/fraction (Gy)	RT fractions	Duration of RT (week)	Total dose (Gy)	EQD_2 ($\alpha/\beta=3$)	EQD_2 ($\alpha/\beta=10$)
5	5	1	25	40	31
6	5	1	30	54	33
1.8	28	5.5	50.4	48.4	49.6
2	25	5	50	50	50

EQD_2, equivalent doses in 2 Gy; RT, radiotherapy.

lating from pancreatic cancer studies, two papers studying the feasibility of photon [16] and proton [17] neoadjuvant SCRT showed that the former was associated with more toxicities than the latter due to increased fibrosis that the surgeons reported intra-operatively while performing a Whipple's procedure. Other studies [18] have shown that neoadjuvant SCRT with chemotherapy is safe for downsizing pancreatic cancer pre-Whipple's procedure and hence, this patient is more likely to have developed complications due to other medical factors rather than due to the SCRT given to him. Another patient's surgery was aborted due to COVID-19 infection because this study was conducted amidst the initial pandemic. She continued to demonstrate sustained control of her recurrent tumors for at least 18 months post-SCRT. The SCRT probably contributed significantly to her extended survival on top of the palliative trabectedin.

Of the six patients who underwent resection and had longer-term follow-up, all six did not have complications peri-operatively other than one who had persistent chyle-leak, which was conservatively managed. One developed an out-of-field relapse almost two years after initial SCRT as only the tumor near the abdominal aorta, inferior vena cava and mesenteric vessels were irradiated. In the STRASS study, 39% developed at least a grade 3 complication throughout the study, and 14% developed peri-operative complications, although it is hard to ascertain how much radiotherapy contributed to these complication rates specifically [1]. Although our numbers are small, we have shown SCRT to be safe and feasible.

The current standard dose fractionation for RPS would be 50.4 or 50 Gy in 28 or 25 fractions. The equivalent dose for the short-course regimen as compared to the standard is described below (Table 2). Extrapolating from truncal and extremity soft tissue sarcomas, hypofractionated radiotherapy is gaining traction, with a few prospective trials reporting safety and equivalent tumor control ranging from 20 to 35 Gy in 5 fractions [4,5,19,20]. In terms of acute toxicities, SCRT is expected to have less ($\alpha/\beta=10$), and in terms of sarcoma control ($\alpha/\beta=3$), similar for 30 Gy in 5 fractions but lower for 25 Gy in 5 fractions (Table 2). As RPS is located near sensitive organs, unlike truncal and soft tissue sarcomas, we would recommend applying more caution. Hence, we propose future trials to use 30 Gy in 5 fractions as a starting point for investigations.

Many questions remained unanswered for the radiotherapy management of RPS, other than dose-fractionation. We are not sure if radiotherapy to the margins only is sufficient, and it is also difficult to predict where the at-risk margins are pre-operatively based on imaging. We await longer-term results from STRASS and STREXIT. STRASS 2 will be informative on the role of chemotherapy in high-risk retroperitoneal sarcomas, but the paradigm of low-risk retroperitoneal sarcomas remains status quo.

Our study's strengths are that target delineation was performed with both the radiation oncologist and the primary surgeon to ensure that the areas at high risk of close or involved surgical margins were irradiated. This is also the first publication, as far as we are aware, to report on the feasibility and safety of RPS using SCRT. The surgeries were performed in a single high-volume tertiary center. The weaknesses of our study are small numbers and short follow-up. It is documented in existing literature that the risk of local recurrence does not plateau even after 15–20 years [21]. The definition of at-risk margin is also dependent on surgeons' opinions.

This feasibility study showed that hypofractionated neoadjuvant radiotherapy to margins-at-risk is safe. We have demonstrated early results to provide insights on safety, and potential impact on surgical outcomes and early tumor control. If proven safe and efficacious in the long run with larger prospective studies, SCRT may be a valuable addition to the treatment armamentarium for this challenging disease.

Statement of Ethics

The study protocol was approved by the institutional review board (SingHealth reference 2020/2905). Patients gave informed consent for this procedure.

Conflict of Interest

No potential conflict of interest relevant to this article was reported.

https://doi.org/10.3857/roj.2024.00297

Acknowledgments

The authors would like to thank our research coordinators, administrators, and various colleagues for assisting in this study. We would also like to thank our patients for their participation.

Funding

This study was funded by SingHealth Onco-ACP Proton Therapy Research Funds and the NCCS Cancer Fund (Research). C-AJO is supported by the National Medical Research Council Clinician Scientist-Individual Research Grant (MOH-CIRG21jun-0005) and Clinician Scientist Award (INV category) (MOH-CSAINV22jul-0005). All funding sources had no role in the study design, data interpretation or writing of the manuscript.

Author Contributions

Conceptualization, CAJO, RXW, VSWY; Data curation, RXW; Formal analysis, RXW, CAJO, WSL; Funding acquisition, RXW; Investigation, RXW; Methodology, RXW; Validation, CAJO; Visualization, CAJO; Writing – original draft, RXW; Writing – review & editing, RXW, CAJO, VSWY, WSL, WLN, CSC.

Data Availability Statement

Anonymised data is stored in an institutional repository and can be made available upon personal request to the authors.

References

1. Bonvalot S, Gronchi A, Le Pechoux C, et al. Preoperative radiotherapy plus surgery versus surgery alone for patients with primary retroperitoneal sarcoma (EORTC-62092: STRASS): a multicentre, open-label, randomised, phase 3 trial. Lancet Oncol 2020;21:1366–77.
2. Murray Brunt A, Haviland JS, Wheatley DA, et al. Hypofractionated breast radiotherapy for 1 week versus 3 weeks (FAST-Forward): 5-year efficacy and late normal tissue effects results from a multicentre, non-inferiority, randomised, phase 3 trial. Lancet 2020;395:1613–26.
3. Sebag-Montefiore D, Stephens RJ, Steele R, et al. Preoperative radiotherapy versus selective postoperative chemoradiotherapy in patients with rectal cancer (MRC CR07 and NCIC-CTG C016): a multicentre, randomised trial. Lancet 2009;373:811–20.
4. Kalbasi A, Kamrava M, Chu FI, et al. A phase II trial of 5-day neoadjuvant radiotherapy for patients with high-risk primary soft tissue sarcoma. Clin Cancer Res 2020;26:1829–36.
5. Parsai S, Lawrenz J, Kilpatrick S, et al. Early outcomes of preoperative 5-fraction radiation therapy for soft tissue sarcoma followed by immediate surgical resection. Adv Radiat Oncol 2020;5:1274–9.
6. Salerno KE, Alektiar KM, Baldini EH, et al. Radiation therapy for treatment of soft tissue sarcoma in adults: executive summary of an ASTRO clinical practice guideline. Pract Radiat Oncol 2021;11:339–51.
7. Benedict SH, Yenice KM, Followill D, et al. Stereotactic body radiation therapy: the report of AAPM Task Group 101. Med Phys 2010;37:4078–101.
8. Diez P, Hanna GG, Aitken KL, et al. UK 2022 Consensus on normal tissue dose-volume constraints for oligometastatic, primary lung and hepatocellular carcinoma stereotactic ablative radiotherapy. Clin Oncol (R Coll Radiol) 2022;34:288–300.
9. Bonvalot S, Rivoire M, Castaing M, et al. Primary retroperitoneal sarcomas: a multivariate analysis of surgical factors associated with local control. J Clin Oncol 2009;27:31–7.
10. Gronchi A, Miceli R, Allard MA, et al. Personalizing the approach to retroperitoneal soft tissue sarcoma: histology-specific patterns of failure and postrelapse outcome after primary extended resection. Ann Surg Oncol 2015;22:1447–54.
11. Callegaro D, Raut CP, Ajayi T, et al. Preoperative radiotherapy in patients with primary retroperitoneal sarcoma: EORTC-62092 trial (STRASS) versus off-trial (STREXIT) results. Ann Surg 2023;278:127–34.
12. Istl AC, Gronchi A. Neoadjuvant therapy for primary resectable retroperitoneal sarcomas-looking forward. Cancers (Basel) 2022;14:1831.
13. Tzeng CW, Fiveash JB, Popple RA, et al. Preoperative radiation therapy with selective dose escalation to the margin at risk for retroperitoneal sarcoma. Cancer 2006;107:371–9.
14. Liveringhouse CL, Palm RF, Bryant JM, et al. Neoadjuvant simultaneous integrated boost radiation therapy improves clinical outcomes for retroperitoneal sarcoma. Int J Radiat Oncol Biol Phys 2023;117:123–38.
15. Gogineni E, Chen H, Istl AC, Johnston FM, Narang A, Deville C Jr. Comparative in silico analysis of ultra-hypofractionated intensity-modulated photon radiotherapy (IMRT) versus intensity-modulated proton therapy (IMPT) in the pre-operative treatment of retroperitoneal sarcoma. Cancers (Basel) 2023;15:3482.
16. Wo JY, Mamon HJ, Ferrone CR, et al. Phase I study of neoadjuvant accelerated short course radiation therapy with photons and capecitabine for resectable pancreatic cancer. Radiother Oncol 2014;110:160–4.
17. Hong TS, Ryan DP, Blaszkowsky LS, et al. Phase I study of preop-

erative short-course chemoradiation with proton beam therapy and capecitabine for resectable pancreatic ductal adenocarcinoma of the head. Int J Radiat Oncol Biol Phys 2011;79:151–7.
18. Burkon P, Trna J, Slavik M, et al. Stereotactic body radiotherapy (SBRT) of pancreatic cancer: a critical review and practical consideration. Biomedicines 2022;10:2480.
19. Kosela-Paterczyk H, Szacht M, Morysinski T, et al. Preoperative hypofractionated radiotherapy in the treatment of localized soft tissue sarcomas. Eur J Surg Oncol 2014;40:1641–7.
20. Bedi M, Singh R, Charlson JA, et al. Is 5 the new 25? Long-term oncologic outcomes from a phase II, prospective, 5-fraction preoperative radiation therapy trial in patients with localized soft tissue sarcoma. Adv Radiat Oncol 2022;7:100850.
21. Danieli M, Swallow CJ, Gronchi A. How to treat liposarcomas located in retroperitoneum. Eur J Surg Oncol 2023;49:1068–80.

 https://doi.org/10.3857/roj.2024.00297

ROJ Radiation Oncology Journal

Original Article

pISSN 2234-1900 · eISSN 2234-3156
Radiat Oncol J 2025;43(1):13-21
https://doi.org/10.3857/roj.2024.00059

Reducing clinical target volume margins for multifocal glioblastoma: a multi-institutional analysis of patterns of recurrence and treatment response

Francesco Marampon[1,*], Giovanni Luca Gravina[2,*], Elisa Cinelli[3], Lucy Zaccaro[1], Miriam Tomaciello[1], Nunzia Di Meglio[4], Francesco Gentili[4], Alfonso Cerase[5], Armando Perrella[3], Mariya Yavorska[3], Sami Aburas[3], Luciano Mutti[2,6], Maria Antonietta Mazzei[3,4], Giuseppe Minniti[1,7,*], Paolo Tini[3,4,*]

[1]*Department of Radiological, Oncological and Pathological Sciences, University of Rome Sapienza, Rome, Italy*
[2]*Department of Biotechnological and Applied Clinical Sciences, University of L'Aquila, L'Aquila, Italy*
[3]*Department of Medicine, Surgery and Neurosciences, University of Siena, Siena, Italy*
[4]*Diagnostic Imaging, Azienda Ospedaliera Universitaria Senese, Siena, Italy*
[5]*Unit of Neuroradiology, Azienda Ospedaliera Universitaria Senese, Siena, Italy*
[6]*Sbarro Institute for Cancer Research and Molecular Medicine, Center for Biotechnology, College of Science and Technology, Temple University, Philadelphia, PA, USA*
[7]*Istituti di Ricovero e Cura a Carattere ScientificoNeuromed, Pozzilli, Italy*

Received: January 19, 2024
Revised: July 2, 2024
Accepted: July 22, 2024

Correspondence:
Paolo Tini
Unit of Radiology, Department of Medicine, Surgery and Neurosciences, University of Siena, Banchi di Sotto, 55, 53100 Siena SI, Italy.
Tel: +0039 0763 711229
E-mail: paolo.tini@unisi.it
ORCID:
https://orcid.org/0000-0003-4826-4809

*These authors contributed equally to this work.

Purpose: No guidelines exist to delineate radiation therapy (RT) targets for the treatment of multiple glioblastoma (mGBM). This study analyzes margins around the gross tumor volume (GTV) to create a clinical target volume (CTV), comparing response parameters and modalities of recurrence.

Material and Methods: One-hundred and three mGBM patients with a CTV margin of 2 cm (GTV + 2.0 cm) or 1 cm (GTV + 1.0 cm) were retrospectively analyzed. All patients received a total dose of 59.4–60 Gy in 1.8–2.0 Gy daily fractions, delivered from 4 to 8 weeks after surgery, concomitantly with temozolomide (75 mg/m^2). Overall survival (OS) and progression-free survival (PFS) were calculated from the date of surgery until diagnosis of disease progression performed by magnetic resonance imaging and classified as marginal, in-field, or distant, comparing site of progression with dose distribution in RT plan.

Results: OS in mGBM CTV1 group was 11.2 months (95% confidence interval [CI], 10.3–12.1), and 9.2 months in mGBM CTV2 group (95% CI, 9.0–11.3). PFS in mGBM CTV1 group occurred within 8.3 months (95% CI, 7.3–9.3), and 7.3 months in mGBM CTV2 group (95% CI, 6.4–8.1). No difference was observed between the two groups in terms of OS and PFS time distribution. Adjusted to a multivariate Cox risk model, epidermal growth factor receptor amplification resulted a negative prognostic factor for both OS and PFS.

Conclusion: In mGBM, the use of a 1 cm CTV expansion seems feasible as it does not significantly affect oncological outcomes and progression outcome.

Keywords: Multifocal glioblastoma, Radiotherapy delineation, Clinical target volume, Recurrence patterns

© 2025 The Korean Society for Radiation Oncology
This is an Open Access article distributed under the terms of the Creative Commons Attribution Non-Commercial License (http://creativecommons.org/licenses/by-nc/4.0/) which permits unrestricted non-commercial use, distribution, and reproduction in any medium, provided the original work is properly cited.

Introduction

Glioblastoma (GBM) is the most common malignant primary brain tumor with a median overall survival (OS) of 3 months in untreated patients and approximately of 14 months in patients treated with a surgery-based multimodality approach [1-4].

GBM usually presents on imaging as a single peripherally enhancing lesion even though multiple enhancing lesions may occur, resulting in a poorer prognosis. Multiple GBMs (mGBMs) are distinguished as multifocal or multicentric depending on whether a macroscopic and/or microscopic connection between the uptake lesions can be demonstrated. Notably, there is no significant difference in the management of unifocal or multiple GBM [5-12], despite what has recently been suggested that personalized therapies should be used in these patients [13].

External beam radiotherapy (RT) plays a crucial role in the treatment of GBM, resulting an integral part of the multimodal primary therapy of GBM. Thus, after the maximal safe debulking of the tumor, standard therapy for GBM patients up to age 70 with good performance status is a total dose of 60 Gy in 30–33 fractions, 180–200 cGy per day, with the addition of concurrent and adjuvant temozolomide chemotherapy [4]. Hypofractionated RT, 40 Gy in 15 fractions, 266 cGy per day, can be used for patients older than 70 years or with poor performance status [14]. Notably, the spread of clonogenic GBM cells far from the gross tumor volume (GTV) has been shown to be responsible for the persistent tumor recurrence [15-23]. Thus, the current standard approach to define the clinical target volume (CTV) for RT of unifocal GBM involves the application of a margin of 1–1.5 cm around the GTV, which is reduced compared to previous indications of 2–3 cm [24,25]. This allowed us to mitigate the cognitive consequences of RT on healthy brain tissue, without compromising the survival advantages established by standard chemoradiotherapy [24,25]. However, specific indications for mGBM are lacking, and CTV margins of 2–3 cm are most frequently used [5,26].

In this study, we aimed to retrospectively analyze a cohort of mGBM patients, dividing them into two subgroups based on CTV margins of 2 cm or 1 cm. The purpose of this research is to compare the oncological outcomes and progression patterns between these two distinct groups.

Materials and Methods

1. Study design and patients

Patients with primary diagnosis of a multifocal growth pattern GBM, who underwent RT at the Department of Radiotherapy of Le Scotte Hospital, Siena (Italy) and Policlinico Umberto I, Rome (Italy) between January 2016 and December 2022 were retrospectively analyzed. Only patients with (1) histologically confirmed GBM exhibiting a multifocal growth pattern at the time of initial diagnosis and (2) pre- and post-RT magnetic resonance imaging (MRI) with contrast enhanced T1 and T2 or fluid attenuated inversion recovery (FLAIR) sequences were included. The presence of a multifocal growth pattern was evaluated by an experienced neuroradiologist. This pattern was defined as the existence of at least two separate areas with enhanced contrast in the MRI T1 contrast-enhanced sequence. To be included in the study, patients had to have undergone chemoradiotherapy within 4–8 weeks after surgery (partial or complete resection) based on the Stupp protocol [4]. Additionally, MRI imaging of the tumor recurrence at the time of analysis was required. Patients were excluded from the study if their Karnofsky performance scale (KPS) score was below 60, if they had undergone previous whole brain radiation therapy, or if their tumor histology did not confirm GBM. The O^6-methylguanine-DNA-methyltransferase (MGMT) promoter methylation status and epidermal growth factor receptor (EGFR) amplification status, available for all patients selected for this analysis, were assessed by using a methylation-specific polymerase chain reaction (PCR). Briefly, genomic DNA was extracted from paraffin-embedded tumor sections and treated with sodium bisulfite using the EZ DNA Methylation-Gold kit (HISS Diagnostics GmbH, Freiburg, Germany). Primer sequences were used to detect methylated and unmethylated MGMT promoter sequences. PCR products were separated on 2% agarose gel. A glioma cell line with a completely methylated MGMT promoter, and peripheral blood mononucleated cells, served as positive and negative control samples, respectively [27,28]. A methylation percentage of 5% was used as a cut-off value: samples with methylation $<5\%$ and $>5\%$ were classified as unmethylated (unmetMGMT) and methylated (methMGMT), respectively. This study was approved by the Institutional Review Board of "Le Scotte" Hospital of Siena (No. 2023-01-001). All patients signed informed consent to participate in the study.

2. Radiotherapy protocol

All patients were provided with an individual thermoplastic mask to ensure that patient positioning during planning computed tomography (CT) and subsequent RT sessions were reproducible. For treatment planning, a CT was conducted using sections that were 2.5/3 mm thick. CT images were then co-registered with gadolinium contrast medium enhanced T1 sequences obtained from a diagnostic MRI. To delineate treatment volumes, MRI T1 contrast-enhanced sequence scans were used, along with FLAIR sequences to identify grossly visible lesions such as the GTV. The CTV consisted of the GTV along with a 1 cm margin (CTV1) or a 2 cm margin (CTV2)

https://doi.org/10.3857/roj.2024.00059

to account for microscopic tumor spread and perifocal edema that was visible on the T2 or FLAIR sequence. T2 FLAIR abnormality beyond the delineated CTV1 and CTV2 was not intentionally included in the CTV [4]. The primary determinant influencing CTV margin selection was the amount of macroscopic disease lesions, as typically a greater number of lesions requires the use of a narrower margin to mitigate irradiation of healthy brain tissue. However, the choice to use a more or less wide CTV was always at the discretion of the radiation oncologist.

The margins surrounding the CTV were minimized to 1–3 mm around natural barriers impeding tumor growth (skull, ventricles, sickle). This reduction was implemented to ensure the preservation of the optic nerve and chiasm. The CTV was subsequently expanded by 3–5 mm to generate the planning target volume (PTV) in adherence to setup protocols. The prescribed dose was normalized to the 100% isocenter, ensuring that the 95% isodose area adequately covered the PTV (ICRU Report 50 [4]). The maximum allowable doses for the organs at risk were specified as follows: brainstem (D < 54 Gy), optic nerves (D < 54 Gy), chiasm (D < 55 Gy), eyes (Macula < 45 Gy), cochlea (D < 45 Gy), and lens (D < 6 Gy) [4]. Radiation treatment plans were generated using three-dimensional conformal RT (3DCRT), intensity-modulated radiation therapy (IMRT) or volumetric modulated arc therapy (VMAT). RT consisted of fractionated irradiation at a dose of 59.4–60 Gy divided into fractions of 1.8-2.0 Gy each (median total dose 60 Gy; median fractional dose 2 Gy; median number of fraction 30), plus concomitant 75 mg/m^2 of temozolomide [4]. Simultaneous integrated boost or field reduction was not used in any patient. Adjuvant temozolomide was began 4 weeks after the completion of RT and was continued for 5 consecutive days every 28 days for a maximum of 12 cycles. In the first cycle of adjuvant chemotherapy, temozolomide was administered at a dosage of 150 mg/m^2, which was then escalated to 200 mg/m^2 starting from the second cycle

3. Response evaluation and pattern of relapse

The MRI was conducted approximately 30 days after completion of RT, and then repeated every 12 weeks or as necessary depending on the individual's neurological status. The radiological response was assessed using the Response Assessment in Neuro-Oncology (RANO) criteria [25].

Tumor progression was defined if a growth of more than 25% in tumor size was observed or the appearance of a new lesion on the imaging scans. Two separate MRI evaluations, with at least a 2-month interval between them, were required to confirm radiological tumor progression. Tumor progression was recorded at the time of the first MRI showing progression. The imaging data set for the study of tumor progression consisted of post-contrast T1-weighted MRI and FLAIR MRI imaging. All MRI datasets were recorded alongside planning CT and compared with the pretreatment MRI. Progression was categorized as "in-field" if more than 80% of the intersection area was covered by the 95% isodose line, "marginal" if 20%–80% of the intersection region fell within the 95% isodose line, or "distant" if less than 20% of the volume was within the 95% isodose line. The mean dose received by 50% of the brain volume was compared between the plans [29].

4. Outcome study measures

The progression-free survival (PFS) and OS were used as key study outcome measures. PFS was defined as the time from initial surgery to the occurrence of the first radiological progression, as determined by MRI according to the RANO response assessment criteria [30,31]. OS was defined as the time elapsed between the date of the initial surgery and either the patient's death from any cause or the last known date when the patient was confirmed to be alive.

5. Statistical analysis

The investigated variables were analyzed using descriptive statistics. Continuous variables were normally distributed according with the Shapiro-Wilk test and were summarized as means and 95% confidence interval (CI) and compared using Student t-test. Nominal variables were summarized as absolute and relative frequencies and compared using the Pearson chi-square test, as appropriate. PFS and OS were estimated using the log-rank test (Kaplan-Meier method). Multivariate survival analysis was performed using the Cox regression model. A significance level of $p < 0.05$ was considered statistically significant. Data collection and analysis were conducted using IBM SPSS Statistics (version 21; IBM Corp., Armonk, NY, USA).

Results

This analysis included a total of 103 patients with mGBM, after excluding those who had previous radiation treatment or histotypes other than GBM or had not histologically proven GBM. The mean age of the entire population was 63.1 years (95% CI, 60.5–65.5). The mean age for the mGBM CTV1 group was 62.1 years (95% CI, 60.3–65.3), while for the mGBM CTV2 group it was 63.4 years (95% CI, 56.4–63.5), with no significant difference between the two groups ($p = 0.760$). The mean follow-up for the entire population was 9.9 months (95% CI, 9.2–10.6). Regarding the initial surgery, gross resection was performed in four patients (3.9%), subtotal in 54 patients (52.4%), and stereotactic biopsy in 45 patients (43.7%). A summary of patient characteristics can be found in Table 1, and a representative contouring example of the two CTVs is

Table 1. Summary of patient characteristics

Variable	mGBM CTV1 group (n = 54)	mGBM CTV2 group (n = 49)	p-value
Age (yr)	62.8 (60.3–65.3)	63.3 (60.7–66.1)	0.760
Karnofsky performance status	78.5 (75.8–81.2)	82.6 (79.8–85.5)	0.038
Extent of surgery			0.600
Gross total	4 (7.4)	0 (0)	
Subtotal	26 (48.2)	28 (57.1)	
Biopsy	24 (44.4)	21 (42.9)	
Number of lesions	2.8 (2.6–3.1)	3.3 (3.0–3.5)	0.013
MGMT status			0.090
Methylated	18 (33.3)	22 (44.9)	
Unmethylated	36 (66.7)	27 (55.1)	
EGFR amplification			0.004
Yes	33 (61.1)	43 (87.7)	
No	21 (38.9)	6 (12.3)	
Concomitant TMZ			1.000
Yes	54 (100)	49 (100)	
No	0 (0)	0 (0)	
Adjuvant TMZ			0.570
Yes	37 (68.5)	37 (75.5)	
No	17 (31.5)	12 (24.5)	
CTV	231.9 (209.6–254.1)	271.8 (248.5–295.2)	0.016

Values are presented as mean (95% confidence interval) or number (%).
mGBM, multifocal glioblastoma; CTV, clinical target volume; MGMT, O^6-methylguanine-DNA-methyltransferase; EGFR, epidermal growth factor receptor; TMZ, temozolomide.

presented in Fig. 1. Significant differences between the two study groups were observed in terms of EGFR amplification, number of tumor lesions, KPS and CTVs. Specifically, group mGBM CTV1 demonstrated a CTV of 231.9 cm^3 (range, 209.6 to 254.1 cm3) compared to 271.8 cm^3 (range, 248.5 to 295.2 cm^3) in the other group ($p = 0.016$). This finding indicates a potential reduction in irradiation volume within the group with reduced CTV margin. The dose-volume distribution in normal brain in patients undergoing localized external beam RT was assessed. The mean dose received by 50% of the brain volume was 18.5 Gy (95% CI, 17.7–19.4) in the CTV1 group and 22.4 Gy (95% CI, 21.7–23.1) and in CTV2 group, respectively. A significant reduction in the mean dose received by 50% of the brain volume was observed between the two groups ($p < 0.001$).

The pattern of progression was comparable with no statistically significant difference ($\chi^2 = 1.078$; degrees of freedom = 2; $p = 0.580$) between the two groups. Both in the mGBM CTV1 group (54 patients), and in CTV2 group (49 patients) all patients experienced progression. In the mGBM CTV1 group 77.8% (42 out of 54) experienced in-field, 9.3% (5 out of 54) marginal, and 13.0% (7 out of 54) distant progression. In the mGBM CTV2 group, 73.5% (36 out of 49) experienced in-field, 12.2% (6 out of 49) marginal, and 14.3% (7 out of 49) distant progression (Table 1).

An explorative analysis was performed to assess the potential relationship between the extent of surgical resection and the frequency of in-field, marginal, and distant progression within the two study groups.

In the mGBM CTV1 group, 44.4% patients (24 out of 54) exclusively underwent biopsy, then experiencing 62.5% patients (15 out of 24) in-field, progression, 16.6% patients (4 out of 24) marginal progression, and 20.8% patients (5 out of 24) distant progression. Subtotal resections were performed on 48.1% patients (26 out of 54) who then experienced 92.3% of cases (24 out of 26) in-field progression, 3.8% of cases (1 out of 26) marginal progression, and 3.8% of cases (1 out of 26) distant progressions. Gross total resection was performed on 7.4% patients (4 out of 54), 75.0% of them (3 out of 4) then experiencing in-field progressions and 25.0% (1 out of 4) distant progression. In the mGBM CTV2 group, 42.8% of cases (21 out of 49) underwent biopsy, then experiencing 71.4% (15 out of 21) in-field progression, 14.3% (3 out of 21) marginal progression, and 14.3% (3 out of 21) distant progression. Subtotal resections were performed on 57.1% of patients (28 out of 49), then all (28 out of 28) experiencing in-field progressions. No gross total resections were performed in this group. Pearson chi-square test was utilized to analyze these data. No significant difference was found between the extent of surgical resection and the occurrence of in-field, marginal, and distant progression, even when patients were classified based on CTV margins (Table 2).

The median OS in mGBM CTV1 group was 12.0 months (95% CI, 10.0–13.0), wherea mGBM CTV2 group had a mean OS of 11.8

https://doi.org/10.3857/roj.2024.00059

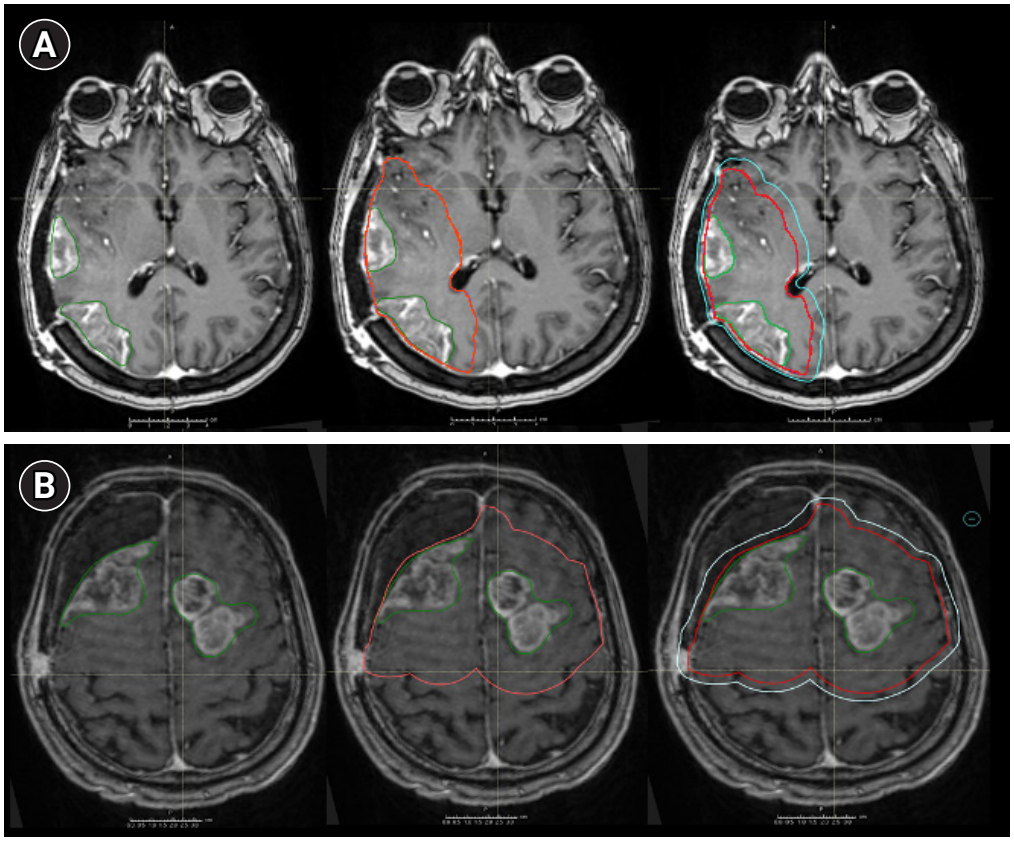

Fig. 1. Representative contouring of a patient affected by multifocal glioblastoma treated with 1 cm margin of CTV (A) and with 2 cm margin of CTV (B). mGBM, multifocal glioblastoma; Gross tumor volume (green line); CTV, clinical target volume (red line); Planning target volume (cyan line).

Table 2. Pattern of relapse according surgery extent (Pearson chi-square test)

Extent of surgery	mGBM CTV1 group (n = 54)			p-value	mGBM CTV2 group (n = 49)			p-value
	Gross total (n = 4)	Subtotal (n = 26)	Biopsy (n = 24)		Gross total (n = 0)	Subtotal (n = 28)	Biopsy (n = 21)	
In-field progression	3	24	15		0	28	15	
Marginal progression	0	1	4		0	0	3	
Distant progression	1	1	5	0.070	0	0	3	0.100

mGBM, multifocal glioblastoma; CTV, clinical target volume.

months (95% CI, 10.0–13.0) (Fig. 2). In terms of PFS, mGBM CTV1 group had a mean PFS of 7.2 months (95% CI, 6.0–8.0), while mGBM CTV2 group had a mean PFS of 6.7 months (95% CI, 6.0–8.0) (Fig. 3). No statistically significant difference was observed between the two groups for OS (Fig. 2) and PFS (Fig. 3) time distribution. To further explore these results, we conducted a multivariate Cox risk model analysis adjusting for known variables such as age, MGMT methylation, EGFR amplification, number of tumor lesions, KPS score, and type of surgery. Our analysis revealed that both OS and PFS (Table 3) were associated with MGMT status and KPS. For OS, we had a hazard ratio (HR) of 1.71 (95% CI, 1.06–2.73; p = 0.023), and the unmetMGMT status had a HR of 1.52 (95% CI, 1.03–2.92; p = 0.036) indicating an increased risk of mortality. Similarly, in terms of PFS, the KPS < 70 and the unmetMGMT status had an HR of 1.88 (95% CI, 1.21–2.94; p = 0.006) and 1.95 (95% CI, 1.11–3.01; p = 0.016) further supporting its prognostic significance (Table 3).

Discussion and Conclusions

Despite the generally poorer prognosis associated with mGBM when compared to unifocal GBM [5-10], there is a lack of specific guidelines regarding the management approaches for this clinical entity. Specifically, the controversy regarding the role of surgical

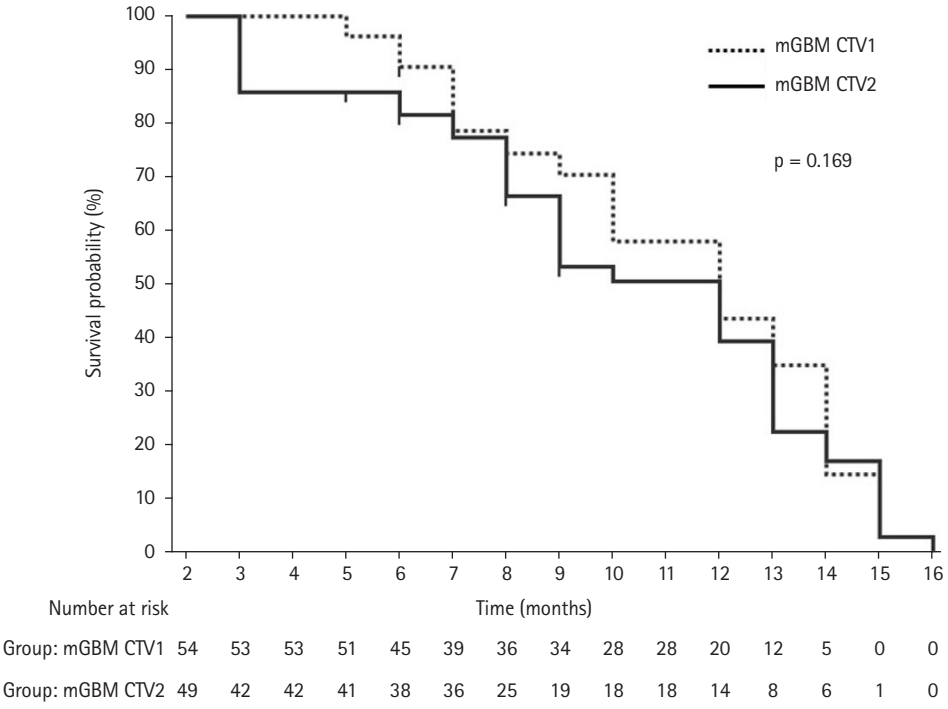

Fig. 2. Overall survival curve. mGBM, multifocal glioblastoma; CTV, clinical target volume.

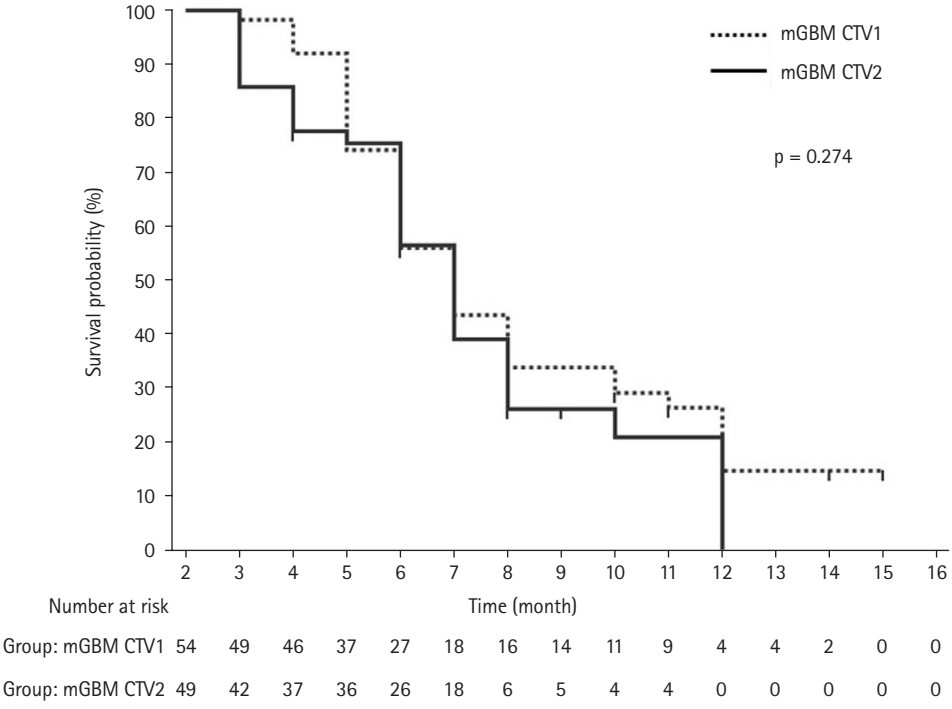

Fig. 3. Progression-free survival curve. mGBM, multifocal glioblastoma; CTV, clinical target volume.

treatment in mGBM [5-10] is in contrast with the confirmed efficacy of concomitant RT and temozolomide as a treatment option [4-10]. Nevertheless, there is a lack of clear guidelines regarding the precise target delineation for RT in mGBM. Indeed, whether the CTV for unifocal GBM has been recently defined as a 1–1.5 cm margin around the GTV [24,25], a margin of 2–3 cm is still applied around the GTV of mGBM [5,26], despite the most common pattern of treatment is central "in-field" relapse [32], similarly to unifocal

 https://doi.org/10.3857/roj.2024.00059

Table 3. Univariate (OS) and multivariate Cox proportional-hazards regression analysis (OS, PFS)

	Univariate		Multivariate			
	OS		OS		PFS	
	p-value	OR (95% CI)	p-value	OR (95% CI)	p-value	OR (95% CI)
KPS	0.038	0.53 (0.29–0.96)	0.022	0.51 (0.28–0.90)	0.005	0.44 (0.24–0.78)
MGMT status	0.051	0.75 (0.56–0.99)	0.035	0.74 (0.56–0.97)	0.016	0.71 (0.55–0.93)
CTV	0.662	1.00 (0.99–1.00)	0.692	1.04 (0.97–1.06)	0.440	0.99 (0.99–1.00)
EGFR amplification	0.610	1.12 (0.70–1.79)	0.778	1.09 (0.72–1.64)	0.078	0.78 (0.53–1.03)
Number of lesions	0.392	1.01 (0.98–1.03)	0.425	1.10 (0.97–1.05)	0.221	1.02 (0.98–1.08)
GTV	0.952	0.99 (0.92–1.07)	0.978	1.00 (0.96–1.08)	0.876	0.96 (0.92–1.04)

OS, overall survival; PFS, progression-free survival; KPS, Karnofsky performance scale; MGMT, O^6-methylguanine-DNA-methyltransferase; CTV, clinical target volume; EGFR, epidermal growth factor receptor; GTV, gross tumor volume; OR, odds ratio; CI, confidence interval.

GBM [33-35]. Thus, in clinical practice the factor that mainly determines the choice of the CTV margin is the quantity of macroscopic lesions since, to mitigate the irradiation of healthy brain tissue, a greater number of lesions generally requires the use of a margin closer.

Based on these findings gathered on unifocal GBM, we made the decision to explore, for the first time, the feasibility of reducing treatment volume delineation margins from 2 cm to 1 cm in mGBM. The purpose of this investigation was to evaluate the feasibility of implementing such a reduction comparing the progression patterns, PFS, and OS rates in this context.

Our study suggested that minimizing the CTV margin to 1 cm in mGBM may have no significant impact on the speed of progression patterns, as well as PFS and OS. It is noteworthy that many tumor progressions were observed within the treatment field with no difference between the two groups. This evidence confirms early studies on patterns of failure in unifocal GBM indicated that 70%–90% of recurrent lesions occurred within 2–3 cm of the primary tumor, even after whole-brain RT [33-35]. Several authors have suggested that these early studies come with several limitations that are inherent in their design. Firstly, the data in these studies was based on early-generation CT technology, which has lower image resolution compared to MRI [36]. Secondly, the assessment of recurrences required laborious manual detection between the radiation plan and subsequent imaging, and usually only one or a few slices were selected to measure two-dimensionally, rather than in three dimensions [37]. New evidence from recent studies indicates that 94.8% local recurrences occurred within 0.5–1 cm of the original T1 enhanced lesions [22,38] supporting the use of a reduced CTV margin of 1 cm in reducing the volume of irradiation. Our study also supports this evidence, as we were able to achieve a substantial reduction in the volume of CTV without affecting the PFS, the OS and the rate of progression patterns. Interestingly, no relationship was found between the extent of surgical resection and the frequency of in-field, marginal or distant progression in our study. This finding is consistent with other studies on unifocal GBM, even though it is in contrast with most previous studies that have reported a longer PFS with the gross tumor resection [39]. However, based on these results, we suggested adopting a reduced CTV margin for mGBM, regardless of the degree of resection achieved.

Our study has several limitations. One limitation is the possible presence of selection bias, which can be attributed to the retrospective nature of the study and the absence of prospective randomization in the two delineation of CTV modalities. The lack of information on the mutational status of iDH1, essential for a correct diagnostic/prognostic classification [40], but not available for all patients in our cohort, represented another limitation.

The small sample size restricted the number of variables analyses. Although we have conducted a multivariate Cox regression analysis, it is important to acknowledge that our study results may be influenced by variables beyond those considered in our analysis. The small sample size may also explain why in this study tumor resection status, a factor known to be significantly associated with PFS and OS [41], was not significantly associated with outcome. This may have generated the lack of significance in the difference in outcome based on the CTV margin.

Furthermore, the use of different radiation techniques (3DCRT, IMRT, and VMAT) may have introduced significant biases, particularly with respect to the dose distribution to the target area, which in turn could have significantly impacted on the progression pattern.

In conclusion, this retrospective study suggests that decreasing the irradiation treatment volumes in mGBM does not significantly affect oncological outcomes. However, to validate these findings, it is essential to conduct prospective multicenter studies, which should include a detailed examination of dosimetric parameters and their implications for disease control.

Statement of Ethics

This retrospective study was reviewed and approved by the Institutional Review Board of Siena University Hospital "Le Scotte" (No. 2023-01-001).

Conflict of Interest

No potential conflict of interest relevant to this article was reported.

Funding

None.

Author Contributions

Conceptualization, FM, GLG, EC, MT, NDM, FG, AC, AP, MY, SA, LM, MAM, GM, PT; Investigation and methodology, FM, GLG, EC, MT, NDM, FG, AC, AP, MY, SA, LM; Writing of the original draft, MAM, GM, PT; Formal analysis, FM, GLG, EC, MT, NDM, FG, AC, AP, MY, SA, LM; Data curation, FM, GLG, EC, MT, NDM, FG, AC, AP, MY, SA, LM.

Data Availability Statement

The data that support the findings of this study are available from the corresponding author upon reasonable request.

References

1. Omuro A, DeAngelis LM. Glioblastoma and other malignant gliomas: a clinical review. JAMA 2013;310:1842–50.
2. Ostrom QT, Cioffi G, Gittleman H, et al. CBTRUS statistical report: primary brain and other central nervous system tumors diagnosed in the United States in 2012-2016. Neuro Oncol 2019;21(Suppl 5):v1–100.
3. Grochans S, Cybulska AM, Siminska D, et al. Epidemiology of glioblastoma multiforme: literature review. Cancers (Basel) 2022;14:2412.
4. Stupp R, Mason WP, van den Bent MJ, et al. Radiotherapy plus concomitant and adjuvant temozolomide for glioblastoma. N Engl J Med 2005;352:987–96.
5. Baro V, Cerretti G, Todoverto M, et al. Newly diagnosed multifocal GBM: a monocentric experience and literature review. Curr Oncol 2022;29:3472–88.
6. Giannopoulos S, Kyritsis AP. Diagnosis and management of multifocal gliomas. Oncology 2010;79:306–12.
7. Lahmi L, Idbaih A, Rivin Del Campo E, et al. Whole brain radiotherapy with concurrent temozolomide in multifocal and/or multicentric newly diagnosed glioblastoma. J Clin Neurosci 2019;68:39–44.
8. Di L, Heath RN, Shah AH, et al. Resection versus biopsy in the treatment of multifocal glioblastoma: a weighted survival analysis. J Neurooncol 2020;148:155–64.
9. Haque W, Thong Y, Verma V, Rostomily R, Brian Butler E, Teh BS. Patterns of management and outcomes of unifocal versus multifocal glioblastoma. J Clin Neurosci 2020;74:155–9.
10. Li Y, Zhang ZX, Huang GH, et al. A systematic review of multifocal and multicentric glioblastoma. J Clin Neurosci 2021;83:71–6.
11. Lasocki A, Gaillard F, Tacey M, Drummond K, Stuckey S. Multifocal and multicentric glioblastoma: Improved characterisation with FLAIR imaging and prognostic implications. J Clin Neurosci 2016;31:92–8.
12. Sulman EP, Ismaila N, Armstrong TS, et al. Radiation therapy for glioblastoma: American Society of Clinical Oncology Clinical Practice Guideline Endorsement of the American Society for Radiation Oncology Guideline. J Clin Oncol 2017;35:361–9.
13. Roncevic A, Koruga N, Soldo Koruga A, et al. Personalized treatment of glioblastoma: current state and future perspective. Biomedicines 2023;11:1579.
14. Perry JR, Laperriere N, O'Callaghan CJ, et al. Short-course radiation plus temozolomide in elderly patients with glioblastoma. N Engl J Med 2017;376:1027–37.
15. Sanai N, Alvarez-Buylla A, Berger MS. Neural stem cells and the origin of gliomas. N Engl J Med 2005;353:811–22.
16. Seker-Polat F, Pinarbasi Degirmenci N, Solaroglu I, Bagci-Onder T. Tumor cell infiltration into the brain in glioblastoma: from mechanisms to clinical perspectives. Cancers (Basel) 2022;14:443.
17. Sherriff J, Tamangani J, Senthil L, et al. Patterns of relapse in glioblastoma multiforme following concomitant chemoradiotherapy with temozolomide. Br J Radiol 2013;86:20120414.
18. Wallner KE, Galicich JH, Krol G, Arbit E, Malkin MG. Patterns of failure following treatment for glioblastoma multiforme and anaplastic astrocytoma. Int J Radiat Oncol Biol Phys 1989;16:1405–9.
19. Hochberg FH, Pruitt A. Assumptions in the radiotherapy of glioblastoma. Neurology 1980;30:907–11.
20. Gaspar LE, Fisher BJ, Macdonald DR, et al. Supratentorial malignant glioma: patterns of recurrence and implications for external beam local treatment. Int J Radiat Oncol Biol Phys 1992;24:55–7.
21. McDonald MW, Shu HK, Curran WJ, Crocker IR. Pattern of failure after limited margin radiotherapy and temozolomide for glioblastoma. Int J Radiat Oncol Biol Phys 2011;79:130–6.

 https://doi.org/10.3857/roj.2024.00059

22. Tu Z, Xiong H, Qiu Y, Li G, Wang L, Peng S. Limited recurrence distance of glioblastoma under modern radiotherapy era. BMC Cancer 2021;21:720.
23. Minniti G, Amelio D, Amichetti M, et al. Patterns of failure and comparison of different target volume delineations in patients with glioblastoma treated with conformal radiotherapy plus concomitant and adjuvant temozolomide. Radiother Oncol 2010; 97:377–81.
24. Minniti G, Tini P, Giraffa M, et al. Feasibility of clinical target volume reduction for glioblastoma treated with standard chemoradiation based on patterns of failure analysis. Radiother Oncol 2023;181:109435.
25. Niyazi M, Andratschke N, Bendszus M, et al. ESTRO-EANO guideline on target delineation and radiotherapy details for glioblastoma. Radiother Oncol 2023;184:109663.
26. Fleischmann DF, Schon R, Corradini S, et al. Multifocal high-grade glioma radiotherapy safety and efficacy. Radiat Oncol 2021;16: 165.
27. Tini P, Belmonte G, Toscano M, et al. Combined epidermal growth factor receptor and Beclin1 autophagic protein expression analysis identifies different clinical presentations, responses to chemo- and radiotherapy, and prognosis in glioblastoma. Biomed Res Int 2015;2015:208076.
28. Tini P, Nardone V, Pastina P, et al. Patients affected by unmethylated O(6)-methylguanine-DNA methyltransferase glioblastoma undergoing radiochemotherapy may benefit from moderately dose-escalated radiotherapy. Biomed Res Int. 2017;2017: 9461402.
29. Soderstrom H, Walfridsson A, Martinsson U, et al. Neurocognition and mean radiotherapy dose to vulnerable brain structures: new organs at risk? Radiat Oncol 2023;18:132.
30. Wen PY, Macdonald DR, Reardon DA, et al. Updated response assessment criteria for high-grade gliomas: response assessment in neuro-oncology working group. J Clin Oncol 2010;28:1963–72.
31. Leao DJ, Craig PG, Godoy LF, Leite CC, Policeni B. Response assessment in neuro-oncology criteria for gliomas: practical approach using conventional and advanced techniques. AJNR Am J Neuroradiol 2020;41:10–20.
32. Syed M, Liermann J, Verma V, et al. Survival and recurrence patterns of multifocal glioblastoma after radiation therapy. Cancer Manag Re 2018;10:4229–35.
33. Guberina N, Padeberg F, Pottgen C, et al. Location of recurrences after trimodality treatment for glioblastoma with respect to the delivered radiation dose distribution and its influence on prognosis. Cancers (Basel) 2023;15:2982.
34. Rapp M, Baernreuther J, Turowski B, Steiger HJ, Sabel M, Kamp MA. Recurrence pattern analysis of primary glioblastoma. World Neurosurg 2017;103:733–40.
35. Bette S, Barz M, Huber T, et al. Retrospective analysis of radiological recurrence patterns in glioblastoma, their prognostic value and association to postoperative infarct volume. Sci Rep 2018;8: 4561.
36. Mabray MC, Barajas RF, Cha S. Modern brain tumor imaging. Brain Tumor Res Treat 2015;3:8–23.
37. Castellano A, Bailo M, Cicone F, et al. Advanced imaging techniques for radiotherapy planning of gliomas. Cancers (Basel) 2021;13:1063.
38. Tseng CL, Zeng KL, Mellon EA, et al. Evolving concepts in margin strategies and adaptive radiotherapy for glioblastoma: a new future is on the horizon. Neuro Oncol 2024;26(12 Suppl 2):S3–S16.
39. Shonka NA, Aizenberg MR. Extent of resection in glioblastoma. J Oncol Pract 2017;13:641–2.
40. Hertler C, Felsberg J, Gramatzki D, et al. Long-term survival with IDH wildtype glioblastoma: first results from the ETERNITY Brain Tumor Funders' Collaborative Consortium (EORTC 1419). Eur J Cancer 2023;189:112913.
41. Brown TJ, Brennan MC, Li M, et al. Association of the extent of resection with survival in glioblastoma: a systematic review and meta-analysis. JAMA Oncol 2016;2:1460–9.

ROJ Radiation Oncology Journal

Original Article

pISSN 2234-1900 · eISSN 2234-3156
Radiat Oncol J 2025;43(1):22-29
https://doi.org/10.3857/roj.2024.00339

Promising application of nano-WO_3/epoxy composite in intensity-modulated brachytherapy: a simulation study

Erfan Saatchian[1], Shahrokh Naseri[2], Sare Hosseini[3], Hamid Gholamhosseinian[2]

[1]*Department of Medical Physics, Mashhad University of Medical Sciences, Mashhad, Iran*
[2]*Medical Physics Research Center, Mashhad University of Medical Sciences, Mashhad, Iran*
[3]*Cancer Research Center, Mashhad University of Medical Sciences, Mashhad, Iran*

Received: May 2, 2024
Revised: July 27, 2024
Accepted: August 8, 2024

Correspondence:
Hamid Gholamhosseinian
Medical Physics Research Center, Mashhad University of Medical Sciences, Mashhad 9177899191, Iran
Tel: +98-09153066188
E-mail: gholamhosseinianh@mums.ac.ir
ORCID:
https://orcid.org/0000-0003-2246-6939

Purpose: Implementing intensity-modulated brachytherapy (IMBT) techniques with high-energy sources like ^{60}Co has always been challenging due to the clinical limitations of the applicator dimensions. This study aims to investigate using tungsten trioxide nanoparticles/epoxy composite as a shielding material to enhance the protective properties of a redesigned applicator.

Materials and Methods: The Geant4 application to tomographic emission, the Geant4-based Monte Carlo dose calculation engine (version 9.0), was used to simulate the shielding composite and the IMBT technique with a voxelated patient-based phantom. To evaluate the effectiveness of the new shielding material, IMBT plans created with the redesigned applicator were compared with those with a conventional applicator. ^{60}Co and ^{192}Ir were utilized, and in the same high-risk clinical target volumes D_{90}, the D_{2cc} for the bladder and rectum were evaluated in 18 patients with vaginal cancer.

Results: For the IMBT plans with the ^{60}Co source, the use of the redesigned applicator decreased the D_{2cc} of the bladder and rectum by 11.1% and 12.8%, respectively, while for those with the ^{192}Ir source, the reduction was 16.6% and 18.7%, respectively. Nevertheless, there was an insignificant alteration in the absorbed dose parameter (D_{90}) for the target using both sources.

Conclusion: This study demonstrates that tungsten trioxide nanoparticle/epoxy composite can be advantageous in tackling radiation shielding concerns. Enhancing the shielding properties of this composite, considering the size limitations of applicators, leads to improved protection of organs at risk, such as the bladder and rectum. This substance can be considered a promising shielding material in the construction of applicators.

Keywords: Brachytherapy, Nanoparticles, Monte carlo method, Intensity-modulated brachytherapy

Introduction

Even with improvements in external beam radiation therapy techniques like volumetric-modulated arc therapy, image-guided radiation therapy, and stereotactic body radiation therapy, brachytherapy continues to be a vital treatment choice for numerous cancer patients [1]. External radiotherapy and brachytherapy are the most effective primary treatment options for patients with invasive vaginal cancer. Brachytherapy, used in conjunction with external radiotherapy, plays a crucial role in ensuring the delivery of a therapeutic dose to the tumor [2,3]. Brachytherapy can be administered through various methods, such as intraluminal, intracavitary, multi-catheter interstitial techniques, and intensity-modulated brachytherapy (IMBT) [4]. While the interstitial approach offers improved precision in dose distribution, it is more invasive and subjective [5]. Dose modulation methods utilizing metal shields have been introduced to protect healthy tissues. Nonetheless, a standardized technique for achieving optimal outcomes remains elusive [6].

The practice of using high-Z materials as a protective barrier for

© 2025 The Korean Society for Radiation Oncology
This is an Open Access article distributed under the terms of the Creative Commons Attribution Non-Commercial License (http://creativecommons.org/licenses/by-nc/4.0/) which permits unrestricted non-commercial use, distribution, and reproduction in any medium, provided the original work is properly cited.

a particular organ at risk (OAR) has been established for quite some time. In recent years, methods involving a shielded applicator or source have been explored to adjust the radiation dose intensity during brachytherapy administration, known as IMBT [7]. To perform IMBT effectively, it is crucial for the shield to be of sufficient thickness to successfully modify the intensity of the radiation source, especially when utilizing high-energy sources such as ^{60}Co. The introduction of the ^{60}Co high dose rate (HDR) after-loading system presents an attractive option. The ^{60}Co HDR source's longer half-life of 5.3 years provides logistical and financial benefits compared to the ^{192}Ir HDR source [8,9].

A notable focus is on creating shielding materials to substitute traditional lightweight and body-safe lead. Among these materials is tungsten-based material, which boasts a high atomic number and superior shielding capabilities compared to lead [10]. Tungsten, a material free of lead, is non-toxic and possesses a higher density and atomic number than lead. Consequently, tungsten offers superior shielding characteristics compared to lead [11]. However, other types of materials need to be taken into account. The properties of nanomaterials indicate that their high surface area to volume ratio enhances the ratio of photon absorption potential [12]. Nanoparticle composites possess the potential to meet the requirements for shielding against radiation in medical and industrial environments. Several research studies and theoretical assessments have delved into the effects of nano-WO_3 composite materials on radiation protection [12,13]. However, there is a lack of literature on the application of these nanoparticles in the necessary protection in IMBT techniques. Considering their manufacturability and acceptable weight, the utilization of these nanoparticles can be a feasible option for the required protective materials inside the applicator.

This article introduces our innovative idea of using a cylinder applicator shielded with nano-WO_3/epoxy composite to deliver patient-specific intensity-modulated HDR brachytherapy. This approach aims to enhance target coverage compared to current brachytherapy techniques while reducing radiation exposure to organs at risk. The applicator used in this study is based on the redesign of the IMBT commercial cylinder applicator by Elekta Company (Elekta, Stockholm, Sweden).

Materials and Methods

Fig. 1 categorizes the various stages of conducting this study.

1. Patient data selection

The current study included 18 cases of cervical cancer with stages ranging from IB to IVA. The high-risk clinical target volumes (HR-CTV) had volumes ranging from 5.2 to 95.3 cm^3, with an average of 36.1 cm^3 and a standard deviation of 16.3 cm^3. Patients with a history of surgery in the vaginal and cervical region were excluded from the study. A skilled brachytherapy oncologist contoured OARs

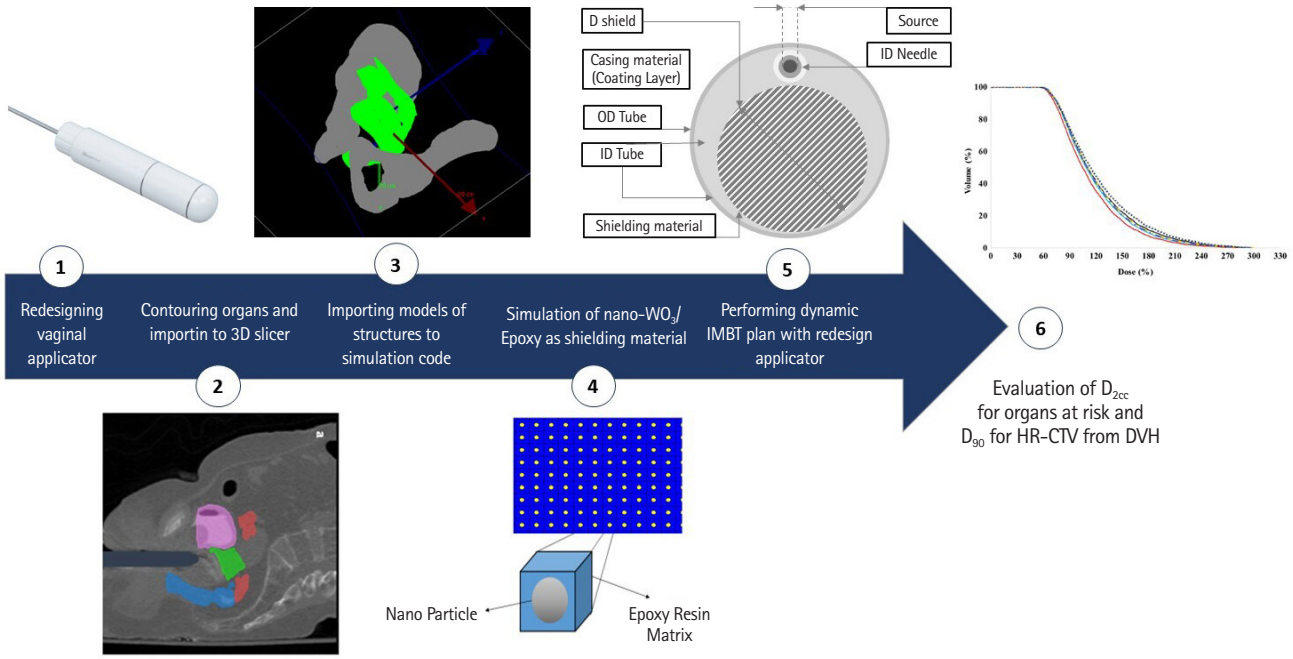

Fig. 1. The study workflow is summarized in various stages. D, diameter; OD, outer diameter; ID, inner diameter; 3D, three-dimensional; IMBT, intensity-modulated brachytherapy; D_{2cc}, minimum dose received by the highest 2 cc of organ; D_{90}, minimum dose received by 90% of target volume; HR-CTV, high-risk clinical target volume; DVH, dose volume histogram.

such as the bladder, sigmoid, rectum, and HR-CTV for all instances using high-resolution computed tomography (CT) scans with a 1 mm slice thickness.

2. IMBT applicator and source design

The vaginal cylinder applicator (Elekta Brachytherapy, Veenendaal, The Netherlands) was redesigned to maximize the IMBT ability in utilizing more amount of shielding in a cylinder tube. To maximize the shield's capacity within the applicator, the internal structure has been redesigned to accommodate a shielding rod with a diameter of 22.1 mm inside a 24.5 mm internal diameter. The overall internal structure consists of a shielding rod and a source channel (with an internal diameter of 1.0 mm and outer diameter 1.3 mm) connected to a rotational system enabling the rotation of structures relative to each other When the outer shell is fixed. The reconstruction of the internal structure of the applicator, such as the repositioning of the source channel and the placement of the shielding cylinder on a rotatable structure, can enable the implementation of dynamic techniques. In the redesigned applicator, some structural features, such as the outer diameter of 25.0 mm and a length of 6.3 cm, have not been modified to maintain consistent clinical usability.

This research employed a simulated form of the ^{60}Co encapsulated source made by Elekta Company. The source was modeled to mimic the Flexisource utilized in the Elekta Flexitron afterloader, a brachytherapy device manufactured by Elekta Brachytherapy [14]. This study used Monte Carlo calculations following the American Association of Physicists in Medicine Task Group No. 229 (TG-229) guidelines to establish the TG-43 parameters of the ^{192}Ir source from Nucletron, Elekta, for high-energy brachytherapy sources. The source's properties, including its geometry, material composition, and densities, were sourced from published materials. Notably, the source is 0.9 mm in diameter and 4.5 mm in length (Fig. 2) [15]. The calculation of total treatment durations utilized a standard activity of 10 Ci for ^{192}Ir and 2 Ci for ^{60}Co.

3. Shielding material simulation

A simulation code based on Geant4 application to tomographic emission (GATE) was employed to model a nano-WO_3/epoxy composite. An epoxy resin with a chemical formula of $C_{21}H_{25}ClO_5$ and a density of 1.18 g/cm^3 was employed as the matrix. The simulation involved tungsten trioxide, which has a density of 7.16 g/cm^3, as

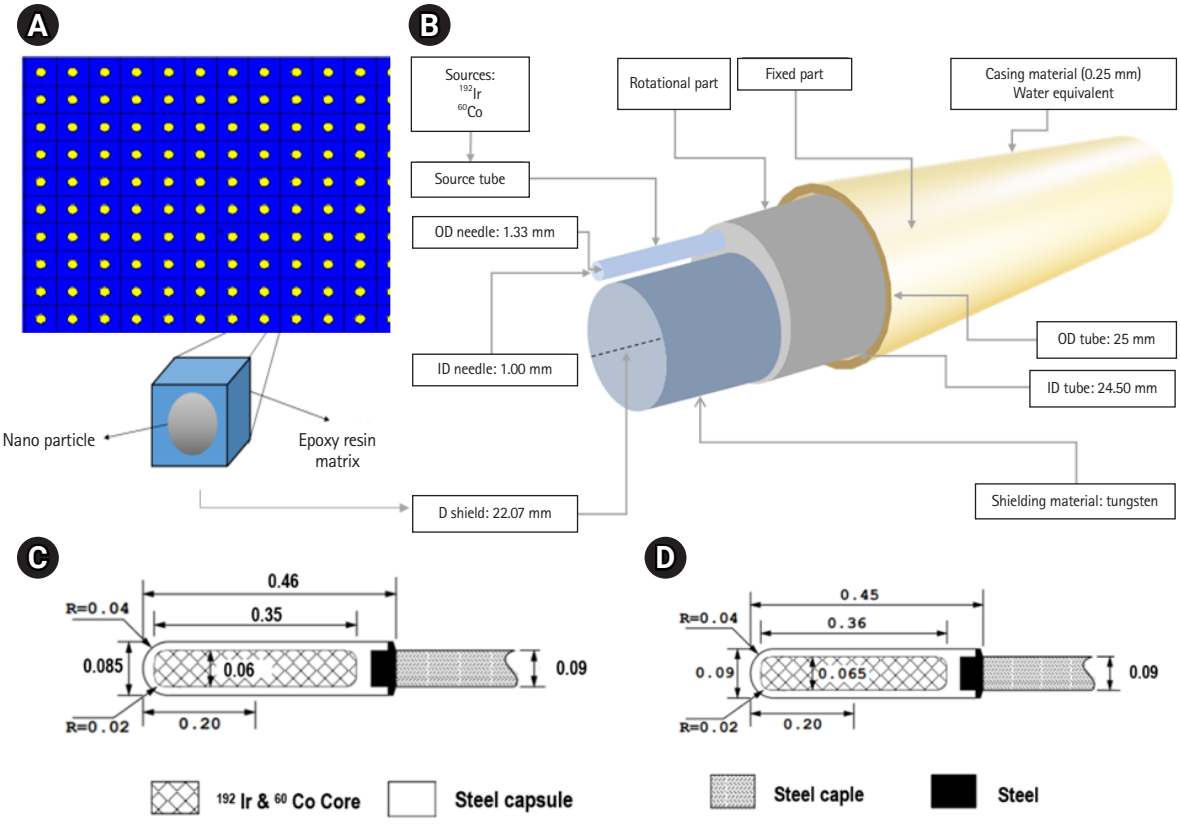

Fig. 2. Graphical representation of (A) spatial arrangement WO_3 nanoparticles (represented as spherical particles) within epoxy resin polymer matrix, (B) modified design of intravaginal applicator with new shielding material, (C, D) dimensions of ^{60}Co and ^{192}Ir sources, respectively (the unit is in cm). OD, outer diameter; ID, inner diameter; D, diameter.

https://doi.org/10.3857/roj.2024.00339

the polymer filler in 30 nm dimensions and at a weight percentage of 80 weight%. Previous research indicated that using WO_3 filler of this size and weight percentage exhibited promising results in attenuating/absorbing high-energy gamma photons [13,16]. The simulation code was utilized to evenly distribute WO_3 particles within the resin polymer matrix as spherical particles measuring 30 nm in diameter. To provide clearer visualization, screenshots of the simulated composite with both micro and nanofiller sizes are presented in Fig. 2.

4. Patient modeling

The anonymized patient data, comprising magnetic resonance images in Digital Imaging and Communications in Medicine (DICOM) format, contours from DICOM radiotherapy structure set files, and dwell positions extracted from DICOM radiotherapy plan files, were imported into the three-dimensional (3D) Slicer software [17]. The CT image had a slice thickness of 1 mm. Each case involved converting the images into voxelized phantoms with a voxel size of 1 × 1 × 1 mm^3. Each organ was individually modeled, maintaining its spatial relationships with other organs, and then exported in Stereolithography format. This format facilitated importing the models into the simulation code. Subsequently, each structure was associated with the appropriate material model from the code library within the simulation code. A female pelvic phantom with properties equivalent to water, sized 30 × 30 × 30 cm^3, was simulated within a larger air box world measuring 80 × 80 × 80 cm^3 using the GATE simulation code based on Geant4. The OARs and HR-CTV models were positioned at the center of the phantom. To evaluate the conventional brachytherapy (CBT) and IMBT treatment planning methods for 18 patients with identical source path geometry, simulations were conducted using the GATE simulation code. The simulations aimed to ensure that the prescribed dose to the HR-CTV met acceptable standards and complied with Groupe Europeen de Curietherapiee-European Society for Radiotherapy and Oncology (GEC-ESTRO) constraints [18]. This approach enabled a comparison of the administered dose to the organs at risk.

5. IMBT plan simulation

The GATE, Geant4-based simulation code was utilized to optimize and streamline the plans. To minimize any potential bias from the planner, all plans were optimized using the same parameters without any manual adjustments thereafter. The optimized dose distributions were fine-tuned to ensure the minimum dose received by 90% of target volume (D_{90}) value for the HR-CTV aligned with the prescribed dose of 5.5 Gy per fraction. This normalization was performed to facilitate a fair comparison across various combinations of modality and radionuclide. Key dosimetric comparisons metrics, such as minimum dose received by the highest 2 cc of organ (D_{2cc}) for organs at risk and D_{90} for HR-CTV, were derived from the results following the guidelines outlined by the GEC-ESTRO. The statistical significance of dose-volume histogram metrics variations was evaluated using a paired sample t-test, with a significance level set at $p < 0.05$. In planning conventional and IMBT high-dose-rate plans, the active core materials chosen were ^{192}Ir and ^{60}Co. In the CBT method, the entire procedure was repeated by replacing the nanoparticle shielding material with a water-equivalent Plexiglas applicator, which is a conventional acting applicator. A standard activity level of 10 Ci for ^{192}Ir and 2 Ci for ^{60}Co was considered when calculating the total treatment durations. To ensure uncertainties remained within the range of 1% to 2%, a total of 108 decay events were simulated for each radionuclide at every dwell position, with a voxel resolution of 2 mm^3 employed in the GATE simulation. Actors are tools that allow to interact with the simulation. They can collect information during the simulation, such as energy deposit, number of particles created in a given volume, etc. They can also modify the behavior of the simulation. In the GATE simulation code, DoseActors for scoring were defined and linked to all specified organs. The output data format was set as .mhd and .hdr, which were then processed using 3D Slicer and Amide software. In a Monte Carlo simulation, a physics list library refers to a collection of predefined physics processes and models that can be used to simulate the interactions of particles in a simulation. These processes can include electromagnetic interactions, particle decay, hadronic interactions, and more. By choosing and configuring a physics list from the library, users can customize the behavior of particles in the simulation to accurately model the physical processes they are interested in studying. The emstandard_opt3-physics list, recognized for its high precision in electromagnetic interactions, was utilized throughout the research. This physics library encompasses critical radiation-matter interactions essential in dosimetry and radiotherapy applications [19]. The algorithms were run on a high-performance computing system featuring the following configuration: 16 gigabytes of RAM, an Intel CoreTM i7-6700 processor clocked at 3.4 GHz with 8 cores, Mesa Intel HD Graphics, and a GTX 1080 Ti graphics card equipped with 11 gigabytes of GDDR5X memory. This supercomputer operates on a Linux operating system and is situated at the imaging center of Mashhad University of Medical Sciences in Iran.

6. Monte Carlo simulation validation

A quantitative measure called the transmission factor (TF) is defined to assess the alignment of simulated data with measured data. Following the principles of TG-43 [20], we use the polar angle (or zenith angle), denoted as β, which is measured from the z-axis.

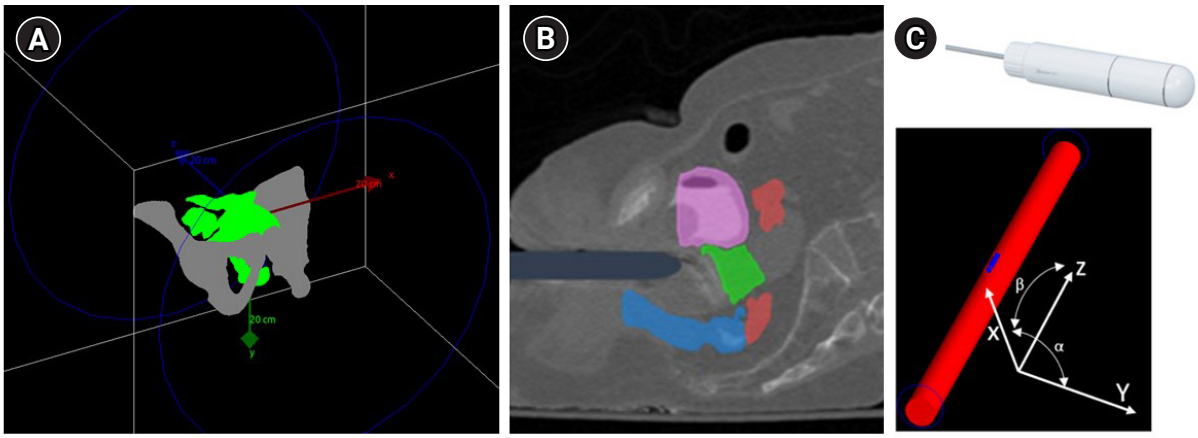

Fig. 3. Schematic images of the stages of modeling and simulating structures. (A) Placement of structures in a virtual water phantom. (B) A sagittal computed tomography scan image of the pelvic region with contoured structures in the three-dimensional (3D) Slicer software environment. Importing contoured structures into the software 3D Slicer and modeling of the organ. (C) A visual representation of the coordinate system for calculating transmission factor.

The azimuthal angle in the x-y plane, denoted as α, is defined as the axis shielding for dose modulation. The distance from the origin is defined as the radius, denoted as r. Fig. 3 provides a visual representation of the coordinate system. TF is calculated as the ratio of the dose at a distance of 2 cm from the center of the tandem on the x-y plane of the shielded side to that of the unshielded side. This parameter has been simulated and measured to determine its value. A 0.6 cm^3 Farmer-type ionization chamber manufactured by PTW (Freiburg GmbH, Freiburg, Germany) was inserted into the corresponding point at the water phantom. Due to the offsetting of the central source channel through different applicators, the effect of distance squared has been considered and adjusted to compare the applicators.

$$\text{Transmission factor} = \frac{D\,(r = 2\ \text{cm}, \beta = 90°, \alpha = 180°)}{D\,(r = 2\ \text{cm}, \beta = 90°, \alpha = 0°)}$$

Results

The findings from utilizing dynamic IMBT techniques and traditional approaches with cobalt and iridium HDR sources were acquired and assessed, and the essential parameters were extracted and detailed in Table 1. Furthermore, their visual representation can be seen in Fig. 4. There is a slight relative variation of less than 1.0% in the absorbed dose parameter D_{90} for the target in both techniques using ^{60}Co and ^{192}Ir sources. The plan comparison indices of D_{2cc} (which represents the maximum dose for OARs) decreased by 2.3%–18.7% for dynamic IMBT, as shown in Table 1. Overall, IMBT with ^{192}Ir and ^{60}Co exhibited significant enhancements in sparing organs at risk compared to conventional methods. IMBT also showcased a notable decrease in rectal D_{2cc} compared to CBT while maintaining the same level of HR-CTV D_{90} coverage. The rectum and bladder D_{2cc} parameter obtained from vaginal IMBT and CBT techniques showed that the dynamic IMBT technique offered greater protection to the rectum and bladder compared to conventional techniques (Fig. 4). Additionally, the level of protection for OARs was slightly higher for the iridium source than for the cobalt source.

The Monte Carlo statistical uncertainties were calculated for the target, rectum, and bladder in the brachytherapy methods. The average statistical uncertainties were obtained by averaging the uncertainties of all voxels in both the IMBT and conventional techniques. All uncertainties were below two percent, with a slightly higher value for the target (1.72%) compared to the organs at risk (0.62%). The TF was used to evaluate the alignment of simulated and measured data for both sources with IMBT applicator. Simulated values were 5.1% and 12.5%, and the measured values were 5.0% and 12.5% for the ^{192}Ir and ^{60}Co sources, respectively, which reports a difference of less than one percent in both sources.

Discussion and Conclusion

This research was carried out to evaluate the effectiveness of a newly designed nanoparticle tungsten-shielded dynamic cylinder applicator in comparison to a traditional applicator for brachytherapy treatment of vaginal cancer, utilizing the GATE Monte Carlo code. In order to conduct IMBT, a shielded applicator with off-center channels is required to offer effective shielding to OARs and administer a precise dose to the target area. The protective capability of OARs was enhanced by utilizing a WO_3 nanoparticle mate-

https://doi.org/10.3857/roj.2024.00339

Table 1. The percentage dosimetric data for treating vaginal cancer with ^{60}Co and ^{192}Ir sources were compared between the IMBT technique and the conventional method

Volume	Metric	CBT (mean ± SD, Gy)		IMBT (mean ± SD, Gy)		Diff (%)	
		^{60}Co	^{192}Ir	^{60}Co	^{192}Ir	^{60}Co	^{192}Ir
HR-CTV	D_{90}	82.1 ± 7.9	81.6 ± 10.6	82.1 ± 8.1	81.6 ± 10.1	0.5 (p = 0.159)	0.5 (p = 0.312)
Bladder	D_{2cc}	45.6 ± 10.8	41.7 ± 10.1	40.1 ± 7.1	35.1 ± 10.7	11.1 (p < 0.001[a])	16.6 (p < 0.001[a])
Rectum	D_{2cc}	35.3 ± 7.8	33.4 ± 7.0	27.4 ± 8.1	24.4 ± 9.1	12.8 (p < 0.001[a])	18.7 (p < 0.001[a])
Sigmoid	D_{2cc}	38.8 ± 8.1	36.4 ± 9.2	37.9 ± 8.7	35.3 ± 8.5	2.3 (p = 0.136)	2.9 (p = 0.572)

IMBT, intensity-modulated brachytherapy; CBT, conventional brachytherapy; SD, standard deivation; Diff, difference; HR-CTV, high-risk clinical target volumes; D_{90}, minimum dose received by 90% of target volume; D_{2cc}, minimum dose received by the highest 2 cc of organ.
[a]Significant values.

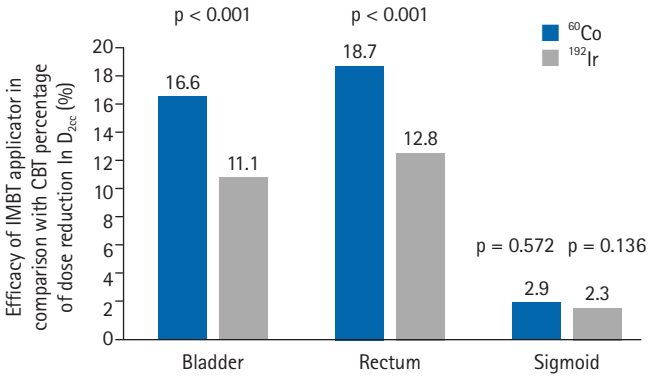

Fig. 4. Percentage of dose reduction in minimum dose received by the highest 2 cc of organ (D_{2cc}) parameters of organ at risks in intensity-modulated brachytherapy (IMBT) compared with conventional brachytherapy (CBT) technique with ^{60}Co and ^{192}Ir sources. The white box represents p-values in D_{2cc} of organs when comparing the two methods.

rial for the main body of the applicator.

Choosing an appropriate and effective shielding material against gamma rays requires great precision in the type and thickness of materials. Factors such as weight, volume, and cost considerations play a significant role in the interconnected analysis for choosing the right material for the protective shield. The primary characteristic of a material's protective ability lies in its capacity to attenuate gamma radiation, with heavier materials generally exhibiting greater attenuation abilities. The design of a radiation protective shield is influenced by factors such as the radiation source's type and characteristics, the installation type, and the shield material's properties [21].

Numerous factors advocate for the utilization of nanoparticles in the design of radiation shielding. Conventional materials like lead may not always be able to be manufactured in the specific shapes and geometries needed for diverse applications. The drawbacks of traditional metallic lead shields, including toxicity and weight, have prompted researchers to explore alternative radiation shielding materials that are lighter, flexible, moldable, and non-toxic. Nanoparticle-based composites, for instance, have the capability to fulfill the criteria for radiation protection in both medical and industrial settings.

Although the protective properties of various compounds, including bismuth trioxide (Bi_2O_3), copper (II) oxide, gadolinium oxide, and lead monoxide in powder form, and zirconium ZrO_2, against different spectra of radiation, have been investigated, none of these compounds have been specifically applied for the required protection in IMBT technique [22]. Numerous experimental investigations and modeling analyses have explored the impact of nano-WO_3 composite materials in radiation shielding, yielding promising findings [16,23-26]. Therefore, in this research, we harnessed this capability in a new application within the field of brachytherapy.

The present research validated that IMBT methods with a redesigned commercial applicator using nano-WO_3/epoxy composite surpassed traditional brachytherapy in the treatment of vaginal cancer. Including a shielded segment within the applicator partially blocked the radiation directed toward healthy tissues surrounding the applicator, allowing the targeted area to receive radiation without a significant decrease in its original intensity. Consequently, the IMBT technique could precisely adjust the radiation dose distribution to effectively cover the tumor while also providing adequate protection to OARs. IMBT utilizing ^{192}Ir sources, known for their lower average photon energy, demonstrated superior modulation potential by effectively reducing the radiation dose to OARs, with a more pronounced reduction observed compared to ^{60}Co sources. Dynamic IMBT with ^{60}Co HDR sources led to an 11.1% decrease in the relative D_{2cc} of the bladder and a 12.8% decrease in the rectum compared to conventional applicators. The use of ^{192}Ir HDR sources in IMBT resulted in a 16.6% reduction in the relative D_{2cc} for the bladder and an 18.7% reduction in the rectum. The D_{2cc} of the sig-

moid dose exhibited a non-significant decrease with both cobalt and iridium sources, indicating that the lack of significance in dose reduction may be attributed to the organ's location. The ability to modulate doses in IMBT techniques is influenced by various factors, including tumor size, location, and shape; shielding characteristics such as diameter, material, density, availability, and cost; and source energies. Therefore, in order to design and create an efficient IMBT system, it is essential to take into account, examine, validate, and optimize the impact of all these contributing factors.

In the present study, for the first time, the direct incorporation of nano-WO_3/epoxy composite in the design of brachytherapy applicators has been utilized. While complete organ protection has not been achieved, a significant reduction in organs at risk doses has occurred. This study marks a promising start in the use of nanoparticle compounds in IMBT that can be further enhanced through more extensive research in this area.

The performance of a newly designed dynamic cylinder applicator shielded with nano-WO_3/epoxy composite was simulated and contrasted with a standard applicator using the GATE Monte Carlo code for treating vaginal cancer. This study represents the initial utilization of nano-WO_3/epoxy composite directly integrated into the design of brachytherapy applicators. Although full organ protection was not attained, a notable decrease in doses to organs at risk was observed. This research signifies a hopeful beginning in incorporating nanoparticle compounds in IMBT, with the potential for further advancements through additional research in this field.

Statement of Ethics

Research Ethics Committees of the School of Medicine-Mashhad University of Medical Sciences granted permission for this study (4011349) and written informed consent was obtained from participants to participate in the study.

Conflict of Interest

No potential conflict of interest relevant to this article was reported.

Acknowledgments

This paper was extracted from a PhD thesis in Medical Physics numbered (4011349) at Mashhad university of medical sciences.

Funding

The authors would like to thank the Research Deputy of MUMS for the financial support of this project, numbered (4011349).

Author Contributions

Conceptualization, HG; Data curation, SN; Formal analysis, ES; Funding acquisition, HG; Investigation, ES; Methodology, SN; Project administration, HG; Resources, HG; Software, ES; Supervision, SN; Validation, SH; Visualization, ES; Writing–original draft, ES; Writing–review & editing, ES.

Data Availability Statement

All data generated or analyzed during this study are included in this article. Further inquiries can be directed to the corresponding author.

References

1. Chyle V, Zagars GK, Wheeler JA, Wharton JT, Delclos L. Definitive radiotherapy for carcinoma of the vagina: outcome and prognostic factors. Int J Radiat Oncol Biol Phys 1996;35:891–905.
2. Viswanathan AN, Erickson BE, Rownd J. Image-based approaches to interstitial brachytherapy. In : Viswanathan A, Kirisits C, Erickson B, Potter R, editors. Gynecologic radiation therapy: novel approaches to image-guidance and management. Berlin: Springer; 2011. p. 247–59.
3. Hasbini A, Haie-Meder C, Morice P, et al. Outcome after salvage radiotherapy (brachytherapy +/- external) in patients with a vaginal recurrence from endometrial carcinomas. Radiother Oncol 2002;65:23–8.
4. Mayer C, Gasalberti DP, Kumar A. Brachytherapy. In: StatPearls. Treasure Island, FL: StatPearls Publishing; 2024.
5. Tanderup K, Eifel PJ, Yashar CM, Potter R, Grigsby PW. Curative radiation therapy for locally advanced cervical cancer: brachytherapy is NOT optional. Int J Radiat Oncol Biol Phys 2014;88:537–9.
6. Price MJ, Gifford KA, Horton JL Jr, et al. Monte Carlo model for a prototype CT-compatible, anatomically adaptive, shielded intracavitary brachytherapy applicator for the treatment of cervical cancer. Med Phys 2009;36:4147–55.
7. Callaghan CM, Adams Q, Flynn RT, Wu X, Xu W, Kim Y. Systematic review of intensity-modulated brachytherapy (IMBT): static and dynamic techniques. Int J Radiat Oncol Biol Phys 2019;105:206–21.
8. Tantivatana T, Rongsriyam K. Treatment outcomes of high-dose-rate intracavitary brachytherapy for cervical cancer: a comparison of Ir-192 versus Co-60 sources. J Gynecol Oncol 2018;29:e86.

 https://doi.org/10.3857/roj.2024.00339

9. Wen A, Wang X, Wang B, et al. Comparative analysis of ^{60}Co and ^{192}Ir sources in high dose rate brachytherapy for cervical cancer. Cancers (Basel) 2022;14:4749.
10. Lide DR. CRC handbook of chemistry and physics. Boca Raton, FL: CRC Press; 2004.
11. Ivanov EY, Suryanarayana C, Bryskin BD. Synthesis of a nanocrystalline W–25 wt.% Re alloy by mechanical alloying. Mater Sci Eng A 1998;251:255–61.
12. Azman MN, Abualroos NJ, Yaacob KA, Zainon R. Feasibility of nanomaterial tungsten carbide as lead-free nanomaterial-based radiation shielding. Radiat Phys Chem 2023;202:110492.
13. Mostafa AM, Issa SA, Sayyed MI. Gamma ray shielding properties of PbO-B_2O_3-P_2O_5 doped with WO_3. J Alloys Compd 2017;708:294–300.
14. Granero D, Perez-Calatayud J, Casal E, Ballester F, Venselaar J. A dosimetric study on the Ir-192 high dose rate flexisource. Med Phys 2006;33:4578–82.
15. Safigholi H, Han DY, Soliman A, Song WY. Direction modulated brachytherapy (DMBT) tandem applicator for cervical cancer treatment: choosing the optimal shielding material. Med Phys 2018;45:3524–33.
16. Kazemi F, Malekie S, Hosseini MA. A Monte Carlo study on the shielding properties of a novel polyvinyl alcohol (PVA)/WO_3 composite, against gamma rays, using the MCNPX code. J Biomed Phys Eng 2019;9:465–72.
17. Pieper S, Halle M, Kikinis R. 3D slicer. In: 2004 2nd IEEE International Symposium on Biomedical Imaging: Nano to Macro (IEEE Cat No. 04EX821); 2004 Apr 18; Arlington, VA, USA. New York: Institute of Electrical and Electronics Engineers; 2004. p. 632–5.
18. Haie-Meder C, Potter R, Van Limbergen E, et al. Recommendations from Gynaecological (GYN) GEC-ESTRO Working Group (I): concepts and terms in 3D image based 3D treatment planning in cervix cancer brachytherapy with emphasis on MRI assessment of GTV and CTV. Radiother Oncol 2005;74:235–45.
19. Bakkali JE, Bardouni TE. Validation of Monte Carlo Geant4 code for a 6 MV Varian linac. J King Saud Univ Sci 2017;29:106–13.
20. Melhus CS, Rivard MJ. Approaches to calculating AAPM TG-43 brachytherapy dosimetry parameters for ^{137}Cs, ^{125}I, ^{192}Ir, ^{103}Pd, and ^{169}Yb sources. Med Phys 2006;33:1729–37.
21. El-Refaie ES, El-Gamel AA, Mohamed AH, Kandil M, Hussein AZ. Electrical properties of electrorefined nanostructured lead (Pb) for enhancing radiation safety. Int J Mater Sci Appl 2015;4:283–7.
22. Bawazeer O, Makkawi K, Aga ZB, et al. A review on using nanocomposites as shielding materials against ionizing radiation. J Umm Al-Qura Univ Appl Sci 2023;9:325–40.
23. Mansouri E, Mesbahi A, Malekzadeh R, Mansouri A. Shielding characteristics of nanocomposites for protection against X- and gamma rays in medical applications: effect of particle size, photon energy and nano-particle concentration. Radiat Environ Biophys 2020;59:583–600.
24. Verdipoor K, Alemi A, Mesbahi A. Photon mass attenuation coefficients of a silicon resin loaded with WO_3, PbO, and Bi_2O_3 micro and nano-particles for radiation shielding. Radiat Phys Chem 2018;147:85–90.
25. Malekie S, Hajiloo N. Comparative study of micro and nano size WO_3/E44 epoxy composite as gamma radiation shielding using MCNP and experiment. Chin Phys Lett 2017;34:108102.
26. Palanisami S, Dhandapani VS, Jayachandran V, et al. Investigation on physico chemical and X-ray shielding performance of zinc doped nano-WO_3 epoxy composite for light weight lead free aprons. Materials (Basel) 2023;16:3866.

ROJ Radiation Oncology Journal

Original Article

pISSN 2234-1900 · eISSN 2234-3156
Radiat Oncol J 2025;43(1):30-39
https://doi.org/10.3857/roj.2024.00409

Hounsfield units predict vertebral compression fractures in gastric cancer survivors after adjuvant irradiation

Pervin Hurmuz[1], Yasin Ozyurek[1], Ecem Yigit[1], Suayib Yalcin[2], Fazli Yagiz Yedekci[1], Faruk Zorlu[1], Mustafa Cengiz[1]

[1]*Department of Radiation Oncology, Hacettepe University, Faculty of Medicine, Ankara, Türkiye*
[2]*Department of Medical Oncology, Hacettepe University, Faculty of Medicine, Ankara, Türkiye*

Received: June 24, 2024
Revised: July 25, 2024
Accepted: August 8, 2024

Correspondence:
Pervin Hurmuz
Department of Radiation Oncology, Hacettepe University, Faculty of Medicine, 06230 Ankara, Türkiye
Tel: +90-312-3052900
E-mail: phurmuz@yahoo.com
ORCID:
https://orcid.org/0000-0003-1221-9192

Purpose: This study aimed to investigate the risk factors and predictive value of vertebral Hounsfield units (HUs) for vertebral compression fracture (VCF) development in gastric cancer (GC) patients who received adjuvant radiotherapy (RT).

Materials and Methods: We retrospectively analyzed the data of 271 patients with non-metastatic GC who received adjuvant RT between 2010 and 2020. The vertebral bodies from 9th thoracic (T9) to 2nd lumbar (L2) were contoured in computed tomographies used for RT planning, and V30, V35, V40, mean doses, and HUs of vertebrae were documented. We conducted univariate and multivariate analyses to identify the risk factors for VCF development.

Results: The median follow-up time was 35.7 months. VCF developed in 23 patients (8.5%) in a median of 30.6 months (range, 3.4 to 117.3) after the end of RT. In total, 37 vertebrae were fractured, with 14 located in T12, nine in L1, seven in T11, four in L2, and three in T10. Older age, female sex, non-smoking status, and lower median vertebrae HUs were significantly associated with VCF in the univariate analysis. In the multivariate analysis, lower median HUs of T12 vertebrae (odds ratio, 0.965; 95% confidence interval, 0.942 to 0.989; p = 0.004) remained significant. The optimal cut-off value for T12 HU was 205.1, with an area under the receiver operating characteristic curve of 0.765, sensitivity of 85.7%, and specificity of 65%.

Conclusion: The lower median HU value of T12 vertebrae is a significant and independent risk factor for VCF development in GC patients who received adjuvant RT. HUs values serve as a simple and reliable predictor of VCF development in this population.

Keywords: Spinal fracture; Stomach neoplasms; Radiotherapy; Computed tomography

Introduction

Gastric cancer (GC) ranks among the most prevalent and fatal malignancies globally, with around 1.09 million new cases and 768,000 deaths reported in 2020 [1]. The main treatment option for localized GC is surgery. However, the risk of recurrence and metastasis remains high, particularly in advanced stages [2,3]. Various strategies, including perioperative chemotherapy and adjuvant chemoradiotherapy (CRT), aim to improve long-term survival [2]. While the benefit of radiotherapy (RT) as an adjuvant treatment is debatable, studies show no significant overall survival improvement with RT after quality-assured gastrectomy [4-6]. Adjuvant CRT could improve overall survival for patients, especially those who have undergone D1 lymphadenectomy or R1 resection [7-9].

GC patients undergoing gastrectomy face elevated osteoporosis and fracture risks compared to the general population, with incidences of 36% and 42.1 cases per 1,000 person-years, respectively [10,11]. Cancer treatments like endocrine therapies and chemotherapy are known to reduce bone mineral density (BMD) and increase fracture risks, but the association with RT remains unclear [12,13]. RT can induce bone loss and fragility by directly damaging the bone cells and matrix [14,15], as well as indirectly affecting the

© 2025 The Korean Society for Radiation Oncology
This is an Open Access article distributed under the terms of the Creative Commons Attribution Non-Commercial License (http://creativecommons.org/licenses/by-nc/4.0/) which permits unrestricted non-commercial use, distribution, and reproduction in any medium, provided the original work is properly cited.

hormonal and inflammatory pathways that regulate bone metabolism [16,17]. RT could have negative effects on the bone health of GC survivors, such as decreased BMD, osteoporosis, and vertebral compression fractures (VCFs) [18,19].

VCF is a collapse of the vertebral body that can cause pain, disability, deformity, and increased mortality. VCFs can occur spontaneously or as a result of minor trauma in patients with weakened bones [20]. Several factors have been identified as potential predictors of VCFs in cancer survivors, such as age, sex, body mass index, smoking, alcohol intake, history of osteoporotic fracture, osteoporosis, rheumatoid arthritis, diabetes mellitus, hyperthyroidism, systemic glucocorticoid usage, low BMD, and low Hounsfield units (HUs) [14,21-26]. Treatment-related factors like higher RT doses, technique, surgery type, and chemotherapy usage may also influence VCF risk [14,22,26,27]. VCFs have been reported in a variety of cancers following RT, including cervical, uterine, prostate, rectal, lung, pancreatic, esophageal, and GCs [18,24-26,28-36].

HUs, quantifying material radiodensity on computed tomography (CT) scans, are associated with BMD and predict osteoporosis and VCFs in diverse populations. [19,37-40]. Yet, the utility of the HU in predicting VCFs after adjuvant irradiation for GC has not been thoroughly investigated.

This study aims to investigate the correlation between HU and VCF occurrence in GC patients receiving adjuvant RT or CRT, along with exploring other potential risk factors for VCFs. We hypothesized that lower HU values would correlate with higher VCF rates, and the HU could be a simple and convenient way to assess VCF risk in GC survivors.

Materials and Methods

1. Patient selection

We conducted a single-institution retrospective study of the medical records of 276 patients with non-metastatic GC who received adjuvant RT or CRT at our center between January 2010 and December 2020. We excluded five patients who were under the age of 18. The analysis incorporated the data of 271 patients who received adjuvant RT or CRT.

The local ethics committee approved this study, which followed the Declaration of Helsinki's guidelines [41].

2. Treatment and follow-up

According to our institutional protocol, CT scans of the abdomen with intravenous contrast were performed with a slice thickness of 2.5 mm for RT planning. The clinical target volumes for RT planning included the gastric bed and lymphatics at risk [42]. The prescription dose was 45 Gy administered in 1.8–2 Gy fractions for patients with negative surgical margins. For patients with residual disease, a boost dose of 5.4–14.4 Gy was delivered to the gastric bed. All but six patients (2.0%) were treated using 3-dimensional conformal radiation therapy, intensity-modulated radiation therapy, or volumetric-modulated arc therapy techniques. Treatments were delivered using either Versa HD (Elekta AB, Stockholm, Sweden) or Clinac DHX (Varian Medical Systems, Palo Alto, CA, USA). Chemotherapy was administered in neoadjuvant, adjuvant, and/or concomitant settings.

Following the completion of RT or CRT, patients underwent clinical examinations every 3 months for the first 2 years, then twice a year for the next 3 years, and once a year after that. Each check-up encompassed a physical assessment, a complete blood count, a biochemical profile, and CT scans of the abdomen and thorax. Upper gastrointestinal endoscopy, positron emission tomography–CT, or brain magnetic resonance imaging tests were performed in cases of suspicion of recurrence or metastasis.

3. Procedures

The vertebral bodies from 9th thoracic (T9) to 2nd lumbar (L2) were retrospectively contoured in the CT scans used for RT planning. The entire vertebral body, including both the cortical and trabecular areas, was included in the region of interest (Fig. 1). The average HU value for each vertebra was automatically measured using the RayStation (RaySearch, Stockholm, Sweden) treatment planning system. Additionally, the volume of the vertebral bodies receiving a dose of 30 Gy or more (V30), V35, V40, and mean radiation doses (D_{mean}) were recorded. To diagnose VCF, a reconstructed sagittal image and the semi-quantitative method of Genant were employed in the follow-up CTs [43]. VCF was defined as a loss of ≥ 20%–25% in height or ≥ 10%–20% in area of the vertebral bodies in the sagittal view. Vertebral fractures that developed before RT and were secondary to bone metastases or the direct vertebral invasion of a recurrent tumor were excluded. The assessment was conducted on the relationship between VCF development and age, sex, smoking history, alcohol intake history, surgery type, RT technique, total RT dose, vertebrae doses (V30, V35, V40, and D_{mean}), and vertebrae HUs before treatment.

4. Statistical analysis

The follow-up time was calculated from the final day of RT, and time to VCF development was defined as the period from the end of RT to the detection of VCF on follow-up CT scans. The median values were used as the cut-off for the analyses. Chi-square or Fischer's exact test were used to compare ratios between independent categorical groups. The Mann-Whitney U test was used to compare non-normally distributed numerical variables. Univariate

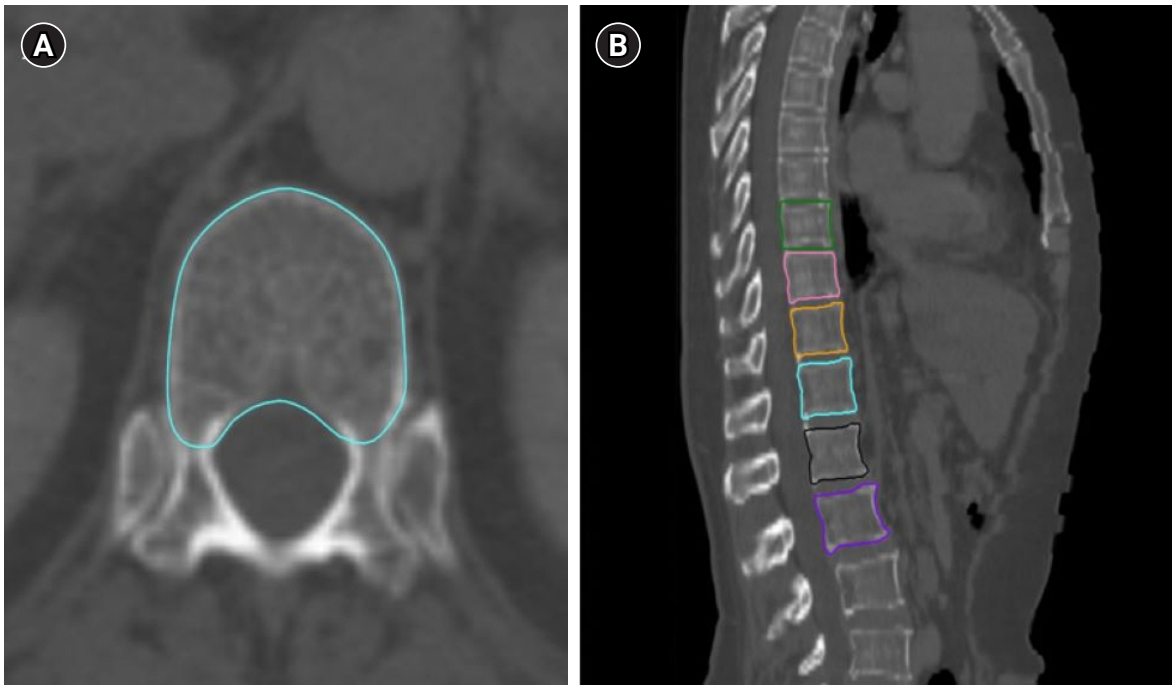

Fig. 1. Vertebral body contouring. (A) T12 vertebral body contour in axial view. (B) T9 to L2 vertebrae contours in sagittal view.

and multivariate analyses used binary logistic regression with backward selection, expressing results with odds ratios and 95% confidence intervals (CIs). Variables with $p < 0.10$ in univariate analyses were used for multivariate analyses to determine independent predictors for VCFs. Receiver operating characteristic (ROC) analysis identified significant risk factors' cutoff points for VCF development. Statistical significance was determined by a p-value less than 0.05. The Statistical Package for the Social Sciences version 21.0 (IBM Corp., Armonk, NY, USA) was utilized for all statistical analyses.

Results

The median age at diagnosis was 58 (range, 20 to 83). The detailed patient, tumor, and treatment characteristics are presented in Table 1. The most frequently applied neoadjuvant chemotherapy regimen was docetaxel, cisplatin, and 5-fluorouracil in nine patients (45.0%), followed by 5-fluorouracil, folinic acid, oxaliplatin, and docetaxel in eight patients (40.0%). The most frequently used concomitant chemotherapy regimen was capecitabine in 148 patients (58.5%). The most frequently applied adjuvant chemotherapy regimen was capecitabine and oxaliplatin in 79 patients (31.2%), followed by 5-fluorouracil and folinic acid in 63 patients (24.9%).

The median follow-up time was 35.7 months (range, 2.8 to 136.5). VCFs developed in 23 out of 271 patients (8.5%). The median development time for VCFs was 30.6 months (range, 3.4 to

Table 1. Baseline patient, tumor, and treatment characteristics

Characteristic	Value (n = 271)
Age (year)	58 (20–83)
Sex	
Male	177 (65.3)
Female	94 (34.7)
History of smoking	
Yes	144 (53.1)
No	127 (46.9)
History of alcohol intake	
Yes	37 (13.7)
No	234 (86.3)
Histology	
Diffuse	142 (52.4)
Intestinal	114 (42.1)
Mixed	15 (5.5)
Differentiation degree	
Well	18 (6.6)
Moderate	53 (19.6)
Poor	176 (64.9)
Unknown	24 (8.9)
Tumor location	
Proximal	123 (45.4)
Distal	135 (49.8)
Diffuse	13 (4.8)
pT classification[a)]	
T1	15 (5.5)
T2	19 (7.0)
T3	94 (34.7)

(Continued to the next page)

 https://doi.org/10.3857/roj.2024.00409

Table 1. Continued

Characteristic	Value (n = 271)
T4	143 (52.8)
pN classification[a]	
N0	55 (20.3)
N1	42 (15.5)
N2	75 (27.7)
N3	99 (36.5)
Pathological stage[a]	
IB	9 (3.3)
IIA	37 (13.6)
IIB	40 (14.8)
IIIA	88 (32.5)
IIIB	62 (22.9)
IIIC	35 (12.9)
Tumor size (cm)	5 (1–18)
Metastatic lymph node ratio (median)	0.18
Perineural invasion (positive)	128 (47.2)
Lymphovascular space invasion (positive)	150 (55.4)
Neoadjuvant chemotherapy	
Yes	20 (7.4)
No	251 (92.6)
Surgery type	
Total gastrectomy	140 (51.7)
Subtotal gastrectomy	131 (48.3)
Dissection type	
D1	170 (62.7)
D2	90 (33.2)
D3	10 (3.7)
D4	1 (0.4)
Surgical margins	
Positive	33 (12.2)
Negative	238 (87.8)
Concomitant chemotherapy	
Yes	261 (96.3)
No	10 (3.7)
Adjuvant chemotherapy	
Yes	253 (93.4)
No	18 (6.6)
RT dose (Gy)	
45	241 (88.9)
> 45	30 (11.1)
RT technique	
2DRT-3DCRT	166 (61.3)
IMRT-VMAT	105 (38.7)

Values are presented as median (range) or number of patients (%) unless otherwise indicated.
RT, radiotherapy; 2DRT, 2-dimensional radiotherapy; 3DCRT, 3-dimensional conformal radiotherapy; IMRT, intensity-modulated radiotherapy; VMAT, volumetric-modulated arc therapy.
[a]According to the American Joint Committee of Cancer Staging Manual, 8th edition.

117.3). Six patients (26.1%) developed fractures within the first year, and 11 patients (47.8%) within 2 years. Five patients (21.7%) developed fractures after 5 years. Nine patients (39.1%) had VCFs at multiple vertebral levels. Of these, five had fractures at two levels, three had fractures at three levels, and one had fractures at four levels. VCF was observed in 37 vertebrae. Fourteen of them (37.9%) were located at T12 level, nine (24.3%) at L1 level, seven (18.9%) at T11 level, four (10.8%) at L2 level, and three (8.1%) at T10 level. All fractured bones were within the irradiated volumes.

The effects of clinical features on the development of VCFs are shown in Table 2. Older age ($p = 0.007$), female sex ($p = 0.021$), and non-smoking status ($p = 0.023$) are associated with a higher incidence of VCFs. The effects of vertebral doses and HUs on the development of VCFs are shown in Table 3. Patients who developed VCF had significantly lower median HUs for T10, T11, T12, L1, and L2 vertebrae (212.9, 197.2, 182.4, 187.6, and 188.3) compared to those who did not (239.3, 224.5, 217.6, 208.8, and 214.7), respectively ($p = 0.005$, $p = 0.003$, $p = 0.002$, $p = 0.009$, and $p = 0.003$). The development of VCFs was not significantly affected by the history of alcohol intake, surgery type, RT technique, RT total dose, or the doses of radiation received by the vertebrae (V30, V35, V40, and D_{mean}).

Univariate and multivariate analyses were performed for factors found to be associated with VCF development (Table 4). Older age, female sex, non-smoking status, and lower median HUs of T10-L2 vertebrae were significantly associated with a higher probability of developing VCFs in the univariate analysis. Only lower median HUs of T12 vertebrae (odds ratio, 0.965; 95% CI, 0.942 to 0.989; $p = 0.004$) remained significantly associated with VCF development in the multivariate analysis.

In the analysis of whether age (< 58 vs. ≥ 58 years) and sex (male vs. female) affect T12 HU values, it was found that neither sex ($p = 0.499$) nor age ($p = 0.151$) had a significant impact on the T12 HU values. The impact of T12 HU values on VCF incidence stratified by age and sex is shown in Table 5. In all subgroups, patients with VCF had significantly lower T12 HU values compared to those without VCF.

ROC analysis was performed to find the cut-off value for T12 HUs that best predicted VCF development (Fig. 2). The ideal cut-off value for T12 HUs forecasting VCF development was found to be 205.1. Area under the ROC curve for T12 HUs was 0.765 (95% CI, 0.645 to 0.886; $p = 0.002$). The optimal sensitivity and specificity for the T12 HUs cut-off level were 85.7% and 65%, respectively. For a threshold value of 221 HUs, the sensitivity was found to be 93%, and for a threshold value of 171.5 HUs, the specificity was found to be 90%.

Table 2. The effect of clinical features on the development of VCF

	VCF (n = 23)	No VCF (n = 248)	Total (n = 271)	p-value
Age (year)	63 (49–79)	57 (20–83)	58 (20–83)	0.007[a]
Sex				
Female	13 (56.5)	81 (32.7)	94 (34.7)	0.021[b]
Male	10 (43.5)	167 (67.3)	177 (65.3)	
History of smoking				
Yes	7 (30.4)	137 (55.2)	144 (53.1)	0.023[b]
No	16 (69.6)	111 (44.8)	127 (46.9)	
History of alcohol intake				
Yes	1 (4.3)	36 (14.5)	37 (13.7)	0.335[b]
No	22 (95.7)	212 (85.5)	234 (86.3)	
Surgery				
Total gastrectomy	14 (60.9)	126 (50.8)	140 (51.7)	0.356[b]
Subtotal gastrectomy	9 (39.1)	122 (49.2)	131 (48.3)	
RT technique				
2DRT-3DCRT	10 (43.5)	95 (38.3)	105 (38.7)	0.626[b]
IMRT-VMAT	13 (56.5)	153 (61.7)	166 (61.3)	
RT total dose (Gy)				
45	21 (91.3)	220 (88.7)	241 (88.9)	> 0.99[b]
> 45	2 (8.7)	28 (11.3)	30 (11.1)	

Values are presented as median (range) or number (%).
VCF, vertebral compression fracture; RT, radiotherapy; 2DRT, 2-dimensional radiotherapy; 3DCRT, 3-dimensional conformal radiotherapy; IMRT, intensity-modulated radiotherapy; VMAT, volumetric-modulated arc therapy.
[a]Calculated by the Mann-Whitney U test. [b]Calculated by the chi-square test.

Discussion and Conclusion

To our knowledge, this is the most extensive research on VCFs following adjuvant RT or CRT for GC, comprising the data of 271 patients. In this study, T12 vertebrae HUs were associated with the risk of VCF development in GC patients who underwent RT. The cut-off value was determined to be 205.1, with 85.7% sensitivity and 65% specificity.

Numerous studies have explored VCF prevalence and associated risk factors, revealing incidence rates ranging from 1.7% to 89% in patients undergoing treatment for various cancers such as gynecologic, gastrointestinal, lung, pancreatic, or prostate cancer [14,34-36]. Various methodological differences, such as study designs (retrospective or prospective), varying follow-up scan frequencies, different imaging techniques, RT doses, and the inclusion of asymptomatic VCFs, collectively account for the observed wide range. Our study reported a VCF rate of 8.5%, which is consistent with the literature [18,28,33-36]. We observed that the vertebral fracture rates in studies examining VCF in patients receiving RT due to cervical cancer in Japan were higher than the fracture rate in our study [24,25,30,31]. We think that this could possibly be explained by the population being predominantly female, known to have higher fracture risks, and the higher prevalence of vertebral osteoporosis in Japanese society compared to the United States and Europe [14,44].

In our study, the median time for the development of VCFs was 30.6 months, longer than previously reported in the literature, which ranged from 6 to 20 months [14]. This discrepancy may be attributed to the extended follow-up period in our study. Among patients who developed VCF, 21.7% experienced fractures after 5 years. The longest VCF development time observed was 117.3 months, which, to our knowledge, is the longest duration reported for VCF development in the literature. Most VCFs (62.2%) occurred in the T12 and L1 vertebrae, which are junctional and weight-bearing, mirroring findings in cervical cancer patients in whom fractures frequently appear in the weight-bearing sacrum and sacroiliac joints [29]. These findings indicate that even though RT affects all bones in the treatment field, the weight-bearing vertebrae are the most susceptible to fracture development.

In evaluating factors influencing VCF development, older age, female sex, non-smoking status, and low vertebral HU values were associated with increased VCF incidence in univariate analysis. Subsequent analysis revealed a significant association between smoking status and sex ($\chi^2 = 12.72$; $p < 0.001$). We concluded that the relationship between non-smoking status and VCF formation was mainly due to sex, as most males (61.0%) were smokers and most females (61.7%) were non-smokers, which indicates smoking status as a confounding factor. Similar to our findings, numerous studies on VCF risk factors in cancer patients have also linked advanced age and female sex with higher VCF incidence

https://doi.org/10.3857/roj.2024.00409

Table 3. The effect of vertebrae doses and HUs on the development of VCF

	VCF	No VCF	Total	p-value[a]
T10 vertebra				
D_{mean} (Gy)	31.0 (21.0–39.0)	30.5 (10.0–37.5)	30.5 (12.0–38.0)	0.640
V30 (%)	49.0 (24.0–85.0)	56.5 (8.5–93.0)	55.5 (10.0–92.0)	0.790
V35 (%)	40.5 (14.0–70.0)	39.0 (5.0–69.5)	39.5 (6.0–70.0)	0.836
V40 (%)	30.5 (7.0–54.0)	20.0 (3.5–43.0)	20.5 (4.0–44.0)	0.655
HUs	212.9 (199.6–221.0)	239.3 (214.2–267.7)	229.8 (206.9–256.8)	0.005
T11 vertebra				
D_{mean} (Gy)	37.0 (34.0–40.0)	38.0 (34.0–40.5)	38.0 (34.0–40.0)	0.924
V30 (%)	78.5 (66.0–95.0)	96.0 (68.0–99.0)	95.0 (68.0–99.0)	0.232
V35 (%)	62.0 (41.0–85.0)	75.5 (46.5–90.0)	70.5 (45.0–90.0)	0.355
V40 (%)	38.0 (27.0–51.0)	46.0 (31.0–63.0)	46.0 (31.0–63.0)	0.738
HUs	197.2 (192.3–207.4)	224.5 (203.7–250.1)	216.8 (198.8–242.8)	0.003
T12 vertebra				
D_{mean} (Gy)	38.0 (37.0–42.0)	40.0 (37.0–41.0)	40.0 (37.0–41.0)	0.288
V30 (%)	92.5 (78.0–100.0)	96.0 (88.0–100.0)	96.0 (86.0–100.0)	0.334
V35 (%)	68.5 (51.0–90.0)	84.0 (59.5–91.5)	82.0 (59.0–91.0)	0.313
V40 (%)	40.5 (32.0–72.0)	54.0 (39.5–60.5)	53.0 (39.0–61.0)	0.230
HUs	182.4 (170.7–203.3)	217.6 (194.6–234.1)	212.9 (186.6–229.9)	0.002
L1 vertebra				
D_{mean} (Gy)	35.5 (33.0–39.0)	38.0 (28.0–41.0)	38.0 (30.0–40.0)	0.499
V30 (%)	84.0 (59.0–96.0)	94.0 (50.0–100.0)	92.5 (50.0–99.0)	0.429
V35 (%)	55.5 (40.0–76.0)	82.0 (25.0–88.0)	78.0 (28.0–88.0)	0.274
V40 (%)	31.0 (27.0–41.0)	40.0 (15.0–53.0)	38.5 (16.0–51.0)	0.426
HUs	187.6 (166–201.8)	208.8 (190.2–226.5)	206.3 (186.4–224.3)	0.009
L2 vertebra				
D_{mean} (Gy)	32.0 (11.0–36.0)	27.0 (6.0–37.0)	28.5 (6.0–37.0)	0.293
V30 (%)	54.5 (11.0–87.0)	61.0 (6.5–72.0)	59.5 (7.0–72.0)	0.987
V35 (%)	37.5 (6.0–60.0)	46.5 (4.5–56.5)	44.5 (5.0–58.0)	0.987
V40 (%)	22.0 (2.0–30.0)	15.5 (2.0–37.0)	17.0 (2.0–36.0)	0.597
HUs	188.3 (161.5–205.7)	214.7 (189.5–235.7)	209.7 (187.1–233.2)	0.003

Values are presented as median (IQR).
HUs, Hounsfield units; VCF, vertebral compression fracture; D_{mean}, mean dose; V30, volume that received a dose of 30 Gy or more; V35, volume that received a dose of 35 Gy or more; V40, volume that received a dose of 40 Gy or more; IQR, interquartile range.
[a]Calculated by the Mann-Whitney U test.

Table 4. Univariate and multivariate logistic regression analysis of variables predicting VCF

	Univariate			Multivariate		
	Odds ratio	95% CI	p-value	Odds ratio	95% CI	p-value
Age	4.986	1.649–15.076	0.004	1.040	0.970–1.115	0.272
Sex						
Male	1			1		
Female	2.680	1.127–6.372	0.026	2.417	0.702–8.322	0.162
History of smoking						
Yes	1			1		
No	2.821	1.121–7.099	0.028	1.067	0.242–4.693	0.932
T10 HUs	0.973	0.953–0.994	0.011	0.993	0.958–1.029	0.684
T11 HUs	0.968	0.945–0.993	0.011	1.003	0.950–1.060	0.902
T12 HUs	0.965	0.942–0.988	0.003	0.965	0.942–0.989	0.004
L1 HUs	0.971	0.950–0.993	0.011	1.015	0.971–1.062	0.507
L2 HUs	0.968	0.947–0.989	0.004	0.975	0.932–1.021	0.282

VCF, vertebral compression fracture; CI, confidence interval; HUs, Hounsfield units.

Table 5. Impact of T12 HU values on VCF incidence stratified by age and sex

	T12 HUs		p-value[a]
	VCF	No VCF	
Age (year)			
< 58	178.1 (168.3–190.2)	215.4 (200.8–236.5)	0.044
≥ 58	186.7 (170.7–203.3)	217.9 (179.4–232.1)	0.017
Sex			
Male	182.4 (174.6–189.6)	218.0 (194.9–236.1)	0.015
Female	183.3 (170.5–212.1)	214.6 (194.6–227.1)	0.042

Values are presented as median (IQR).
HUs, Hounsfield units; VCF, vertebral compression fracture; IQR, interquartile range.
[a]Calculated by the Mann-Whitney U test.

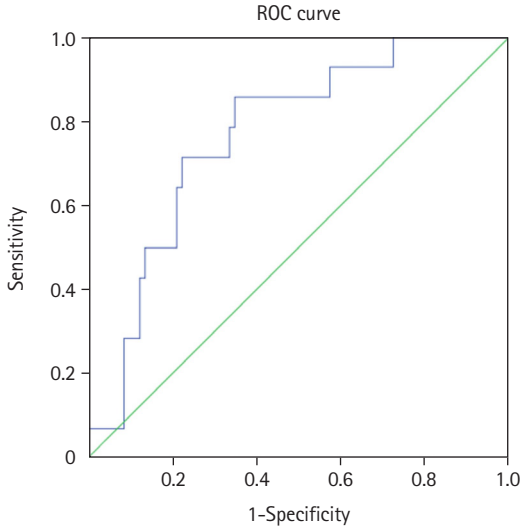

Fig. 2. Receiver operating characteristic (ROC) curve demonstrating the accuracy of T12 Hounsfield units for the assessment of vertebral compression fracture development.

[26,33,35].

The pathophysiology of radiation-induced bone damage remains incompletely understood. Irradiation lowers the number of osteoblasts, stops their cell cycle, and makes them more prone to cell death, meaning that less bone formation is a key factor in bone damage caused by RT. Radiation also seems to harm the bone matrix, increase fat in the marrow, and impair the blood supply to bone, all of which likely affect the direct impact of RT on bone health and strength [14]. Our study found no association between total RT dose, vertebral doses (V30, V35, V40, and D_{mean}), and VCF development, despite conflicting literature data. Studies show that every 5-Gy increase in the mean vertebral dose raises the risk of VCF development by factors of 1.19 and 1.22, according to Fujii et al. [26] and Wu et al. [36], respectively. In both studies, the median total RT dose was 60 Gy. This exceeded the median total RT dose in our study, which was 45 Gy. In addition, Uezono et al. [24] examined the risk factors for pelvic fractures in cervical cancers that received RT. They also found no significant association between fractures and vertebral doses, consistent with our study. The median total RT dose was 50.4 Gy, which closely resembled that of our study. Considering all these data, it was thought that the RT dose threshold for vertebral bones could be so high that we could not observe the effect of the RT dose on VCF development.

Osteoporosis, which is indicated by low BMD, is a significant risk factor and an indirect predictor of VCF development [14]. While dual-energy X-ray absorptiometry (DEXA) is considered the gold standard for assessing BMD [45], it is not routinely used for cancer survivors. This, coupled with the focus of BMD measurements on areas like the lumbar spine and femoral neck, makes it difficult to assess bone loss in radiation-affected areas. Hence, considering bone density measurements using CT before RT could be valuable in predicting the development of fractures. Numerous studies have shown that there is a strong relationship between BMD assessed by DEXA and HUs derived from CT scans [19,37-40]. One of the most important findings of our study was that pre-RT HU values of vertebrae were the best parameter to show the probability of VCF development, as well as the findings of previous studies [24,25]. While all vertebral HU values were associated with VCF development in univariate analysis, only the T12 HU value remained significant in multivariate analysis. Uezono et al. [24] and Ishikawa et al. [25] conducted studies investigating the risk of pelvic fractures in patients with cervical cancer who received definitive RT. In both studies, it was observed that only pre-RT CT HU values were associated with the development of pelvic fractures, consistent with our study.

We identified 205.1 as the optimal cut-off point for the T12 vertebrae HU value. A threshold of 221 HUs showed 93% sensitivity, and 171.5 HUs had 90% specificity. Wu et al. [36] found a higher risk of thoracic vertebral fracture in esophageal squamous cell carcinoma patients with initial CT scan HU values below 128. However, their study did not include the cortical edges of vertebrae in the region of interest for HU determination, possibly accounting for the discrepancy.

Our study aimed to simplify VCF risk assessment for radiation oncologists. The HU values of the vertebrae indicated the likelihood of VCF occurrence. Therefore, the VCF risk could be estimated by using treatment planning systems. We can also use the HUs from CT scans to estimate BMD, save money, and reduce radiation exposure from DEXA tests. Moreover, the sagittal views of the vertebrae from CT scans can be used for detecting hidden and asymptomatic bone fractures. By incorporating these measurements into regular practice, osteopenia, osteoporosis, and fracture risk could be iden-

https://doi.org/10.3857/roj.2024.00409

tified.

Our study has several strengths, such as a relatively large sample size, a long follow-up period, a homogeneous population of GC patients, a standardized adjuvant RT or CRT protocol, and objective measurement of HUs and VCFs. However, our study also has some limitations, mostly due to its retrospective nature. The patients' comorbidity status, body mass index, basal calcium level, and vitamin D level, as well as whether they received replacement therapy during follow-up, were unknown. The patients' baseline BMD was not assessed using the DEXA method, which is the most reliable technique. The clinical outcomes of VCFs, such as pain, disability, quality of life, and mortality, that are important aspects to be considered in the management of cancer patients, were not evaluated. As all patients in our study population received adjuvant RT, we were unable to compare the development of VCF and associated factors between patients who received RT and those who did not. Furthermore, the effect of RT on the HU value was not observed by measuring HUs in the sequential CT scans of the patients during the follow-up. Finally, since there are several techniques for HU measurement, cut-off values for HUs should be interpreted with attention to the measurement technique used in each study.

In conclusion, our study suggests that GC patients who receive adjuvant RT or CRT are at increased risk of VCF. Additionally, low pre-RT or CRT vertebral HU values are simple and reliable indicators of VCF risk. These results imply that HU measurement from CT scans can be used as a screening tool to identify high-risk patients who may benefit from preventive interventions, such as replacement therapy with calcium and vitamin D, vertebral augmentation, or prophylactic vertebroplasty. Therefore, further studies with prospective, long-term, and comprehensive assessments are needed to validate and extend our findings and to explore the possible mechanisms and preventive strategies for VCFs in GC patients who receive RT.

Statement of Ethics

This study protocol was reviewed and approved by the Institutional Ethics Committee of Hacettepe University (Project No: GO 22/312, Decision No: 2022/06-37). A written informed consent for the treatment and use of data for the present study were obtained from every patient prior to treatment.

Conflict of Interest

No potential conflict of interest relevant to this article was reported.

Funding

None.

Author Contributions

Conceptualization, PH, SY, MC; Data curation, YO, EY, FYY; Formal analysis, YO, EY, FYY; Methodology, PH, SY, FYY; Project administration, PH; Supervision, PH, MC; Visualization, FZ; Writing – original draft, PH, YO, EY; Writing – review & editing, FZ, MC.

Data Availability Statement

The data that support the findings of this study are available from the corresponding author upon reasonable request.

References

1. Sung H, Ferlay J, Siegel RL, et al. Global cancer statistics 2020: GLOBOCAN estimates of incidence and mortality worldwide for 36 cancers in 185 countries. CA Cancer J Clin 2021;71:209–49.
2. Guan WL, He Y, Xu RH. Gastric cancer treatment: recent progress and future perspectives. J Hematol Oncol 2023;16:57.
3. Smyth EC, Nilsson M, Grabsch HI, van Grieken NC, Lordick F. Gastric cancer. Lancet 2020;396:635–48.
4. Lee J, Lim DH, Kim S, et al. Phase III trial comparing capecitabine plus cisplatin versus capecitabine plus cisplatin with concurrent capecitabine radiotherapy in completely resected gastric cancer with D2 lymph node dissection: the ARTIST trial. J Clin Oncol 2012;30:268–73.
5. Cats A, Jansen EP, van Grieken NC, et al. Chemotherapy versus chemoradiotherapy after surgery and preoperative chemotherapy for resectable gastric cancer (CRITICS): an international, open-label, randomised phase 3 trial. Lancet Oncol 2018;19:616–28.
6. Park SH, Lim DH, Sohn TS, et al. A randomized phase III trial comparing adjuvant single-agent S1, S-1 with oxaliplatin, and postoperative chemoradiation with S-1 and oxaliplatin in patients with node-positive gastric cancer after D2 resection: the ARTIST 2 trial. Ann Oncol 2021;32:368–74.
7. Macdonald JS, Smalley SR, Benedetti J, et al. Chemoradiotherapy after surgery compared with surgery alone for adenocarcinoma of the stomach or gastroesophageal junction. N Engl J Med 2001;345:725–30.
8. Smalley SR, Benedetti JK, Haller DG, et al. Updated analysis of SWOG-directed intergroup study 0116: a phase III trial of adjuvant radiochemotherapy versus observation after curative gastric cancer resection. J Clin Oncol 2012;30:2327–33.

9. Stiekema J, Trip AK, Jansen EP, et al. Does adjuvant chemoradiotherapy improve the prognosis of gastric cancer after an r1 resection? Results from a Dutch cohort study. Ann Surg Oncol 2015;22:581–8.
10. Oh HJ, Lim CH, Yoon BH, et al. Fracture after gastrectomy for gastric cancer: a long-term follow-up observational study. Eur J Cancer 2017;72:28–36.
11. Oh HJ, Yoon BH, Ha YC, et al. The change of bone mineral density and bone metabolism after gastrectomy for gastric cancer: a meta-analysis. Osteoporos Int 2020;31:267–75.
12. D'Oronzo S, Stucci S, Tucci M, Silvestris F. Cancer treatment-induced bone loss (CTIBL): pathogenesis and clinical implications. Cancer Treat Rev 2015;41:798–808.
13. Stava CJ, Jimenez C, Hu MI, Vassilopoulou-Sellin R. Skeletal sequelae of cancer and cancer treatment. J Cancer Surviv 2009;3:75–88.
14. Higham CE, Faithfull S. Bone halth and pelvic radiotherapy. Clin Oncol (R Coll Radiol) 2015;27:668–78.
15. Okoukoni C, Farris M, Hughes RT, et al. Radiation-induced bone toxicity. Curr Stem Cell Rep 2017;3:333–41.
16. Wydmanski J, Polanowski P, Tukiendorf A, Maslyk B. Radiation-induced injury of the exocrine pancreas after chemoradiotherapy for gastric cancer. Radiother Oncol 2016;118:535–9.
17. Webb GJ, Brooke R, De Silva AN. Chronic radiation enteritis and malnutrition. J Dig Dis 2013;14:350–7.
18. Yaprak G, Gemici C, Temizkan S, Ozdemir S, Dogan BC, Seseogullari OO. Osteoporosis development and vertebral fractures after abdominal irradiation in patients with gastric cancer. BMC Cancer 2018;18:972.
19. Yaprak G, Gemici C, Seseogullari OO, Karabag IS, Cini N. CT Derived hounsfield unit: an easy way to determine osteoporosis and radiation related fracture risk in irradiated patients. Front Oncol 2020;10:742.
20. Pentecost RL, Murray RA, Brindley HH. Fatigue, iinsufficiency, and pathologic fractures. JAMA 1964;187:1001–4.
21. Kanis JA, Johnell O, Oden A, Johansson H, McCloskey E. FRAX and the assessment of fracture probability in men and women from the UK. Osteoporos Int 2008;19:385–97.
22. Oh D, Huh SJ. Insufficiency fracture after radiation therapy. Radiat Oncol J 2014;32:213–20.
23. Lee SJ, Graffy PM, Zea RD, Ziemlewicz TJ, Pickhardt PJ. Future osteoporotic fracture risk related to lumbar vertebral trabecular attenuation measured at routine body CT. J Bone Miner Res 2018;33:860–7.
24. Uezono H, Tsujino K, Moriki K, et al. Pelvic insufficiency fracture after definitive radiotherapy for uterine cervical cancer: retrospective analysis of risk factors. J Radiat Res 2013;54:1102–9.
25. Ishikawa K, Yamashiro T, Ariga T, et al. Predictive factors of post-treatment fracture by definitive radiotherapy for uterine cervical cancer. Jpn J Radiol 2021;39:93–9.
26. Fujii K, Sakanaka K, Uozumi R, et al. Association of chemoradiotherapy with thoracic vertebral fractures in patients with esophageal cancer. JAMA Netw Open 2020;3:e2013952.
27. Oh H, Yoon BH, Park JW, et al. The risk of osteoporotic fracture in gastric cancer survivors: total gastrectomy versus subtotal gastrectomy versus endoscopic treatment. Gastric Cancer 2023;26:814–22.
28. Salcedo MP, Sood AK, Jhingran A, et al. Pelvic fractures and changes in bone mineral density after radiotherapy for cervical, endometrial, and vaginal cancer: a prospective study of 239 women. Cancer 2020;126:2607–13.
29. Ramlov A, Pedersen EM, Rohl L, et al. Risk factors for pelvic insufficiency fractures in locally advanced cervical cancer following intensity modulated radiation ttherapy. Int J Radiat Oncol Biol Phys 2017;97:1032–9.
30. Yamamoto K, Nagao S, Suzuki K, et al. Pelvic fractures after definitive and postoperative radiotherapy for cervical cancer: a retrospective analysis of risk factors. Gynecol Oncol 2017;147:585–8.
31. Tokumaru S, Toita T, Oguchi M, et al. Insufficiency fractures after pelvic radiation therapy for uterine cervical cancer: an analysis of subjects in a prospective multi-institutional trial, and cooperative study of the Japan Radiation Oncology Group (JAROG) and Japanese Radiation Oncology Study Group (JROSG). Int J Radiat Oncol Biol Phys 2012;84:e195–200.
32. Igdem S, Alco G, Ercan T, et al. Insufficiency fractures after pelvic radiotherapy in patients with prostate cancer. Int J Radiat Oncol Biol Phys 2010;77:818–23.
33. Kim HJ, Boland PJ, Meredith DS, et al. Fractures of the sacrum after chemoradiation for rectal carcinoma: incidence, risk factors, and radiographic evaluation. Int J Radiat Oncol Biol Phys 2012;84:694–9.
34. Uyterlinde W, Chen C, Belderbos J, et al. Fractures of thoracic vertebrae in patients with locally advanced non-small cell lung carcinoma treated with intensity modulated radiotherapy. Radiother Oncol 2016;118:437–41.
35. Otani K, Teshima T, Ito Y, et al. Risk factors for vertebral compression fractures in preoperative chemoradiotherapy with gemcitabine for pancreatic cancer. Radiother Oncol 2016;118:424–9.
36. Wu XQ, Zhang TY, Yang F, et al. Association of radiotherapy with thoracic vertebral fractures in esophageal squamous cell carcinoma: a retrospective cohort study. Medicine (Baltimore) 2023;102:e35304.
37. Yang G, Wang H, Wu Z, Shi Y, Zhao Y. Prediction of osteoporosis

 https://doi.org/10.3857/roj.2024.00409

and osteopenia by routine computed tomography of the lumbar spine in different regions of interest. J Orthop Surg Res 2022; 17:454.
38. Li YL, Wong KH, Law MW, et al. Opportunistic screening for osteoporosis in abdominal computed tomography for Chinese population. Arch Osteoporos 2018;13:76.
39. Vadera S, Osborne T, Shah V, Stephenson JA. Opportunistic screening for osteoporosis by abdominal CT in a British population. Insights Imaging 2023;14:57.
40. Pickhardt PJ, Pooler BD, Lauder T, del Rio AM, Bruce RJ, Binkley N. Opportunistic screening for osteoporosis using abdominal computed tomography scans obtained for other indications. Ann Intern Med 2013;158:588–95.
41. World Medical Association. World Medical Association Declaration of Helsinki: ethical principles for medical research involving human subjects. JAMA 2013;310:2191–4.
42. Tepper JE, Foote RL, Michalski JM. Gunderson and Tepper's clinical radiation oncology. Philadelphia, PA: Elsevier; 2021.
43. Genant HK, Wu CY, van Kuijk C, Nevitt MC. Vertebral fracture assessment using a semiquantitative technique. J Bone Miner Res 1993;8:1137–48.
44. Wade SW, Strader C, Fitzpatrick LA, Anthony MS, O'Malley CD. Estimating prevalence of osteoporosis: examples from industrialized countries. Arch Osteoporos 2014;9:182.
45. Blake GM, Fogelman I. The role of DXA bone density scans in the diagnosis and treatment of osteoporosis. Postgrad Med J 2007; 83:509–17.

ROJ Radiation Oncology Journal

Original Article

pISSN 2234-1900 · eISSN 2234-3156
Radiat Oncol J 2025;43(1):40-48
https://doi.org/10.3857/roj.2024.00521

Planning evaluation of stereotactic magnetic resonance–guided online adaptive radiosurgery for kidney tumors close to the organ at risk: is it valuable to wait for good timing to perform stereotactic radiosurgery?

Takaya Yamamoto, Shohei Tanaka, Noriyoshi Takahashi, Rei Umezawa, Yu Suzuki, Keita Kishida, So Omata, Kazuya Takeda, Hinako Harada, Kiyokazu Sato, Yoshiyuki Katsuta, Noriyuki Kadoya, Keiichi Jingu

Department of Radiation Oncology, Tohoku University Graduate School of Medicine, Sendai, Japan

Received: August 9, 2024
Revised: October 12, 2024
Accepted: October 30, 2024

Correspondence:
Takaya Yamamoto
Department of Radiation Oncology, Tohoku University Graduate School of Medicine, 1-1 Seiryo-machi, Aoba-ku, Sendai 980-8574, Japan
Tel: +81-22-717-7312
E-mail: takaya.yamamoto.c3@tohoku.ac.jp
ORCID:
https://orcid.org/0000-0003-3562-1037

Purpose: This study aimed to investigate changes in target coverage using magnetic resonance–guided online adaptive radiotherapy (MRgoART) for kidney tumors and to evaluate the suitable timing of treatment.

Materials and Methods: Among patients treated with 3-fraction MRgoART for kidney cancer, 18 tumors located within 1 cm of the gastrointestinal tract were selected. Stereotactic radiosurgery planning with a prescription dose of 26 Gy was performed using pretreatment simulation and three MRgoART timings with an adapt-to-shape method. The best MRgoART plan was defined as the plan achieving the highest percentage of planning target volume (PTV) coverage of 26 Gy. In clinical scenario simulation, MRgoART plans were evaluated in the order of actual treatment. Waiting for the next timing was done when the PTV coverage of 26 Gy did not achieve 95%–99% or did not increase by 5% or more compared to the pretreatment plan.

Results: The median percentages of PTV receiving 26 Gy in pretreatment and the first, second, and third MRgoART were 82% (range, 1 to 99), 63% (range, 7 to 99), 88% (range, 31 to 99), and 95% (range, 3 to 99), respectively. Comparing pretreatment simulation plans with the best MRgoART plans showed a significant difference ($p = 0.025$). In the clinical scenario simulation, 16 of the 18 planning series, including nine plans with 95%–99% PTV coverage of 26 Gy and seven plans with increased PTV coverage by 5% or more, would be irradiated at a good timing.

Conclusion: MRgoART revealed dose coverage differences at each MRgoART timing. Waiting for optimal irradiation timing could be an option in case of suboptimal timing.

Keywords: Radiotherapy, Stereotactic technique, Kidney cancer, Radiotherapy planning, MR-Linac, MR-guided online adaptive radiotherapy

Introduction

Set-up accuracy is important for patients receiving radiotherapy. Current techniques of image-guided radiotherapy such as radiotherapy using cone-beam computed tomography (CT) provide accurate set-up and high repeatability [1,2]. If there are remaining issues, the relative positions of organs and tumors may not be consistent at each time. Kidney cancer is usually located near the stomach, duodenum, small intestine, and colon. The relative positions of these radiosensitive organs and kidney cancer can be changed by various factors including peristalsis, accumulation of food or feces residue, intestinal gases, and level of muscular ten-

© 2025 The Korean Society for Radiation Oncology
This is an Open Access article distributed under the terms of the Creative Commons Attribution Non-Commercial License (http://creativecommons.org/licenses/by-nc/4.0/) which permits unrestricted non-commercial use, distribution, and reproduction in any medium, provided the original work is properly cited.

sion at the time of treatment. One solution for these issues is the use of magnetic resonance (MR)–guided online adaptive radiotherapy (MRgoART) with Unity MR-Linac (Elekta Unity, Elekta, Stockholm), which is equipped with a linear accelerator and a 1.5 Tesla magnetic resonance imaging (MRI) system [3]. In Unity MR-Linac, MR images can be used for radiotherapy image guidance: patients' set-up and target shift (adapt-to-position method). The adapt-to-shape (ATS) method, which provides modification of tumor and organ delineation, can also be used with Unity MR-Linac. Optimization recalculation based on the modification is performed immediately before each fraction, and doses based on the recalculated plan are delivered [4]. In this way, inter-fractional relative position changes between kidney cancer and surrounding organs are modified, and more precise radiotherapy can be delivered than adapt-to-position method. Here, a new question arises regarding MRgoART: when kidney cancer is located adjacent to the small bowel, leading to a disturbance of sufficient radiotherapy dose delivery, could this situation be changed on another day? The timing of irradiation might be more important in hypofractionated radiotherapy especially in single-fraction radiotherapy (stereotactic radiosurgery [SRS]) which has been reported to provide better local control than multifraction radiotherapy [5]. In this planning study, a kidney lesion located near the gastrointestinal tract was simulated for SRS using the ATS method. The purpose of this study was to estimate the delivery dose to targets at each MRgoART timing and to investigate the values of waiting for good timing to perform SRS.

Materials and Methods

1. Patient and tumor selection

Patients who received stereotactic radiotherapy (SRT) for primary kidney cancer using the 1.5 Tesla Unity MR-Linac system between February 2022 and February 2024 at Tohoku University Hospital were identified from our database. Targeted tumors that were located within 1 cm from the organs at risk (OARs) were selected. In this study, the OARs included the stomach, duodenum, small bowel, and colon (gastrointestinal tract). Other non-irradiated tumors such as cystic lesions located within 1 cm from the OARs were identified with a limitation of one tumor per kidney. A flowchart of the selection for this study is shown in Supplementary Fig. S1. All eligible tumors were replanned for SRS and analyzed.

2. Set-up and SRT procedure in actual treatment

Patients were placed in the supine position with or without a waist belt for abdominal compression (Beruetto, Taketora, Kanagawa, Japan). At the time of pretreatment simulation, both MRI and CT scans were performed for radiotherapy planning. At each treatment, patients were immobilized at the same position as that for pretreatment planning, and then a T2-weighted MRI for MRgoART was obtained. The pretreatment contours were adapted by deformable image registration onto the online planning MRI and the contours were manually modified. Then, optimization recalculation was performed, checked, verified, and finally the beam was delivered. Our treatment workflow of Unity MR-Linac was described elsewhere [6]. The step-and-shoot method of intensity-modulated radiotherapy with 7 MV flattening-filter-free photons was used for the radiotherapy treatment plan. The interval between each fraction was at least 40 hours, and the overall treatment time was within 14 days.

3. Contouring and planning simulation in this study

Contouring and planning were performed in Monaco v5.51.11 (Elekta, Stockholm). The eligible tumors, including both the irradiated tumors and non-irradiated tumors, were contoured as exhalation phase gross tumor volume (GTV) on a T2-weighted planning MR image of the exhalation phase using a breathing navigator [7]. The inhalation phase GTV was also contoured from the inhalation phase of T2-weighted planning MR image. Then the internal target volume (ITV) was created from the exhalation phase GTV by adding minimum asymmetric margins to fully cover the inhalation phase GTV. The planning target volume (PTV) was created from the ITV plus 0.5 cm for all directions to account for inter-fractional tumor motion variation and intra-fractional respiratory and positioning uncertainties. The PTV was not trimmed in this study to facilitate easier comparison of the dose coverage change of the PTV although some institutions report trimming the PTV to avoid overlap with the OAR [8].

When SRT with the ATS method was used, only T2-weighted MR image of the exhalation phase was scanned. The exhalation phase GTV was recontoured on this MRI, and then the ITV was created from the exhalation phase GTV by adding the same margin as that in the pretreatment planning MRI. The ITV plus 0.5 cm margin was used to define the PTV. The PTV was used for motion monitoring, and the GTV was assessed to ensure it remained within the PTV during respiratory motion on the treatment day using cine MRI [6]. If the GTV moved beyond the PTV, the abdominal belt was retightened. In cases where the GTV still exceeded the PTV despite retightening the belt, the PTV margin was expanded beyond 0.5 cm. Following this, the OAR was recontoured, and inter-fractional changes and movements of the OAR were modified. However, additional margins for intra-fractional changes were not applied to the OARs, based on a prospective study in which planning organ-at-risk volume margins were not mandatory, even though the ATS

method was not used [9].

In this study, SRT was planned as single-fraction radiotherapy, i.e., SRS. Twenty-six Gy was delivered to cover the highest percentage, up to 99%, of the PTV, and 32.5 Gy was delivered to 0.03 cm^3 of the PTV (80% isodose), adhering strictly to the upper limit of the OAR dose constraints (Table 1). The highest percentage of PTV coverage by the prescribed dose of each plan was investigated. The prescribed dose and dose constraints were based on the protocol of clinical trial (TROG 15.03) and other well-known constraints [9,10]. We created 18 planning series: 18 pretreatment simulation plans and 54 MRgoART plans (3 MRgoART plans per 1 tumor). The MRgoART plan was created as three separate SRS plans obtained from the 3-fraction MRgoART for kidney cancer. The ATS method was used in all MRgoART plans. In all pretreatment simulation plans and MRgoART plans, dose-volume data were evaluated using the following parameters: the percentage of the PTV covered by prescribed dose (26 Gy), the minimum dose covering at least 99% of the PTV, ITV, and GTV, mean doses of the PTV, ITV and GTV, the minimum dose covering at least 0.03 cm^3 of the PTV, ITV and GTV, prescription isodose volume (PIV) which is the volume covered by the 26 Gy isodose line, prescription isodose target volume (PITV) which is the target volume covered by the 26 Gy isodose line, conformity index (CI) which is calculated as PITV/PIV, Paddick conformity index (PCI) which is calculated as (PITV)2/(PTV × PIV), homogeneity index (HI) which is calculated as $(D_{2\%}–D_{98\%})/D_{50\%}$ where $D_{x\%}$ is the minimum dose covering at least x% of the PTV, and OAR doses [11-13]. The best and worst MRgoART plan were defined as the plan that achieved the highest and the lowest percentage of the PTV coverage of the prescribed dose. We also evaluated the magnitude of overlap between the PTV and gastrointestinal tract, as well as between the PTV plus 0.5 cm and the gastrointestinal tract, in both pretreatment and MRgoART plans.

Table 1. Dose constraints for stereotactic radiosurgery in the planning study

Organ	Volume	Limitation
Skin (0.5 cm subcutis)	1.5 cm^3	< 18 Gy
Spinal canal	0.03 cm^3	< 12 Gy
Stomach	0.03 cm^3	< 18.3 Gy
	5 cm^3	< 13.9 Gy
Duodenum	0.03 cm^3	< 18.3 Gy
	5 cm^3	≤ 13.9 Gy
Small bowel	0.03 cm^3	< 18.3 Gy
	5 cm^3	< 11.9 Gy
Colon	1.5 cm^3	< 26 Gy
Contralateral kidney	V10 Gy	≤ 33%
Ipsilateral kidney–ITV	1.5 cm^3	ALARA
	V10 Gy	ALARA

V10 Gy, percentage volume of the kidney receiving at least 10 Gy; ITV, internal target volume; ALARA, as low as reasonable achievable.

4. Statistical and simulated clinical treatment analysis

A two-sided Wilcoxon signed-rank sum test was used to compare pretreatment simulation plans and MRgoART plans. The Pearson's correlation coefficients were calculated to measure the strength and direction of the relationship between two factors. A p-value less than 0.05 was defined as significant. Statistical analyses were performed using EZR version 1.54 (Saitama Medical Center, Jichi Medical University, Saitama, Japan), a modified version of R commander (R Foundation for Statistical Computing, Vienna, Austria) [14].

To reveal the effectiveness of waiting for good timing to perform SRS in a clinical setting, clinical scenario simulation which was the evaluation of MRgoART plan in the order of actual treatment was performed. In the clinical MRgoART simulation, each plan selected the maximum coverage (up to 99%) of the PTV within the dose constraints of the OARs and a change in the PTV coverage by 5% was used as a cut-off. This is because although the TROG 15.03 trial required 99% prescribed dose coverage of the PTV, a PTV coverage of 95% (within a 4% change) was acceptable to fulfill the dose constraints of the OAR [9]. If the PTV coverage decreased from 99% to 94% (5% decrease), the plan would be considered the protocol violation. Therefore, this simulation used the 5% difference as the cut-off. If the prescribed dose (26 Gy) covered 95% or more of the PTV within the dose constraints, the plan was acceptable and SRS would be performed [9]. If the prescribed dose coverage of the PTV improved by 5% or more from pretreatment plans within the dose constraints, the plan was also regarded as acceptable and SRS would be performed. MRgoART timing of these two plans was regarded as good timing. On the other hand, the timings of other MRgoART plans in which the change of PTV coverage of the prescribed dose was within 5% (plan with almost no difference) or decreased by 5% or more to fulfill the dose constraints were regarded as fair timing and bad timing, respectively. MRgoART plans of these two timings were unacceptable, and they proceeded to the next round of MRgoART. Similarly, the MRgoART plans for the remaining tumors were estimated at the second and third MRgoART timings. Finally, all remaining patients would be treated at the third adaptive radiotherapy (ART).

Results

Eighteen tumors met the inclusion criteria: five tumors were actually irradiated and 13 tumors were not irradiated (Supplementary Fig. S1). The characteristics of 14 patients and 18 tumors used for

https://doi.org/10.3857/roj.2024.00521

analysis in this study are summarized in Table 2. The median overall treatment time was 8 days (range, 7 to 8) and all intervals between each fraction were 40 hours or more. There was no patient who needed the PTV margin beyond 0.5 cm on the treatment day. The results of pretreatment simulation planning and MRgoART planning using ATS are summarized in Table 3. Among these factors, Spearman correlation coefficients between the percentage of PTV covered by the prescribed dose and PIV, PITV, CI, PCI, HI, the overlap between the PTV and gastrointestinal tract, the overlap between the PTV plus 0.5 cm and gastrointestinal tract, and the minimum dose covering at least 1.5 cm^3 of the ipsilateral kidney were 0.48 ($p < 0.001$), 0.44 ($p < 0.001$), 0.10 ($p = 0.378$), 0.88 ($p < 0.001$), −0.71 ($p < 0.001$), −0.27 ($p = 0.020$), −0.35 ($p = 0.002$), 0.77 ($p < 0.001$), respectively. Among the 18 planning series, 4 planning series achieved 100% dose coverage of 99% of the PTV through pretreatment planning and MRgoART. Other series included at least one plan that required a reduction of the prescribed dose coverage of the PTV to fulfill the dose constraints of the OAR. Among these plans that did not achieve 100% dose coverage of 99% of the PTV, the dose coverage limiting OARs were the stomach in one plan, the duodenum in 14 plans, the small bowel in 29 plans, and the colon in four plans. The prescribed dose moderately or greatly differed at the MRgoART timing, as shown in Table 3. Some examples are shown in Supplementary Figs. S2 and S3. In Supplementary Fig. S2, no overlap between PTV and OARs was observed on the day (A and B), however,

Table 2. Characteristics of patients and tumors in the planning study

Category	Median (range) or distribution
No. of patients and kidneys	14 patients and 28 kidneys
Age (years)	77 (69–83)
Sex	Male: 11, Female: 3
Waist belt	Yes: 13, No: 1
Eligible tumor location	Right kidney: 10, Left kidney: 8
PTV of eligible tumor (cm^3)	20.0 (2.9–65.7)

PTV, planning target volume.

Table 3. Summary of the parameters at pretreatment simulation timing (planning), first timing (MRgoART 1), second timing (MRgoART 2), and third timing (MRgoART 3)

Parameter	Planning			MRgoART 1			MRgoART 2			MRgoART 3		
	Median	Q1–Q3	Range	Median	Q1–Q3	Range	Median	Q1–Q3	Range	Median	Q1–Q3	Range
PTV (cm^3)	20.0	7.9–31.9	2.8–65.3	20.4	7.5–31.6	3.6–63.9	21.9	7.5–30.8	3.6–70.1	21.4	7.8–30.9	4.0–69.5
% of PTV receiving 26 Gy (%)	82	49–99	1–99	63	39–99	7–99	88	55–99	31–99	95	65–99	3–99
PIV (cm^3)	14.7	6.2–32.3	0.1–60.6	13.0	8.9–24.3	0.6–65.8	13.3	9.3–32.0	2.6–71.1	16.3	9.9–28.5	1.4–73.3
PITV (cm^3)	14.4	5.0–29.6	0.1–53.6	12.3	5.2–20.4	0.3–54.3	13.1	5.5–24.3	1.5–62.3	14.7	5.2–42.9	0.5–58.4
Dose of covering 99% PTV (Gy)	19.4	15.3–26.0	12.7–26.0	18.5	14.7–26.0	13.4–26.0	23.4	15.5–26.0	14.3–26.0	23.4	15.9–26.0	11.7–26.0
Dose of covering 99% ITV (Gy)	27.3	19.8–31.1	14.9–31.7	25.2	19.8–30.6	15.7–34.5	27.2	22.4–31.0	17.7–33.7	29.3	20.4–31.0	14.2–34.1
Dose of covering 99% GTV (Gy)	27.4	24.6–31.6	17.1–32.5	26.4	24.1–31.3	19.4–35.8	28.2	25.7–32.1	20.1–33.8	29.6	24.9–31.3	17.1–36.5
Mean PTV dose (Gy)	28.4	25.2–30.3	19.0–31.8	27.0	24.4–30.1	20.7–34.0	29.0	25.5–30.7	24.1–33.0	29.6	26.9–30.5	20.7–34.4
Mean ITV dose (Gy)	30.5	26.4–33.0	19.4–34.3	28.7	26.6–32.5	22.8–36.3	30.7	27.4–33.2	23.9–35.7	32.0	27.9–33.2	22.0–37.9
Mean GTV dose (Gy)	31.1	27.3–33.2	20.0–34.7	30.6	27.4–32.9	22.1–36.7	31.4	28.6–36.3	25.1–36.3	32.4	29.3–33.5	21.3–38.9
$D_{0.03cc}$ of PTV (Gy)	33.7	30.8–34.8	26.1–36.7	33.2	29.6–35.2	26.6–37.3	33.6	31.8–35.0	29.0–38.4	34.4	33.3–35.5	26.7–40.2
$D_{0.03cc}$ of ITV (Gy)	33.7	30.6–34.8	24.4–36.7	32.9	29.6–34.2	24.8–37.2	33.6	31.8–35.0	28.2–38.4	34.4	33.1–35.2	25.0–40.0
$D_{0.03cc}$ of GTV (Gy)	33.6	30.6–34.8	20.9–36.7	32.8	29.6–34.2	22.2–37.1	33.6	31.7–34.8	26.7–38.5	34.0	32.2–35.2	22.1–39.9
Conformity index	0.87	0.79–0.98	0.24–1.00	0.89	0.68–0.99	0.29–1.00	0.87	0.68–0.97	0.34–1.00	0.85	0.67–0.92	0.28–1.00
Paddick conformity index	0.75	0.37–0.81	0.01–0.88	0.50	0.27–0.78	0.02–0.91	0.69	0.33–0.83	0.22–0.90	0.78	0.33–0.85	0.02–0.90
Homogeneity index	0.41	0.25–0.57	0.23–0.68	0.36	0.26–0.58	0.22–0.72	0.33	0.26–0.51	0.22–0.63	0.33	0.24–0.58	0.22–0.72
PTV∩GI tract	0.3	0.1–1.5	0.0–9.9	0.3	0.0–1.8	0.0–10.2	0.47	0.0–1.8	0.0–10.2	0.30	0.0–1.20	0.0–10.0
PTV + 0.5 cm∩GI tract	3.4	1.5–7.5	0.1–22.8	3.6	1.3–7.7	0.0–19.1	3.3	0.5–6.5	0.0–22.9	3.4	0.7–5.9	0.1–23.1

MRgoART, magnetic resonance–guided online adaptive radiotherapy; Q1, the first quartile; Q3, the third quartile; PTV, planning target volume; PIV, prescription isodose volume; PITV, prescription isodose target volume; ITV, internal target volume; GTV, gross tumor volume; $D_{0.03cc}$, the minimum dose covering at least 0.03 cm^3 of the structure; PTV∩GI tract, the magnitude of the PTV and the gastrointestinal tract; PTV + 0.5 cm∩GI tract, the magnitude of the PTV plus 1 cm and the gastrointestinal tract.

some overlap between the PTV and small bowel emerged while the duodenum moved away from PTV on another day (C and D). Supplementary Fig. S3 is an example of almost the same axial slice on different days (A, B, C, and D). The magnitude of overlap between PTV and small bowel and overlap between PTV and colon were different on each day, therefore, dose-limiting OARs changed. In addition to organ movement, gastrointestinal delineation was deformed by accumulation of food or feces residue.

The individual data for the percentage of covering the PTV by 100% of the prescribed dose (26 Gy) at pretreatment and three times of MRgoART are shown in Fig. 1. The difference between pretreatment simulation plans and MRgoART plans ranged from a 78% increase to a 92% decrease, with a mean ± standard deviation of –2.7% ± 26.5%. Among the MRgoART SRS plans, the best and worst MRgoART plans are summarized in Table 4. A comparison of pretreatment simulation plans and the best MRgoART plans showed significant changes in all of the parameters of PTV, ITV, and GTV. On the other hand, a comparison of pretreatment simulation plans and the worst ART plans showed no significant change in any of the parameters. There were only six of the 18 planning series (33%) that consistently showed change in PTV coverage of the prescribed dose within 5% at all timings.

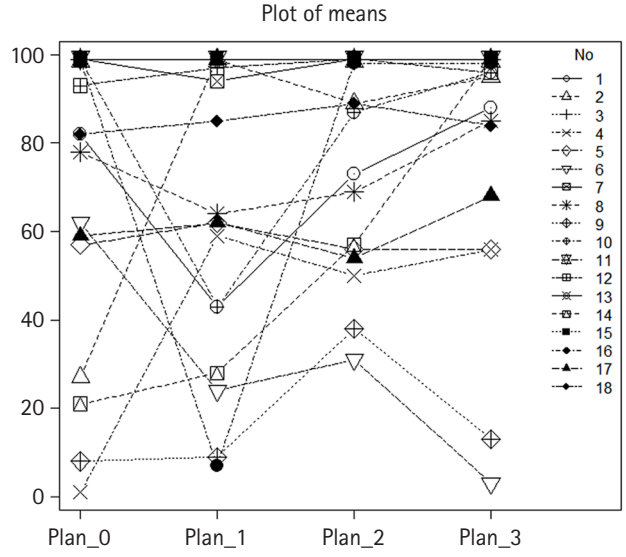

Fig. 1. The individual data for the percentage of the planning target volume (PTV) covered by 100% of the prescribed dose (26 Gy) within the upper limit of the dose constraints of organs at pretreatment and three times of magnetic resonance–guided online adaptive radiotherapy. The vertical axis shows the percentage of the PTV covered by the prescribed dose. On the horizontal axis, Plan_0 represents the results of pretreatment simulation data, while Plan_1, Plan_2, and Plan_3 represent the study results of online adaptive radiotherapy using the first, second, and third fraction data, respectively, in the order of actual 3-fraction radiotherapy.

To estimate the optimal timing to perform SRS, the MRgoART plans were investigated in the order of actual treatment (Fig. 2). Seven of the pretreatment simulation plans showed 95% or more of the PTV covered by the prescribed dose, and these plans would fall into only two categories at MRgoART: achieving 95%–99% PTV coverage by the prescribed dose or experiencing a decline of 5% or more in PTV coverage by the prescribed dose. On the other hand, one plan showed 5% or less PTV coverage by the prescribed dose and this plan would never show a decline of 5% or more in PTV coverage by the prescribed dose. At the first MRgoART, six of the 18 plans achieved 95% or more PTV coverage by the prescribed dose. These six plans consisted of four plans with 99% PTV coverage at both the pretreatment timing and the first MRgoART timing, and the other two plans showed an increase from less than 95% PTV coverage at pretreatment simulation. Additionally, two plans and one plan showed 95% or more PTV coverage by the prescribed dose at the second MRgoART timing and third MRgoART timing, respectively. Two plans achieved more than 5% increase from the pretreatment simulation plan at the first MRgoART timing, and two plans and three plans achieved more than 5% increase at the second MRgoART timing and MRgoART timing, respectively. At the last chance of MRgoART, there was one tumor that showed almost no difference in the plan from the pretreatment simulation plan and there was only one tumor that showed a more than 5% decrease in the prescribed dose coverage of PTV from the pretreatment simulation plan. In summary, 16 of the 18 planning series would be irradiated at a good timing within the three-time chance of MRgoART, whereas nine of the 18 planning series would be irradiated at a good timing at first MRgoART.

Discussion and Conclusion

Although this study was a planning study, to the best of our knowledge, this study is the first study in which dose coverage differences at MRgoART timing was investigated. MRgoART has been used for many sites and many kinds of cancers including the location that was close to OAR [15-20]. In this study, the best benefit-risk balance of kidney tumors located close to the OAR differed depending on the MRgoART timing (Fig. 1). If the benefit-risk balance leans towards risks, radiation oncologists might postpone performing radiotherapy, especially SRS, with the expectation that the next chance of MRgoART will show a better balance. This expectation and waiting for next timing is possibly one of the options considering the result of Fig. 1. Because there was no guidance to irradiate or to wait, the clinical treatment scenario simulation was investigated using a 5% difference as the cut-off (Fig. 2). Although we

https://doi.org/10.3857/roj.2024.00521

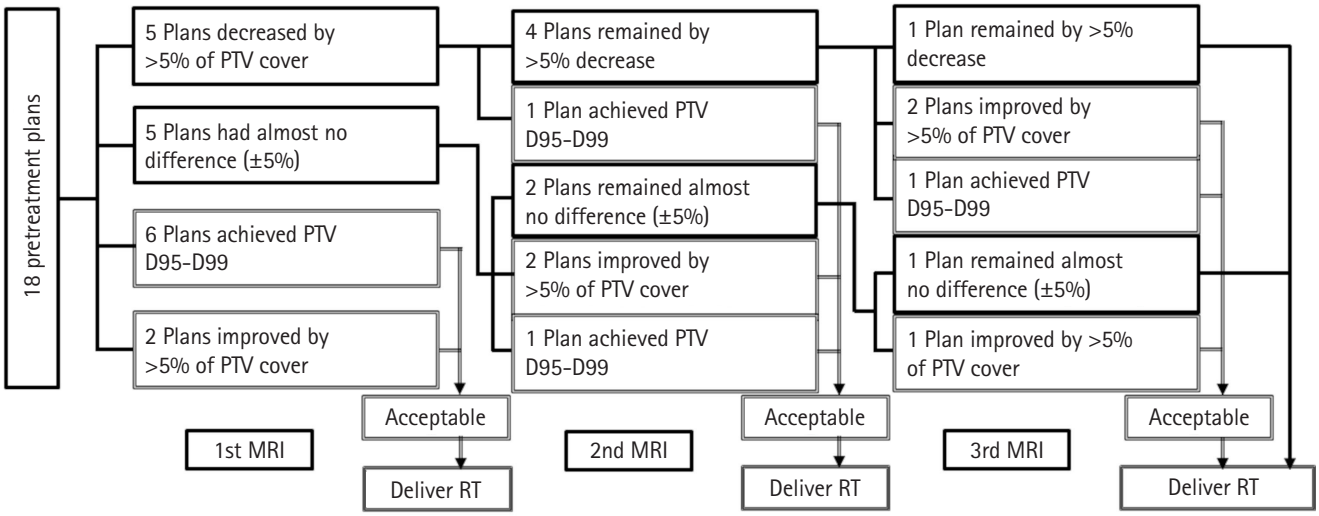

Fig. 2. Timing schema of the results of clinical scenario simulation: online stereotactic adaptive radiosurgery for a kidney tumor located near organs at risk. magnetic resonance–guided online adaptive radiotherapy for stereotactic radiosurgery (SRS) was performed using the adapt-to-shape method for all tumors. In the first timing (1st magnetic resonance imaging [MRI]), if planning target volume (PTV) coverage achieved 95%–99% of the prescribed dose (26 Gy) or improved by 5% or more, the timing was judged to be good and SRS would be performed. Others would proceed to the next timing (second timing and third timing) of adaptive radiotherapy (2nd MRI and 3rd MRI, respectively). The third timing was the last chance, and all remaining tumors would undergo SRS regardless of good or bad timing. RT, radiotherapy.

Table 4. Summary of target doses at different timings

Parameter	Planning		Best MRgoART timing			Worst MRgoART timing		
	Median	Range	Median	Range	p-value	Median	Range	p-value
% of PTV receiving 26 Gy (%)	82	1–99	97	31–99	0.025	60	3–99	0.396
Dose of covering 99% PTV (Gy)	19.4	12.7–26.0	25.1	14.3–26.0	0.042	18.5	11.7–26.0	0.286
Dose of covering 99% ITV (Gy)	27.3	14.9–31.7	30.4	17.7–34.5	0.018	24.9	14.2–30.7	0.074
Dose of covering 99% GTV (Gy)	27.4	17.1–32.5	30.6	20.4–36.5	0.034	26.2	17.1–32.0	0.196
Mean PTV dose (Gy)	28.4	19.0–31.8	30.1	24.1–34.4	0.024	26.7	20.7–31.1	0.196
Mean ITV dose (Gy)	30.5	19.4–34.3	32.7	25.9–37.9	0.015	28.4	22.0–33.7	0.229
Mean GTV dose (Gy)	31.1	20.0–34.7	33.0	26.3–38.9	0.020	29.0	21.3–34.1	0.212
$D_{0.03cc}$ of PTV (Gy)	33.7	26.1–36.7	34.7	29.0–40.2	0.018	32.3	26.6–36.4	0.098
$D_{0.03cc}$ of ITV (Gy)	33.7	24.4–36.7	34.7	28.2–40.0	0.023	32.3	24.8–36.4	0.142
$D_{0.03cc}$ of GTV (Gy)	33.6	20.9–36.7	34.6	26.8–39.9	0.022	31.9	17.1–32.0	0.229

This table summarizes the stereotactic radiosurgery doses delivered to the targets at pretreatment simulation timing (Planning), the best magnetic resonance–guided online adaptive radiotherapy adaptive radiotherapy timing (Best MRgoART timing), and the worst MRgoART timing (Worst MRgoART timing). Statistical comparisons were performed between Planning and Best MRgoART timing, and between Planning and Worst MRgoART timing, using the two-sided Wilcoxon signed-rank sum test.
MRgoART, magnetic resonance–guided online adaptive radiotherapy; PTV, planning target volume; ITV, internal target volume; GTV, gross tumor volume; $D_{0.03cc}$, the minimum dose covering at least 0.03 cm^3 of the structure.

investigated only three timings for SRS, the result of the clinical scenario simulation would be promising. Among the 18 tumors, 16 tumors would be irradiated at good timing, one tumor would be irradiated at fair timing and one tumor would be irradiated at bad timing using the three timings, in comparison to five tumors irradiated at fair timing and five tumors irradiated at bad timing at the first ART. These results encourage the expectations of radiation oncologists that the next timing of MRgoART will show a better benefit-risk balance, with the caution that each timing involved non-consecutive days and that does not guarantee the future outcome. It was also noted that the good timing was not always a good candidate for SRS. In Fig. 1, patients number 6 and 9 had consistently low percentages of PTV coverage by prescribed dose and were not considered good candidates for SRS. Another method which improve the benefit-risk balance is to reduce the ITV and PTV margins. The future respiratory gating system (known as Com-

prehensive Motion Management in Elekta Unity, Elekta, Stockholm) will provide a better benefit-risk balance.

SRS for kidney cancer has been reported to have a better local control rate than multifraction radiotherapy and has shown good local control in prospective studies [5,21]. Multifraction radiotherapy, such as a 10-fraction schedule, is an option to deliver a higher total dose to the target when kidney cancer close to OAR [22]. However, there are some difficulties, especially in terms of machine time of the Unity MR-Linac. MRgoART with the ATS method takes a long treatment time, with a median time of 42 minutes and a wide range from 30 to 65 minutes [23]. Additionally, MRI for pretreatment radiotherapy planning was often performed using the Unity MR-Linac system and it took further machine time. The disadvantage can affect the choice of multifraction radiotherapy. In our clinical scenario simulation, if SRS was selected, nine of the 18 tumors and six of the 18 tumors required the second MRgoART timing and third MRgoART timing, respectively. Although there is no data showing that SRS for kidney cancer with timing strategy is equivalent to multifraction radiotherapy, it can help to reduce machine time on the Unity MR-Linac.

MRgoART of Unity MR-Linac also has an adapt-to-position method, which provides only a shift of the plan to the patient. The adapt-to-position method is relatively simple and therefore it takes a shorter time than that for the ATS method [23]. However, the ATS method has the advantage of modifications of the relative positions of organs and tumors that cannot be made by using the adapt-to-position method of MR-Linac or by using the method for shift and rotation of patients in the most modern Linac [4]. The ATS method has been shown to be more effective than the adapt-to-position method for prostate cancer and head-and-neck cancers [24,25]. When kidney tumors are adjacent to the OARs, the effectiveness of the ATS method will be enhanced, and the ATS method will offer the best benefit-risk balance immediately before irradiation. It can be deduced from the results of this study that only six of the 18 plan series consistently showed that the change in PTV coverage of the prescribed dose was within 5% at all timings, and the other 12 plan series potentially included adaptive plans of underdose PTV or overdose OAR by the adapt-to-position method. Therefore, the ATS method is desirable for kidney tumors when they are adjacent to the OAR.

A comparison of the pretreatment simulation plans with the best MRgoART plans or the worst MRgoART plans showed a significant difference only between the pretreatment simulation plans and the best plans. This was unexpected to some extent because seven of the 18 plans showed 95% or more PTV coverage by the prescribed dose at pretreatment simulation, which were difficult to improve the coverage in the MRgoART plan. On the other hand, only one plan showed 5% or less PTV covered by the prescribed dose at pretreatment simulation, which hardly worsened the coverage in the MRgoART plan. Although there was such an unexpected result, the result would encourage expecting to obtain the best MRgoART plan at another timing.

There are some limitations in this study. Firstly, this was a planning simulation study using retrospective data, and some of the eligible tumors in this study were not actually irradiated. In ATS, only T2-weighted MR images of the exhalation phase were scanned, and therefore, inter-fractional changes in the ITV were not considered. In the clinical scenario simulation, optimal timing was assessed using retrospective data without consideration of future MRI data, which compromises the validity of the clinical scenario. In addition, a change of 5% was used as a cut-off value; however, the 5% value was not based on clinical evidence and the optimal cut-off value was not investigated. Similarly, the three timing assessments were used for each patient in this study, but how long one should wait for the optimal timing was not investigated. Furthermore, the clinical effectiveness of a PTV coverage of less than 95% remains unclear. Therefore, the results of this study are not always applicable to clinical treatment, and further evidence is needed.

In conclusion, MRgoART revealed that target coverage by the prescribed dose and the dose received by the target were different at each MRgoART timing, and the difference between the pretreatment simulation and the best MRgoART timing was significant. In a clinical scenario simulation, waiting for a good irradiation timing might be one of the option in case of suboptimal timing.

Statement of Ethics

This study was approved by the Ethics Committee of Tohoku University Hospital (reference number: 2023-1-960) and all research conducted adhered to the tenets of the Declaration of Helsinki. Informed consent was waived due to the retrospective study design. All patients were guaranteed the opportunity to opt out of participation in this study by receiving information about this study via the Internet, and written informed consent as a part of general consent for the utilization of treatment data was obtained from all patients.

Conflict of Interest

Keiichi Jingu has received financial support from Elekta KK. Others declare that they have no known competing financial interests or personal relationships relevant to this work.

https://doi.org/10.3857/roj.2024.00521

Acknowledgments

We are grateful to the radiation technologists at Tohoku University Hospital who contributed to the acquisition of MRI data. We acknowledged S.E.S. Translation and Proofreading Services (Sapporo, Japan) for the language proofreading of this manuscript.

Funding

None declared.

Author Contributions

Conceptualization, TY, NT; Investigation and methodology, TY, ST, NT, KT, KS; Acquisition of data, TY, NT, RU, YS, KK, SO, HH, KJ; Formal analysis, TY; Data curation, TY, ST; Validation, TY, ST, KJ; Writing - original draft, TY; Writing - review & editing: TY, ST, NT, RU, YS, KK, SO, KT, HH, KS, YK, NK, KJ; Final approval: TY, ST, NT, RU, YS, KK, SO, KT, HH, KS, YK, NK, KJ.

Data Availability Statement

The data that support the findings of this study are available from the corresponding author upon reasonable request.

Supplementary Materials

Supplementary materials can be found via https://doi.org/10.3857/roj.2024.00521.

References

1. Jaffray DA, Siewerdsen JH, Wong JW, Martinez AA. Flat-panel cone-beam computed tomography for image-guided radiation therapy. Int J Radiat Oncol Biol Phys 2002;53:1337–49.
2. Guckenberger M, Meyer J, Vordermark D, Baier K, Wilbert J, Flentje M. Magnitude and clinical relevance of translational and rotational patient setup errors: a cone-beam CT study. Int J Radiat Oncol Biol Phys 2006;65:934–42.
3. Raaymakers BW, Lagendijk JJ, Overweg J, et al. Integrating a 1.5 T MRI scanner with a 6 MV accelerator: proof of concept. Phys Med Biol 2009;54:N229–37.
4. Winkel D, Bol GH, Kroon PS, et al. Adaptive radiotherapy: the Elekta Unity MR-linac concept. Clin Transl Radiat Oncol 2019;18:54–9.
5. Siva S, Ali M, Correa RJ, et al. 5-year outcomes after stereotactic ablative body radiotherapy for primary renal cell carcinoma: an individual patient data meta-analysis from IROCK (the International Radiosurgery Consortium of the Kidney). Lancet Oncol 2022;23:1508–16.
6. Takahashi N, Tanaka S, Umezawa R, et al. Beginning of clinical treatment using the 1.5 Tesla MR-Linac system in Japan: a narrative review. Transl Cancer Res 2024;13:1131–8.
7. Regini F, Gourtsoyianni S, Cardoso De Melo R, et al. Rectal tumour volume (GTV) delineation using T2-weighted and diffusion-weighted MRI: implications for radiotherapy planning. Eur J Radiol 2014;83:768–72.
8. Siva S, Ellis RJ, Ponsky L, et al. Consensus statement from the International Radiosurgery Oncology Consortium for Kidney for primary renal cell carcinoma. Future Oncol 2016;12:637–45.
9. Siva S, Chesson B, Bressel M, et al. TROG 15.03 phase II clinical trial of Focal Ablative STereotactic Radiosurgery for Cancers of the Kidney - FASTRACK II. BMC Cancer 2018;18:1030.
10. Timmerman R. A Story of hypofractionation and the table on the wall. Int J Radiat Oncol Biol Phys 2022;112:4–21.
11. Lomax NJ, Scheib SG. Quantifying the degree of conformity in radiosurgery treatment planning. Int J Radiat Oncol Biol Phys 2003;55:1409–19.
12. Paddick I. A simple scoring ratio to index the conformity of radiosurgical treatment plans. Technical note. J Neurosurg 2000;93 Suppl 3:219–22.
13. Prescribing, recording, and reporting photon-beam intensity-modulated radiation therapy (IMRT): contents. J ICRU 2010;10:1–3.
14. Kanda Y. Investigation of the freely available easy-to-use software 'EZR' for medical statistics. Bone Marrow Transplant 2013;48:452–8.
15. de Mol van Otterloo SR, Christodouleas JP, Blezer ELA, et al. Patterns of care, tolerability, and safety of the first cohort of patients treated on a novel high-field MR-Linac within the MOMENTUM study: initial results from a prospective multi-institutional registry. Int J Radiat Oncol Biol Phys 2021;111:867–75.
16. Kishan AU, Ma TM, Lamb JM, et al. Magnetic resonance imaging-guided vs computed tomography-guided stereotactic body radiotherapy for prostate cancer: the MIRAGE randomized clinical trial. JAMA Oncol 2023;9:365–73.
17. Parikh PJ, Lee P, Low DA, et al. A multi-institutional phase 2 trial of ablative 5-fraction stereotactic magnetic resonance-guided on-table adaptive radiation therapy for borderline resectable and locally advanced pancreatic cancer. Int J Radiat Oncol Biol Phys 2023;117:799–808.
18. Henke LE, Olsen JR, Contreras JA, et al. Stereotactic MR-guided online adaptive radiation therapy (SMART) for ultracentral thorax malignancies: results of a phase 1 trial. Adv Radiat Oncol

2019;4:201–9.
19. Rosenberg SA, Henke LE, Shaverdian N, et al. A multi-institutional experience of MR-guided liver stereotactic body radiation therapy. Adv Radiat Oncol 2019;4:142–9.
20. Michalet M, Bettaieb O, Khalfi S, et al. Stereotactic MR-guided radiotherapy for adrenal gland metastases: first clinical results. J Clin Med 2022;12:291.
21. Siva S, Bressel M, Sidhom M, et al. Stereotactic ablative body radiotherapy for primary kidney cancer (TROG 15.03 FASTRACK II): a non-randomised phase 2 trial. Lancet Oncol 2024;25:308–16.
22. Yamamoto T, Kawasaki Y, Umezawa R, et al. Stereotactic body radiotherapy for kidney cancer: a 10-year experience from a single institute. J Radiat Res 2021;62:533–9.
23. Lakomy DS, Yang J, Vedam S, et al. Clinical implementation and initial experience with a 1.5 Tesla MR-Linac for MR-guided radiation therapy for gynecologic cancer: an R-IDEAL stage 1 and 2a first in humans feasibility study of new technology implementation. Pract Radiat Oncol 2022;12:e296–305.
24. Dassen MG, Janssen T, Kusters M, et al. Comparing adaptation strategies in MRI-guided online adaptive radiotherapy for prostate cancer: implications for treatment margins. Radiother Oncol 2023;186:109761.
25. Lim SY, Tran A, Tran AN, et al. Dose accumulation of daily adaptive plans to decide optimal plan adaptation strategy for head-and-neck patients treated with MR-Linac. Med Dosim 2022;47:103–9.

 https://doi.org/10.3857/roj.2024.00521

ROJ Radiation Oncology Journal

Case Report

pISSN 2234-1900 · eISSN 2234-3156
Radiat Oncol J 2025;43(1):49-54
https://doi.org/10.3857/roj.2024.00493

Long-term outcomes of radiotherapy for inoperable benign soft tissue tumors in the skull base or head

Joo-Hyun Chung[1], Hak Jae Kim[1,2,3], Hyun-Cheol Kang[1], Il Han Kim[1], Joo Ho Lee[1,2,3]

[1]*Department of Radiation Oncology, Seoul National University Hospital, Seoul National University College of Medicine, Seoul, Republic of Korea*
[2]*Cancer Research Institute, Seoul National University, Seoul, Republic of Korea*
[3]*Institute of Radiation Medicine, Medical Research Center, Seoul National University Hospital, Seoul, Republic of Korea*

Received: July 26, 2024
Revised: August 26, 2024
Accepted: September 3, 2024

Correspondence:
Joo Ho Lee
Department of Radiation Oncology, Seoul National University Hospital, Seoul National University College of Medicine, 101 Daehak-ro, Jongno-gu, Seoul 03080, Republic of Korea
Tel: +82-2-2072-2819
E-mail: jooholee@snu.ac.kr
ORCID:
https://orcid.org/0000-0001-7248-3214

This study aimed to evaluate the long-term efficacy and complication of radiotherapy for benign soft tissue tumors. Five cases of benign soft tissue tumors (two plexiform neurofibromas, two juvenile nasopharyngeal angiofibromas, and one cavernous sinus hemangioma) who underwent radiotherapy were enrolled. All patients had at least 10 years of follow-up. The median follow-up duration was 12 years (range, 10 to 27). Three patients underwent incomplete excision prior to radiotherapy. Radiation doses were either 54 Gy in 30 fractions or 50.4 Gy in 28 fractions (1.8 Gy per fraction). Every patient achieved complete remission (CR) or near-CR. The tumor volume decreased significantly within the first 2 years of follow-up and continued to decrease slowly up to 10 years; no distinct further decrease in tumor volume was observed after 10 years. One patient developed left mandibular hypoplasia 8 years after radiotherapy. Significant volume decrease was achievable within a few years after radiotherapy in benign soft tissue tumors. Therefore, radiotherapy is a viable option for unresectable or incompletely resected benign soft tissue tumors with a minimum risk of complication.

Keywords: Soft tissue neoplasms, Plexiform neurofibroma, Angiofibroma, Cavernous hemangioma, Radiotherapy

Introduction

Plexiform neurofibromas typically develop along major nerves, and their expansion often results in the destruction and compression of surrounding tissues, leading to considerable morbidity [1]. Plexiform neurofibromas uniquely possess the potential to evolve into a malignant peripheral nerve sheath tumor, a risk of malignancy that is not observed in other classes of neurofibromas [2]. Juvenile nasopharyngeal angiofibroma is a benign yet locally aggressive tumor that predominantly occurs in young males. The most frequent vascular source for juvenile nasopharyngeal angiofibroma is the internal maxillary artery, followed by the ascending pharyngeal artery [3]. Intracranial involvement is seen in approximately 10% to 37% of all juvenile nasopharyngeal angiofibroma cases [4]. Cavernous sinus hemangioma is a rare vascular tumor comprising 1%–3% of all cavernous sinus lesions [5]. These extra-axial, inter-dural, and intra-sinus lesions cause symptoms due to tumor growth and mass effect [6].

Plexiform neurofibromas are typically removed surgically due to discomfort or cosmetic reasons, while juvenile nasopharyngeal angiofibromas are often excised for debulking, with postoperative radiotherapy or watchful waiting employed for extensive lesions. However, benign tumors located at the skull base or head are often at risk of being incompletely resected or deemed inoperable. For cavernous sinus hemangiomas, the risk of massive bleeding often impedes complete excision, making radiotherapy a preferred alternative as either a definitive or adjuvant treatment.

Benign soft tissue tumors require long-term follow-up for evalu-

© 2025 The Korean Society for Radiation Oncology
This is an Open Access article distributed under the terms of the Creative Commons Attribution Non-Commercial License (http://creativecommons.org/licenses/by-nc/4.0/) which permits unrestricted non-commercial use, distribution, and reproduction in any medium, provided the original work is properly cited.

ating efficacies and complications. Here, we investigated five patients with benign soft tissue tumors at the skull base and head to evaluate the long-term efficacy and complications of radiotherapy.

Case Report

From 1990 to 2011, five cases of benign soft tissue tumors (two plexiform neurofibromas, two juvenile nasopharyngeal angiofibromas, and one cavernous sinus hemangioma) who underwent definitive radiotherapy were enrolled. All patients had at least 10 years of follow-up. The median follow-up duration was 12 years (range, 10 to 27). The characteristics of five patients are summarized in Table 1.

1. Plexiform neurofibroma

Patient 1 presented with extensive swelling mass at the left neck site, accompanying pain, and limitation of arm elevation. Cervical (C) spine magnetic resonance image (MRI) showed an extensive mass stretching from the suboccipital area to the C6 level, anteriorly to retropharyngeal space, and posteriorly to the left neural foramen at the vertebral body (Fig. 1A). Diagnostic neck excision showed pathology consistent with plexiform neurofibroma. Complete surgical resection was not feasible due to the extensiveness of the disease; thus, definitive radiotherapy was planned. Using the intensity-modulated radiotherapy (IMRT) technique, 54 Gy in 30 fractions was administered. No acute or late toxicities were observed. The limitation of arm elevation persisted for 6 years after radiotherapy; arm elevation was relieved afterward, and the range of motion normalized 8 years after radiotherapy. The extent of the disease slowly regressed after radiotherapy. The tumor continued to regress up to 6 years after radiotherapy and reached a plateau (Fig. 2).

Patient 2 presented with a slowly growing mass at the left retroauricular area and sleep apnea caused by the growing mass. Paranasal sinuses MRI showed an extensive mass at the left submandibular gland, parapharyngeal space, retropharyngeal space, prevertebral space, and encasing left large extracranial vessels (Fig. 1B). Biopsy was performed at the left retroauricular mass, and pathology was reported as plexiform neurofibroma. The patient underwent tracheostomy prior to radiotherapy to relieve dyspnea caused by the compressing mass. The patient received 50.4 Gy in 28 fractions using 3-dimensional conformal radiotherapy (3D-CRT). Sleep apnea gradually improved over 1 year after radiotherapy. The volume of the mass decreased slowly up to 8 years after radiotherapy, reaching near complete remission (CR) 10 years after radiotherapy (Fig. 2). The patient developed left mandibular hypoplasia 8 years after radiotherapy (Fig. 3).

2. Juvenile nasopharyngeal angiofibroma

Patient 3 presented with slowly progressing nasal obstruction. Paranasal sinuses MRI revealed extensive mass in both pterygopalatine fossa with skull base infiltration (Fig. 1C). Prior to diagnostic excision, angioembolization was done to prevent hemorrhage. An excisional biopsy was performed to alleviate nasal obstruction, and the pathology result reported angiofibroma. Due to extensive infiltration into the skull base, definitive radiotherapy was planned. A total dose of 50.4 Gy in 28 fractions was delivered via 3D-CRT technique. The volume of the mass significantly decreased within 5 years after radiotherapy and reached CR within 10 years after radiotherapy (Fig. 2).

Patient 4 presented with nasal obstruction and frequent epistax-

Table 1. Patient characteristics

	Case number				
	1	2	3	4	5
Histologic diagnosis	Plexiform neurofibroma	Plexiform neurofibroma	Angiofibroma	Angiofibroma	Hemangioma
Age at diagnosis (year)	11	7	7	14	44
Duration of follow-up (year)	12	11	16	27	10
Location	Cervical paravertebral, C2–T1	Lt parapharyngeal space, nasopharynx, oropharynx	Nasal cavity, nasopharynx	Nasal cavity, nasopharynx	Rt cavernous sinus, Rt sphenoid sinus
Initial symptom	Limited range of motion	Sleep apnea	Nasal obstruction	Nasal obstruction, mucosal bleeding	Rt eye blind
Radiotherapy dose	54 Gy/30 fx	50.4 Gy/28 fx	50.4 Gy/28 fx	54 Gy/30 fx	54 Gy/30 fx
Radiotherapy modality	IMRT	3D-CRT	3D-CRT	3D-CRT	3D-CRT
Date (year) of radiotherapy	2009	2008	2003	1990	2009
Outcome	Near-CR	Near-CR	CR	Near-CR	Near-CR
Complication	None with normal growth	Lt mandibular hypoplasia	None with normal growth	None	None

C, cervical; T, thoracic; Lt, left; Rt, right; fx, fractions; IMRT, intensity-modulated radiotherapy; 3D-CRT, 3-dimensional conformal radiotherapy; CR, complete remission.

https://doi.org/10.3857/roj.2024.00493

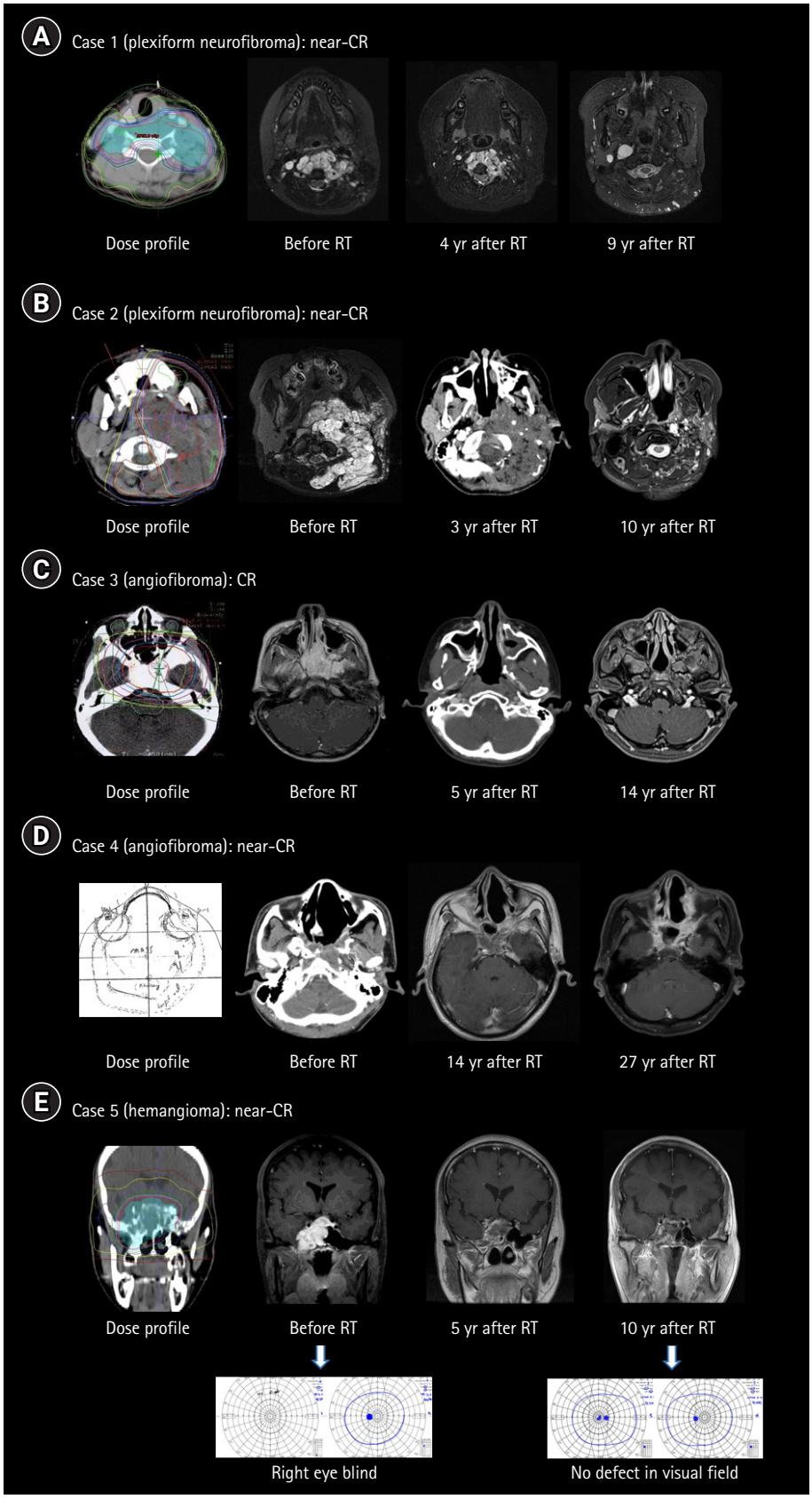

Fig. 1. Dose profiles and images before and after radiotherapy (RT) for cases 1–5 (A–E) are shown. A complete remission (CR) was achieved in case 3 (C), while near-CRs were observed in the others (A, B, D, and E). In case 5, although the right eye was blind prior to RT, visual field defects improved 7 months after RT and maintained throughout the follow-up period (E). yr, year.

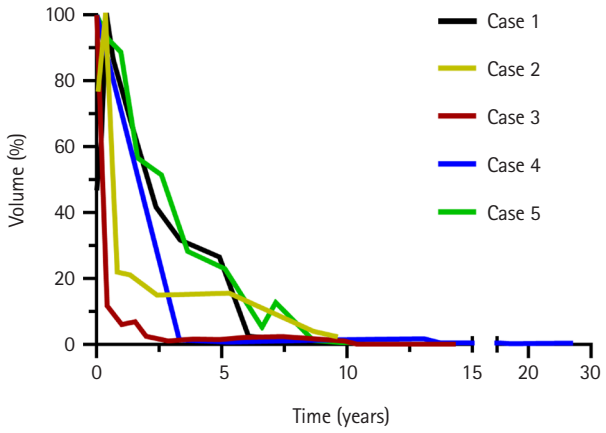

Fig. 2. Volume change after radiotherapy.

is. MRI showed mass infiltration at both nasal cavity, posterior pharyngeal wall, cavernous sinus, and infratemporal fossa extension (Fig. 1D). Intranasal biopsy revealed angiofibroma. Definitive radiotherapy with a total dose of 54 Gy in 30 fractions in 3D-CRT technique was delivered. A significant volume decrease was observed within 2 years after radiotherapy, along with marked improvement in nasal obstruction and no occurence of epistaxis thereafter. Near-CR was reached 3 years after radiotherapy (Fig. 2). No acute or late complications were observed.

3. Cavernous sinus hemangioma

Patient 5 presented with decreased visual acuity. MRI diagnosed a 3.5 cm-sized sellar mass extending to the right cavernous, maxillary, and sphenoid sinus, compressing the optic nerve and chiasm (Fig. 1E). The patient underwent partial resection via transsphenoidal approach and was pathologically diagnosed with capillary hemangioma. However, visual acuity in the right eye deteriorated after the operation, eventually leading to blindness. Postoperative radiotherapy with a total dose of 54 Gy in 30 fractions was delivered via 3D-CRT technique. The patient underwent full recovery in the right visual acuity 7 months after radiotherapy. The volume of the mass decreased constantly throughout 10 years after radiotherapy (Fig. 2). No treatment-related complications occurred.

Discussion

Surgery has always been the treatment of choice when complete removal is possible. However, although benign, advanced soft tissue tumors in the skull base or head often make complete surgical removal challenging. Debulking surgery is the primary goal in such cases, especially for tumors near critical structures such as the spinal cord or airway. Needle et al. [7] reported on 121 children with plexiform neurofibroma undergoing 302 surgeries for 168 tumors over 20 years. Twenty percent of patients with complete resection developed tumor progression. Higher recurrence rates of 39.5% for near-total and 44% for subtotal resections were observed. Tyagi et al. [8] found 80% residual disease and 30% recurrence after surgery in 10 angiofibroma patients, while Fagan et al. [9] reported a 37.5% recurrence after surgery for angiofibroma with intracranial extension. Previous studies reported a notably low rate of total surgical excision and a significant incidence of postoperative morbidity in cavernous sinus hemangiomas [5,10].

Radiotherapy is an effective treatment option for extensive soft tissue tumors not eligible for complete surgical excision. Although benign, disease infiltration into the skull base or intracranial extension makes most patients not amenable to complete excision, as demonstrated in the series of cases presented in this study. Chopra et al. [1] reported four neurofibroma patients treated with radiotherapy (3 patients, 50 to 55 Gy) or stereotactic radiosurgery (SRS) (1 patient, 12.5 Gy) followed from 1.7 to 14.8 years. Local control of 100% was achieved without any significant complications. Mallick et al. [3] reported on 31 patients with unresectable angiofibroma who received 3D-CRT at a median dose of 30 Gy, with a median follow-up period of 36 months. Five-year progression-free survival was 91.7%, with CR in 13 patients, progressive disease in 2, and one case of secondary malignancy. Xin et al. [11] explored 54 patients with giant cavernous sinus hemangiomas who received 50 Gy in 25 fractions of radiation. Every patient experienced symptomatic improvement, with an average tumor reduction of 79.7%, and no significant complications were reported.

Several studies have reported treatment results using stereotactic body radiotherapy (SBRT). A series of studies, including neurofibroma, schwannoma, and meningioma, showed an overall local control rate of over 90% when treated with SBRT of 20–25 Gy within 1 to 5 fractions [12,13]. In the Stanford University series, 24 spinal neurofibromas underwent CyberKnife-based SBRT treatment, with a median dose of 20 Gy over approximately two fractions [12]. Following a median follow-up of 29 months, all lesions were locally controlled, although only 18% showed significant radiographic regression; 17% of patients experienced pain relief, 33% reported worsening pain, and two patients needed surgical resection due to refractory symptoms. On the other hand, other series have found neurofibromas challenging to manage. Sahgal et al. [14] observed one radiographic and one symptomatic failure among 11 spinal neurofibroma patients treated with doses of 21 Gy in 3 fractions and 30 Gy in 3 fractions, respectively, at a median follow-up of 25 months. Wang et al.'s meta-analysis [15] of total 59 cavernous sinus hemangioma patients revealed that 93.2% of patients experienced significant tumor shrinkage following SRS (mean dose, 13.87

 https://doi.org/10.3857/roj.2024.00493

Gy; range 10.0 to 19.0 Gy), with those receiving higher doses showing more tumor shrinkage. Among those 46 patients with cranial nerve impairments before SRS, symptom improvement was achieved in 35 patients. No statistical significance in tumor control between patients treated with or without surgery was observed.

Proton beam therapy (PBT) offers a promising treatment option for angiofibroma, particularly suitable for young patients, as it addresses the concerns of long-term radiation-induced morbidity associated with traditional photon radiotherapy. Hoeltgen et al. [16] compared PBT with conformal photon radiotherapy by analyzing 10 advanced juvenile nasopharyngeal angiofibroma patients treated with PBT at Heidelberg Ion Beam Therapy Center between 2012 and 2022. The local control rate was 100% after a median follow-up of 27.0 months, with reduced estimated risks for neurocognitive impairment and radiation-induced cranial nerve system malignancies compared to photon radiotherapy.

The recent success of MEK inhibitor (MEKi), specifically targeting a downstream effector of RAS, has significantly altered the approach to managing plexiform neurofibromas. Phase I/II clinical trials in children with inoperable, symptomatic plexiform neurofibroma using the MEKi selumetinib showed partial response rates of 71% and 74%, respectively, leading to not only tumor size reduction but also improvement in pain relief [17,18]. Consequently, selumetinib has been approved by the Food and Drug Administration as the first medical therapy for plexiform neurofibroma in children, with similar positive outcomes observed in ongoing phase II trials for adults with symptomatic, inoperable plexiform neurofibroma [19]. Neurofibromas treated with radiotherapy tend to be highly symptomatic and show poor clinical response, partly due to their infiltrative nature leading to unclear margins and higher recurrence risks. Additionally, their association with neurofibromatosis type 1 and its unique potential to evolve into a malignant peripheral nerve sheath tumor not seen in other classes of neurofibromas can complicate treatment effectiveness. The introduction of MEKi in combination with radiotherapy could potentially enhance treatment effectiveness compared to using radiotherapy alone.

In this study, we showed that radiotherapy effectively controlled inoperable benign tumors without severe complications. Tumor volume experienced a significant decrease in the first 2 years of follow-up and continued to decrease gradually over a period of up to 10 years, with no notable further reduction observed after 10 years. Patients experienced a full recovery from dysfunctions such as nasal obstruction and blindness while consistently maintaining either CR or near-CR. Among five patients, only one developed left mandibular hypoplasia 8 years after radiotherapy (Fig. 3). Radiotherapy during childhood frequently poses risks of various late complications, such as growth retardation or secondary malignancies [20]. Patients 2 and 5 received 3D-CRT in 2008 and 2009, respectively, during the period when IMRT was just being gradually introduced. IMRT and proton therapy in the modern radiotherapy era reduced complications, particularly in pediatric patients.

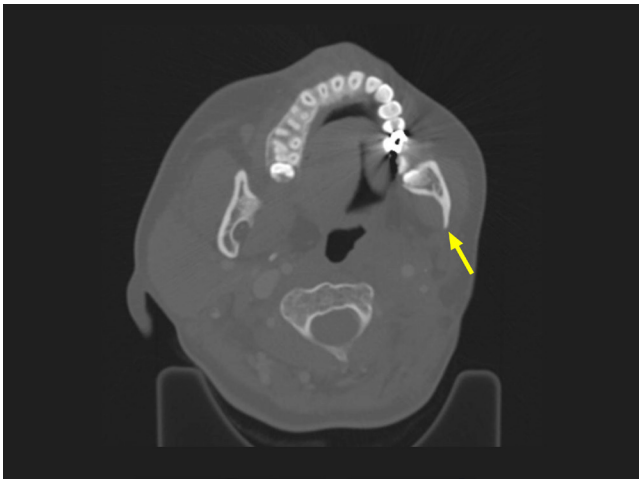

Fig. 3. Left mandibular hypoplasia in patient 2. The patient developed left mandibular hypoplasia 8 years after radiotherapy (arrow).

Our study is limited due to the small number of patients and, as previously noted, includes only a single case of IMRT treatment. Despite the small sample size, this study demonstrates promising outcomes and effective control rates. To achieve more substantial results, further research with a larger patient cohort and advanced radiotherapy technologies such as proton therapy is warranted.

In summary, the radiation dose of 50.4 to 54 Gy inoperable benign soft tissue tumors can successfully be controlled without significant complications: a substantial volume decrease was achievable within a few years, and the tumor volume slowly regresses up to 10 years after radiotherapy, eventually reaching a plateau. Therefore, radiotherapy is recommended as an effective option for unresectable or incompletely resected benign soft tissue tumors with a minimum risk of complication.

Statement of Ethics

This study was reviewed and approved by the Institutional Review Board (IRB) of Seoul National University Hospital (IRB number: H-2003-086-1109), with a waiver of informed consent.

Conflict of Interest

No potential conflict of interest relevant to this article was reported.

Funding

None.

Author Contributions

Conceptualization, IHK; Data curation, JHC, HJK, HCK, and IHK; Formal analysis, JHC, IHK; Investigation, JHC, HJK, HCK, and IHK; Methodology, JHC, IHK; Project administration, all authors; Resources, all authors; Software, all authors; Supervision, JHC, IHK, and JHL; Validation, JHC, IHK, and JHL; Visualization, JHC, IHK, and JHL; Writing-original draft, JHC, IHK; Writing-review & editing, JHC, IHK, and JHL. Approval of final manuscript: all authors.

Data Availability Statement

All data generated or analyzed during this study are included in this article. Further enquiries can be directed to the corresponding author.

References

1. Chopra R, Morris CG, Friedman WA, Mendenhall WM. Radiotherapy and radiosurgery for benign neurofibromas. Am J Clin Oncol 2005;28:317–20.
2. Korf BR. Plexiform neurofibromas. Am J Med Genet 1999;89:31–7.
3. Mallick S, Benson R, Bhasker S, Mohanti BK. Long-term treatment outcomes of juvenile nasopharyngeal angiofibroma treated with radiotherapy. Acta Otorhinolaryngol Ital 2015;35:75–9.
4. Jafek BW, Krekorian EA, Kirsch WM, Wood RP. Juvenile nasopharyngeal angiofibroma: management of intracranial extension. Head Neck Surg 1979;2:119–28.
5. Linskey ME, Sekhar LN. Cavernous sinus hemangiomas: a series, a review, and an hypothesis. Neurosurgery 1992;30:101–8.
6. Song SW, Kim DG, Chung HT, et al. Stereotactic radiosurgery for cavernous sinus hemangiomas. J Neurooncol 2014;118:163–8.
7. Needle MN, Cnaan A, Dattilo J, et al. Prognostic signs in the surgical management of plexiform neurofibroma: the Children's Hospital of Philadelphia experience, 1974-1994. J Pediatr 1997;131:678–82.
8. Tyagi I, Syal R, Goyal A. Staging and surgical approaches in large juvenile angiofibroma: study of 95 cases. Int J Pediatr Otorhinolaryngol 2006;70:1619–27.
9. Fagan JJ, Snyderman CH, Carrau RL, Janecka IP. Nasopharyngeal angiofibromas: selecting a surgical approach. Head Neck 1997;19:391–9.
10. Zhou LF, Mao Y, Chen L. Diagnosis and surgical treatment of cavernous sinus hemangiomas: an experience of 20 cases. Surg Neurol 2003;60:31–6.
11. Xin Z, Yao Y, Chen G, et al. Fractionated radiation therapy for large and giant cavernous sinus hemangioma: a retrospective study. Front Neurol 2020;11:355.
12. Sachdev S, Dodd RL, Chang SD, et al. Stereotactic radiosurgery yields long-term control for benign intradural, extramedullary spinal tumors. Neurosurgery 2011;69:533–9.
13. Hwang L, Okoye CC, Patel RB, et al. Stereotactic body radiotherapy for benign spinal tumors: meningiomas, schwannomas, and neurofibromas. J Radiosurg SBRT 2019;6:167–77.
14. Sahgal A, Chou D, Ames C, et al. Image-guided robotic stereotactic body radiotherapy for benign spinal tumors: the University of California San Francisco preliminary experience. Technol Cancer Res Treat 2007;6:595–604.
15. Wang X, Mei G, Liu X, Dai J, Pan L, Wang E. The role of stereotactic radiosurgery in cavernous sinus hemangiomas: a systematic review and meta-analysis. J Neurooncol 2012;107:239–45.
16. Hoeltgen L, Tessonnier T, Meixner E, et al. Proton therapy for advanced juvenile nasopharyngeal angiofibroma. Cancers (Basel) 2023;15:5022.
17. Gross AM, Wolters PL, Dombi E, et al. Selumetinib in children with inoperable plexiform neurofibromas. N Engl J Med 2020;382:1430–42.
18. Dombi E, Baldwin A, Marcus LJ, et al. Activity of selumetinib in neurofibromatosis type 1-related plexiform neurofibromas. N Engl J Med 2016;375:2550–60.
19. O'Sullivan Coyne GH, Gross AM, et al. Phase II trial of the MEK 1/2 inhibitor selumetinib (AZD6244, ARRY-142886 Hydrogen Sulfate) in adults with neurofibromatosis type 1 (NF1) and inoperable plexiform neurofibromas (PN). J Clin Oncol. 2020;38(15 Suppl):3612.
20. Palmer JD, Tsang DS, Tinkle CL, et al. Late effects of radiation therapy in pediatric patients and survivorship. Pediatr Blood Cancer 2021;68 Suppl 2:e28349.

 https://doi.org/10.3857/roj.2024.00493

Instructions for Authors

ROJ Radiation Oncology Journal

The Radiation Oncology Journal (ROJ) is a peer-reviewed publication of the Korean Society for Radiation Oncology. The ROJ is published quarterly on the last day of March, June, September, and December, one volume per year. Any physicians or researchers throughout the world can submit a manuscript if the scope of the manuscript is appropriate. Articles in the following categories will be published: original articles, invited review articles, case reports, editorials, and letters to the Editor related to basic or clinical radiation oncology.

Manuscripts for submission to ROJ should be prepared according to the following instructions. ROJ follows the Uniform Requirements for Manuscripts Submitted to Biomedical Journals: Writing and Editing for Biomedical Publication (http://www.icmje.org/urm_main.html), commonly known as "the Vancouver style," if not otherwise described below.

1. RESEARCH AND PUBLICATION ETHICS

For the research and publication ethics policies not stated on this site, Good Publication Practice Guidelines for Medical Journals or Guidelines on Good Publication can be applied.

(1) Journal policies on authorship and contributorship

1) Authorship

Authorship credit should be based on 1) substantial contributions to conception and design, acquisition of data, or analysis and interpretation of data; 2) drafting the article or revising it critically for important intellectual content; 3) final approval of the version to be published; and 4) agreeing to be accountable for all aspects of the work in ensuring that the questions related to the accuracy or integrity of any part of the work are appropriately investigated and resolved. Authors should meet these four conditions. For any persons who do not meet the above four criteria, they may be placed as contributors in the Acknowledgments section. Description of co-first authors or co-corresponding authors is also accepted if the corresponding author believes that their roles are equally contributed. After the initial submission of a manuscript, any changes in authorship must be explained by a letter to the Editor-in-Chief from the authors concerned. This letter must be signed by all authors of the paper. Copyright transfer and conflict of interest disclosure forms must be completed by every author. ROJ does not correct authorship after publication unless a mistake has been made by the editorial staff.

2) Originality and Duplicate Publication

All submitted manuscripts should be original and should not be considered by other scientific journals for publication at the same time. Any part of the accepted manuscript should not be duplicated in any other scientific journal without the permission of the editorial board. Submitted manuscripts are screened for possible duplicate publication by Similarity Check upon arrival. If duplicate publication related to the papers of this journal is detected, the authors will be announced in the journal, and their institutes will be informed, and there will also be penalties for the authors.

3) Secondary Publication

It is possible to republish manuscripts if the manuscripts satisfy the conditions of secondary publication of the Uniform Requirements for Manuscripts Submitted to Biomedical Journals. ROJ maintains a zero-tolerance policy when addressing allegations of plagiarism, duplicate publication (self-publication), data falsification, and scientific misconduct. Articles will be retracted if ethics violations are substantiated. Plagiarism is defined by the World Association for Medical Editors (WAME) as the "use of others' published and unpublished ideas or words (or other intellectual property) without attribution or permission and presenting them as new and original rather than derived from an existing source." ROJ participates in the Crosscheck/iThenticate program to investigate incidents of possible plagiarism. Manipulating data through fabrication, omission, or intentional distortion is unacceptable. Authors should be prepared to provide original data to editors if there is a question of authenticity. Claims of scientific misconduct are investigated and addressed, guided by the Committee of Publication Ethics (COPE) Code of Conduct.

(2) Statement of Informed Consent and Institutional Review Board Approval

Authors should have obtained written informed consent from all participants prior to inclusion in the study, and copies of written informed consent should be kept for studies on human subjects. For clinical studies of human subjects, a certificate, agreement, or approval by the Institutional Review Board (IRB) of the author's institution is required. If necessary, the editor or reviewers may request copies of these documents to resolve questions about IRB approval and study conduct.

The statement should be included in the Materials and Methods sec-

tion after the IRB approval. Identifying details of the participants should not be published in written descriptions and photographs. In cases where identifying details are essential for scientific purposes, the participant should have given written informed consent for the identifying information to be published, and it should be stated separately.

Waiver of the informed consent can only be granted by the appropriate IRB and/or national research ethics committee in compliance with the current laws of the country in which the study was performed, and this should be separately stated. It should be noted that manuscripts that do not contain statements on IRB approval and patient informed consent can be returned to the authors before the review process.

(3) Statement of Human and Animal Rights

All studies on human subjects must be conducted according to the principles expressed in the World Medical Association Declaration of Helsinki. Clinical studies that do not meet the Helsinki Declaration will not be considered for publication. The name or initials of the patient should not be displayed, and the patient's identity should not be known when submitting photographs related to the patient. If there is a possibility that the patient's identity may be exposed, it should be stated that the patient has given written consent.

All studies involving animals must state that the guidelines for the use and care of laboratory animals of the authors' institution, or any national law, were followed.

All studies dealing with clinical trials should be registered on the primary national clinical trial registration site, such as Korea Clinical Research Information Service (CRiS, http://cris.nih.go.kr), other primary national registry sites accredited by World Health Organization or ClinicalTrials.gov (http://clinicaltrials.gov), a service of the US National Institutes of Health.

(4) How the journal will handle complaints and appeals

When the Journal faces suspected cases of research and publication misconduct such as a redundant (duplicate) publication, plagiarism, fabricated data, changes in authorship, undisclosed conflicts of interest, an ethical problem discovered with the submitted manuscript, a reviewer who has appropriated an author's idea or data, complaints against editors, and other issues, the resolving process will follow the flowchart provided by the Committee on Publication Ethics (http://publicationethics.org/resources/flowcharts). The Editorial Board of ROJ will discuss the suspected cases and reach a decision. ROJ will not hesitate to publish errata, corrigenda, clarifications, retractions, and apologies when needed.

(5) Journal policies on conflicts of interest/competing interests

Conflict of interest exists when an author or the author's institution, reviewer, or editor has financial or personal relationships that inappropriately influence or bias their actions. Such relationships are also known as dual commitments, competing interests, or competing loyalties. These relationships vary from being negligible to having great potential to influence judgment. Not all relationships represent true conflict of interest. On the other hand, the potential for conflict of interest can exist regardless of whether an individual believes that the relationship affects their scientific judgment. Financial relationships such as employment, consultancies, stock ownership, honoraria, and paid expert testimony are the most easily identifiable conflicts of interest and the most likely to undermine the credibility of the journal, the authors, or the science itself. Conflicts can occur for other reasons as well, such as personal relationships, academic competition, and intellectual passion (http://www.icmje.org/conflicts-of-interest/). If there are any conflicts of interest, the authors should disclose them in the manuscript. The conflicts of interest may occur during the research process as well; however, it is important to provide disclosure. If there is a disclosure, editors, reviewers, and reader can approach the manuscript after understanding the situation and background for the completed research. The corresponding author must inform the editor of any potential conflicts of interest that could influence the authors' interpretation of the data.

(6) Journal policies on data sharing and reproducibility

1) Open data policy

For clarification on result accuracy and reproducibility of the results, raw data or analysis data will be deposited to a public repository after acceptance of the manuscript. Therefore, submission of the raw data or analysis data is mandatory. If the data is already a public one, its URL site or sources should be disclosed. If data cannot be publicized, it can be negotiated with the editor. If there are any inquiries on depositing data or waiver of data sharing, authors should contact the editorial office.

2) Clinical data sharing policy

This journal follows the data sharing policy described in "Data Sharing Statements for Clinical Trials: A Requirement of the International Committee of Medical Journal Editors" (https://doi.org/10.3346/jkms.2017.32.7.1051). As of July 1, 2018, manuscripts submitted to ICMJE journals that report the results of interventional clinical trials must contain a data sharing statement as described below. Clinical trials that begin enrolling participants on or after January 1, 2019, must include a data sharing plan in the trial's registration. The ICMJE's policy regarding trial registration is explained at http://www.icmje.org/recommendations/browse/publishing-and-editorial-issues/clinical-trial-registration.html. If the data sharing plan changes after registration,

this should be reflected in the statement submitted and published with the manuscript and updated in the registry record. All the authors of research articles that deal with interventional clinical trials must submit data sharing plan. Based on the degree of sharing plan, authors should deposit their data after deidentification and report the DOI of the data and the registered site.

(7) Journal's policy on ethical oversight

When the Journal faces suspected cases of research and publication misconduct such as a redundant (duplicate) publication, plagiarism, fabricated data, changes in authorship, undisclosed conflicts of interest, an ethical problem discovered with the submitted manuscript, a reviewer who has appropriated an author's idea or data, complaints against editors, and other issues, the resolving process will follow the flowchart provided by the Committee on Publication Ethics (http://publicationethics.org/resources/flowcharts). The Editorial Board will discuss the suspected cases and reach a decision. We will not hesitate to publish errata, corrigenda, clarifications, retractions, and apologies when needed.

The Research Ethics Committee of the Korean Society for Radiation Oncology covers ethical issues involved with research and publication. This committee is composed of one chairperson and the members of the committee. The director of the ethics committee acts as the chairperson of this committee. The members of the Research Ethics Committee include the vice president, the auditor, the directors of general affairs, research, and publication committees, and two directors without a portfolio of the society become ex officio. The members of this committee serve for a term of two years, and they may be reappointed.

If presented with convincing evidence of dual publication, fragmentation, plagiarism, fabrication, or theft of intellectual property in journals, the committee meeting will be held immediately for investigation. If evidence becomes available that the regulation has been breached, publication of the corresponding manuscript is immediately canceled and all authors, including the corresponding author, are banned from any publication in the ROJ published for the next three years. The investigation results of the committee meeting must be notified for immediate disciplinary measures and reported to the board of directors. Other issues that are not specified in this regulation abide by the decisions made by board members of the society, which conform with the Ethics Code of Science Technology set forth by the Korean Federation of Science Technology Societies.

(8) Journal's policy on intellectual property

All published papers become the permanent property of the Korean Society for Radiation Oncology. Copyrights of all published materials are owned by the Korean Society for Radiation Oncology.

(9) Journal's options for post-publication discussions and corrections

The post-publication discussion is available through a letter to the editor. If any readers have a concern on any articles published, they can submit a letter to the editor on the articles. If there founds any errors or mistakes in the article, it can be corrected through errata, corrigenda, or retraction.

(10) Journal's policy on preprint

A preprint can be defined as a version of a scholarly paper that precedes formal peer review and publication in a peer-reviewed scholarly journal. ROJ allows authors to submit the preprint to the journal. It is not treated as duplicate submission or duplicate publication. ROJ recommends authors to disclose it with DOI in the letter to the editor during the submission process. Otherwise, it may be screened from the plagiarism check program — Similarity Check (Crosscheck). Preprint submission will be processed through the same peer-review process as a usual submission. If the preprint is accepted for publication, authors are recommended to update the information at the preprint with a link to the published article in ROJ, including DOI at ROJ. It is strongly recommended that authors cite the article in ROJ instead of the preprint at their next submission to journals.

2. ELECTRONIC SUBMISSION OF MANUSCRIPT

Manuscript submission is only available through the online submission site at https://submit.e-roj.org. Submission instructions are available on the website. All articles submitted to the ROJ must comply with these instructions. Failure to do so will result in the return of the manuscript and a possible delay in publication. For assistance, please contact us via E-mail (rojeditor@gmail.com, roj@kosro.or.kr), telephone (+82-2-3410-3617).

3. PEER REVIEW PROCESS

The acceptance criteria for all papers are based on the quality and originality of the research and its clinical and scientific significance. Original Articles are generally reviewed at least by two peer reviewers. The Editor-in-Chief is responsible for final decisions regarding the acceptance of a peer-reviewed paper. An initial decision will normally be made within four weeks of receiving a manuscript, and the reviewers' comments are sent to the corresponding authors by E-mail. Revised manuscripts must be submitted online by the corresponding author. The corresponding author must indicate the alterations that

have been made in response to the referees' comments item by item. Failure to resubmit the revised manuscript within 12 weeks of the editorial decision is regarded as a withdrawal.

4. MANUSCRIPT PREPARATION

(1) General Guideline

Authors are required to submit their manuscripts after reading the following instructions. Any manuscript that does not conform to the following requirements will be considered inappropriate and may be returned. When a manuscript is received for consideration, the editors assume that no similar paper has been or will be submitted for publication elsewhere. The main document with manuscript text and tables should be prepared with an MS-word program

- The manuscript should be written in 11-point font with double-line spacing on A4-sized (21.0×29.7 cm) paper with 25 mm margins on the top, bottom, right and left.
- All manuscript pages are to be numbered at the middle of the bottom consecutively.

(2) Language

Manuscripts must be written succinctly in clear, grammatical English. All manuscripts originating from non-English speaking countries must be revised by a professional linguistic reviewer. Medical terminology should be written based on the most recent edition of Dorland's Illustrated Medical Dictionary or the most recent edition of English-Korean Korean-English Medical Terminology, published by the Korean Medical Association. The use of acronyms and abbreviations is discouraged and should be kept to a minimum. When used, they are to be defined where first used, followed by the acronym or abbreviation in parentheses. Drug and chemical names should be stated in standard chemical or generic nomenclature. Units of measure should be presented according to the SI units (e.g., Gy, Sv, Bq, m, kg, L).

(3) Reporting Guidelines for Specific Study Designs

For the specific study design, such as randomized control studies, studies of diagnostic accuracy, meta-analyses, observational studies, and non-randomized studies, it is recommended that the authors follow the reporting guidelines listed in the following table.

ORIGINAL ARTICLES

Original articles are reports of basic or clinical investigations. The manuscript for an original article should be organized on a separate page in the following sequence: title page, abstract and keywords, text (introduction, materials and methods, results, discussion, and conclusion), statements, references, tables, and figure legends.

1) Title page

The title Page should carry the following information.

- The title should be short, informative, and contain the major keywords (no more than 15 words). It is not necessary to lead with expressions like "clinical research on -" or "the study on -."
- Each author's name (first name, middle name, and surname) followed by the highest academic degree (e.g., Gil Dong Hong, MD).
- The name of the department (s) and institution (s) where the work was conducted. If the authors' affiliation is different, indicate individual departments and institutions by inserting a superscript letter immediately after the author's name, and the same letter in front of the appropriate institution.
- Running title of fewer than 60 characters.
- Source(s) of support in the form of grants, equipment, drugs, or all of these.
- Complete mailing address, telephone, and E-mail for correspondence and reprints.

2) Abstract and Keywords

The abstract should be no more than 250 words, and described concisely, in a paragraph, Purpose, Materials and Methods, Results, and Conclusion. Up to six keywords should be listed below the abstract. For selecting keywords, refer to the Medical Subject Headings; if suitable MeSH terms are not yet available for recently introduced terms, present terms may be used.

3) Text

Text should be arranged in the following order: Introduction, Materials and Methods, Results, Discussion, and Conclusion.

Initiative	Type of study	Source
CONSORT	Randomized controlled trials	http://www.consort-statement.org
STARD	Studies of diagnostic accuracy	http://www.stard-statement.org
PRISMA	Preferred reporting items of systematic reviews and meta-analyses	http://www.prisma-statement.org
STROBE	Observational studies inepidemiology	http://www.strobe-statement.org

Introduction

Introduction section should contain 1) the background and rationale of the study and 2) the objective of the study. The former part should state background information and references that inform the reader as to why the study was performed. Please avoid an extensive review of the literature. The final paragraph of the introduction should clearly state the hypothesis and the objective of the study.

Materials and Methods

Materials and Methods section should include sufficient details of the research design, subjects, and methods. Sufficient details need to be addressed in the methodology section of an experimental study so that it can be further replicated by others. The sources of special chemicals or reagents should be given along with the source location (name of the company, city, state/province, and country). Identify and provide references for all the statistical methods used. Statistical methods should be described meticulously. Software used for the statistical analysis should be stated with the name, manufacturer, and version. For studies using human subjects, the detail of IRB approval and patient informed consent should be stated. For animal experiments, a statement of approval by the institutional animal care committee or appropriate substitute should be provided.

Results

Present the results in logical sequence in the text, along with tables and figures. Do not repeat data that are already covered in the tables and/or figures; summarize only important observations. Do not illustrate minor details if their message is adequately conveyed by simple descriptive text. Make sure to give results for all items evaluated as mentioned in Materials and Methods section. State the statistical significance of the results.

Discussion and Conclusion

Emphasize the advances in knowledge provided by the study and the conclusions that follow from them. Do not repeat in detail the data given in the Results section. Include in the Discussion the implications of the findings and their limitations. Relate the observations to other relevant studies. Link the conclusions with the goals of the study, but avoid unqualified statements and conclusions not supported by the data.

4) Statements

All manuscripts must contain the following statements after the main text and before the reference list.

Statement of Ethics

In the manuscript, the authors should state that subjects have given their written informed consent and that the study protocol was approved by the institute's committee on human research.

(1) Study approval statement: Provide name and affiliation of the committee who approved the study and the decision reference number like as "This study protocol was reviewed and approved by [committee name, affiliation, and approval number]." If ethics approval was not required, or if the study has been granted an exemption from requiring ethics approval, this should also be stated, including the name of the ethics committee who made that decision.

(2) Consent to participate statement: For studies using human subjects, state whether written informed consent was obtained from participants to participate in the study. If written informed consent was not required, or if the study has been granted an exemption from requiring written informed consent, this should also be stated, including the name of the ethics committee who made that decision.

Conflicts of Interest Statement

All potential conflicts of interest must be stated within the text of the manuscript, under this heading. This pertains to relationships with pharmaceutical companies, biomedical device manufacturers, or other corporations whose products or services are related to the subject matter of the article. Such relationships include, but are not limited to, employment by an industrial concern, ownership of stock, membership on a standing advisory council or committee, being on the board of directors, or being publicly associated with the company or its products. Other areas of real or perceived conflict of interest could include receiving honoraria or consulting fees or receiving grants or funds from such corporations or individuals representing such corporations. Also, the nonfinancial relationships (personal, political, or professional) that may potentially influence the writing of the manuscript should be declared. Please state "The authors have no conflicts of interest to declare" if no conflicts exist.

Acknowledgement (optional)

If necessary, persons who have made substantial contributions, but who have not met the criteria for authorship, are acknowledged here. An exception is where funding was provided, which should be included in Financial Support.

Financial Support

Authors must give full details about the funding of any research relevant to the study, including the name of the funding agency, country

and the number of the grant provided by the funding agency.

Author Contributions

In the Author Contributions section, a short statement detailing the contributions of each person named as an author should be included. Contributors to the paper who do not fulfil the ICMJE criteria for authorship should be credited in the Acknowledgement section.

Data Availability Statement

Authors are required to provide a Data Availability Statement in their article that details whether data are available and where they can be found. The journal's data sharing policy strongly encourages authors to make all datasets on which the conclusions of the paper rely available to editors, reviewers, and readers without unnecessary restriction wherever possible. In cases where research data are not publicly available on legal or ethical grounds, this should be clearly stated in the Data Availability Statement along with any conditions for accessing the data.

Examples of Data Availability Statements:

- The data that support the findings of this study are openly available in [repository name e.g "figshare"] at http://doi.org/[doi], reference number [reference number]
- Publicly available datasets were used in this study. These can be found in [repository name e.g "figshare"] at http://doi.org/[doi], reference number [reference number]
- All data generated or analyzed during this study are included in this article [and/or] its supplementary material files. Further enquiries can be directed to the corresponding author.
- The data that support the findings of this study are not publicly available due to [REASON WHY DATA ARE NOT PUBLIC e.g., their containing information that could compromise the privacy of research participants] but are available from [e.g., the corresponding author [author initials] OR Data sharing committee [PROVIDE CONTACT DETAILS including email address] upon reasonable request]
- The data in this study was obtained from [third party source] where [RESTRICTIONS/LICENCE] may apply. Such a dataset may be requested from [source contact information].

5) References

In the text, references should be cited with Arabic numerals in brackets, numbered in the order cited. In the references section, the references should be numbered in order of appearance in the text and listed in English. List all authors if there are less than or equal to six authors. List the first three authors followed by "et al." if there are more than three authors. If an article has been published online, but has not yet been given an issue or pages, the digital object identifier (DOI) should be supplied. Journal titles should be abbreviated in the style used in Medline. Other types of references not described below should follow Citing Medicine: The NLM Style Guide for Authors, Editors, and Publishers.

Journal articles:

1. Yu JI, Park HC, Choi DH, et al. Prospective phase II trial of regional hyperthermia and whole liver irradiation for numerous chemorefractory liver metastases from colorectal cancer. Radiat Oncol J 2016;34:34-44.
2. Childs SK, Kozak KR, Friedmann AM, et al. Proton radiotherapy for parameningeal rhabdomyosarcoma: clinical outcomes and late effects. Int J Radiat Oncol Biol Phys. 2011 Mar 4 [Epub]. http://dx.doi.org/10.1016/j.ijrobp.2010.11.048.

Book:

3. Abeloff MD, Armitage JO, Niederhuber JE, Kastan MB, McKenna WG. Abeloff's clinical oncology. 4th ed. Philadelphia, PA: Churchill Livingstone; 2008.
4. Jain RK, Kozak KR. Molecular pathophysiology of tumors. In: Halperin EC, Perez CA, Brady LW, editors. Perez and Brady's principles and practice of radiation oncology. 5th ed. Philadelphia, PA: Lippincott Williams & Wilkins; 2008. p. 126-41.

Conference paper:

5. Medin PM, Foster RD, von der Kogel, Sayre J, Solberg TD. Spinal cord tolerance to reirradiation with radiosurgery: a swine model. In: 52th ASTRO Annual Meeting; 2010 Oct 31 - Nov 11; San Diego, CA, USA. Farifax, VA: ASTRO; 2010.

Online sources:

6. American Cancer Society. Cancer facts & figures [Internet]. Atlanta, GA: American Cancer Society; c2011 [cited 2011 Feb 20]. Available from: http://www.cancer.org/Research/CancerFactsFigures/index.
7. National Cancer Information Center. Cancer incidence [Internet]. Goyang (KR): National Cancer Information Center; c2011 [cited 2011 Oct 20]. Available from: http://www.cancer.go.kr/cms/statics.

6) Tables

Each table should be typed in the separate sheet. The title of the table should be on top-placed, and the first letter of all words (except articles, conjunctions, prepositions) should be capitalized. Tables are numbered in order of citation in the text. Lower case letters in superscripts [a], [b], [c] ... should be used for special remarks. Within a table, if a non-standard abbreviation is used or description may be necessary,

then list them under annotation below. The statistical significance of observed differences in the data should be indicated by the appropriate statistical analysis.

7) Figures

Upload each figure as a separate image file. The figure images should be provided in PowerPoint file, TIFF, JPEG, GIF, or EPS format with high resolution (preferably 300 dpi for figures and 600 dpi for line art and graph). The figures should be sized to column width (8.5 cm or 17.5 cm). If figures are not original, the author must contact each publisher to request permission, and this should be remarked on the footnote of the figure. Figures should be numbered, using Arabic numerals, in the order in which they are cited. All figures should be cited in the text (e.g., Fig. 1, Fig. 1A-C, Figs. 1 and 2). In the case of multiple prints bearing the same number, use capital letters after the numerals to indicate the correct order (e.g., Fig. 1A, Fig. 1B). A figure legend should be in English and a one-sentence description rather than a phrase or a paragraph. Capitalize the first letter of the first word. A legend for each light microscopic photograph should include the name of stain and magnification. Electron microscopic photographs should have an internal scale marker.

REVIEWS

Reviews should be comprehensive analyses of specific topics. They are organized as follows: title page, abstract and keywords, introduction, body text, conclusion, conflicts of interest, acknowledgments (if necessary), references, tables, and figure legends. Upload each figure as a separate image file. There should be an unstructured abstract equal to or less than 200 words. References should be obviously related to documents and should not exceed 50.

CASE REPORTS

Case reports will be published only in exceptional circumstances, when they illustrate a rare occurrence of clinical importance. The manuscript for a case report should be organized in the following sequence: title page, abstract and keywords, introduction, case report(s), discussion, conflicts of interest, acknowledgments (if necessary), references, tables, and figure legends. Upload each figure as a separate image file. The abstract should be unstructured, and its length should not exceed 150 words. References should be obviously related to documents and should not exceed 20. It is not necessary to use the word "introduction."

EDITORIAL

Editorials should be commentaries on articles published recently in the journal. Editorial topics could include active areas of research, fresh insights, and debates. Editorials should be no more than four to five pages in length, including references, tables, and figures.

LETTERS TO THE EDITOR

Letters to the Editor should include brief constructive comments that concern previously published papers. Letters to the Editor should be no more than two pages. It should have maximum five references, 1 table, and 1 figure. Letters could be edited by the Editorial Board. Responses by the author of the subject paper may be provided in the same issue or next issue of the Journal

5. COMMUNICATIONS TO THE PUBLISHER

We invite inquiries to the editorial office at any time during the editorial process. For all matters concerning presubmission, editorial policies, procedures, business inquiries, subscription information, orders, or changes of address, please contact the editorial office.

Editorial Committee Office
Department of Radiation Oncology, Samsung Medical Center, Proton Therapy Center, B2, 81, Irwon-ro, Gangnam-gu, Seoul 06351, Republic of Korea
Tel: +82-2-3410-3617
E-mail: rojeditor@gmail.com ,roj@kosro.or.kr

6. ADDITIONAL INFORMATION

(1) Copyright

All published papers become the permanent property of The Korean Society for Radiation Oncology. Upon acceptance of the manuscript, the authors will be required to sign a statement confirming that the manuscript contains no material the publication of which violates any copyright or other personal or proprietary right of any person or entity.

(2) Page Proofs

Corresponding authors are provided with page proofs and are asked to carefully review them for data and typesetting errors. When proofs are available, the corresponding author will receive a notification. Corrections to proofs must be returned via e-mail within 48 hours. Publication may be delayed if proofs are not returned by the publisher's deadline.

(3) Charges

There are no charges for submission and publication.

***NOTICE*:** These recently revised instructions for authors will be applied beginning with the June 2022 issue.

Checklist

ROJ Radiation Oncology Journal

1. Copyright transfer form has been signed by all authors.
2. Ethics disclosure form has been signed by corresponding author.
3. The manuscript shall be written by Microsoft Office Word or HWP processing programs.
4. A title page including author details and a manuscript without author details of the original file of the article should be submitted separately.
5. The original file of the article should not include the affiliations and names of the authors.
6. Standard abbreviations are defined in a key at their first appearance in the manuscript, and are consistent throughout the text.
7. Generic names are used for all drugs. Trade names are avoided.
8. Normal laboratory values are provided in parentheses when first used.
9. Research or project support/funding is noted in cover letter.
10. Internal review board approval of study is indicated in cover letter.
11. References are accurate, complete and in numerical order as they appear in the text, only the first 3 authors are listed.
12. No more than 50 references are cited in review article.
13. No more than 55 references are cited in original article.
14. No more than 20 references are cited in case report.
15. A corresponding author and complete address, telephone number and e-mail address are provided in cover letter.
16. Written permission from publishers to reproduce or adapt previously published illustrations or tables is included.
17. Informed consent forms for identifiable patient descriptions, photographs and pedigrees are included.

Copyright Transfer Form

ROJ Radiation Oncology Journal

This form applies to manuscripts submitted for the possible publication

Manuscript Title: _____

Date (MM/DD/YYYY): _____

Manuscripts will not be processed until the Radiation Oncology Journal Editorial Office has received this signed form. Please upload the completed form when you submit a manuscript on the E-Submission website (submit.e-roj.org).

The copyright to this article is transferred to the Radiation Oncology Journal (ROJ) effective if and when the article titled above is accepted for publication. If the article has more than two authors, each author must individually transfer his or her right in the article to the ROJ by signing this form. If the article is not published in the ROJ, this form is void and will not take effect. If it is signed and the article is published, the copyright transfer covers the exclusive right to reproduce and distribute the article, including reprints, translation, photographic reproduction, microfilm, electronic form (offline, online) or any other reproductions of similar feature.An author or authors may store it in his or her archive an author-made version of his/her article on his/her own website and his/her affiliated institution's depository library, including his/her final version; however he/she may not use the ROJ's PDF version which is posted on its own website. Provided permission is given to the author/authors by ROJ, he/she may only post his/her version of the article and a link to the original source of publication is inserted to the published article on the ROJ's website.Please use the exact and correct DOI for the article to ensure appropriate linking between sites. Articles listed on the ROJ's website are indexed, abstracted, and referenced by many indexing services and consortia such as SCIE, EMBASE, Google Scholar and KMCI.Each author guarantees that this contribution is original and that he/she has full responsibility to make this grant. The author signs for and accepts full responsibility for releasing this content. The author should declare that, to the best of his/her knowledge and belief, this manuscript does not infringe on the copyright or other proprietary rights of any third party. The author should understand that his/her submission of this manuscript does not guarantee publication in the ROJ. If there are multiple authors, names will appear in the ROJ in the order in which you listed them during the online submission and on this sheet. Therefore, please be sure to list names according the order you want to see in the final version. Each author should sign on the following, as appropriate.

Name (Print)	Signature